Anomalous dimensions of composite operators for off-forward hard scattering processes

Dissertation

zur Erlangung des Doktorgrades
an der Fakultät für Mathematik,
Informatik und Naturwissenschaften

Fachbereich Physik
der Universität Hamburg

vorgelegt von
Sam Van Thurenhout
aus Mechelen, Belgien

Hamburg
2022

Gutachter der Dissertation:	Prof. Dr. Sven-Olaf Moch Prof. Dr. Bernd Kniehl
Zusammensetzung der Prüfungskommission:	Dr. Markus Diehl Dr. Achim Geiser Prof. Dr. Bernd Kniehl Prof. Dr. Sven-Olaf Moch Prof. Dr. Robin Santra
Vorsitzende/r der Prüfungskommission:	Prof. Dr. Robin Santra
Datum der Disputation:	06.07.2022
Vorsitzender Fach-Promotionsausschuss PHYSIK:	Prof. Dr. Wolfgang J. Parak
Leiter des Fachbereichs PHYSIK:	Prof. Dr. Günter H. W. Sigl
Dekan der Fakultät MIN:	Prof. Dr. Heinrich Graener

Contents

List of abbreviations **7**

Introduction **11**

1 Overview of QCD, renormalization and the OPE **15**
1.1 QCD 15
1.1.1 Qualitative introduction 15
1.1.2 The QCD Lagrangian 16
1.1.3 Symmetries 21
1.1.4 Note on factorization 25
1.2 Renormalization 26
1.2.1 Quantum corrections and infinities 26
1.2.2 Regularization 27
1.2.3 Renormalization schemes 28
1.2.4 The renormalization group 29
1.2.5 Renormalization in QCD 31
1.2.6 Renormalization of local composite operators 33
1.3 Operator products 35

2 Scattering experiments **39**
2.1 Deep-inelastic scattering 40
2.1.1 Kinematics 40
2.1.2 The inclusive cross-section 41
2.1.3 Parton distribution functions 44
2.2 Deeply-virtual Compton scattering 46
2.2.1 Kinematics 46
2.2.2 Cross-section 47
2.2.3 Properties of GPDs 48

3 Mathematical background **51**
3.1 Special functions 51
3.1.1 Harmonic sums 51
3.1.2 Euler-Gamma and polygamma functions 52
3.1.3 Gegenbauer polynomials 53
3.2 The binomial transform 53

3.3 Evaluating finite sums . . . 57
3.3.1 Telescoping algorithms . . . 57
3.3.2 Evaluating sums using SIGMA . . . 59
3.3.3 Explicit single and double sums . . . 61

4 Renormalization of non-singlet spin-N operators **67**
4.1 Calculation of operator matrix elements . . . 68
4.2 Operator renormalization I: Forward limit . . . 72
4.3 Operator renormalization II: Off-forward limit . . . 74
4.3.1 Operator bases . . . 75
4.3.2 Renormalization in the total derivative basis . . . 79
4.3.3 Constraints on the anomalous dimensions . . . 81

5 Anomalous dimensions of Wilson operators **87**
5.1 The leading-n_f limit . . . 87
5.2 One-loop anomalous dimensions . . . 88
5.3 Two-loop anomalous dimensions . . . 90
5.4 Three-loop anomalous dimensions . . . 93
5.5 Four-loop anomalous dimensions . . . 95
5.6 Discussion of the results in the total derivative basis . . . 97
5.6.1 Application: Five-loop anomalous dimensions . . . 99
5.7 Anomalous dimensions beyond the leading-n_f limit . . . 100
5.7.1 Two-loop anomalous dimensions in the leading-color limit . . . 101
5.7.2 Spin-five ADM in full QCD . . . 104

6 Anomalous dimensions of transversity operators **109**
6.1 Transversity operators . . . 110
6.2 One-loop anomalous dimensions . . . 111
6.3 Two-loop anomalous dimensions . . . 112
6.4 Three-loop anomalous dimensions . . . 113
6.5 Four-loop anomalous dimensions . . . 114

7 Ongoing research **117**
7.1 A mathematics based relation for the anomalous dimensions . . . 117
7.2 A one-loop relation for gluon operators . . . 118
7.2.1 Extension to even-N operators . . . 120
7.3 Renormalization of polarized non-singlet operators . . . 121
7.3.1 Introduction . . . 121
7.3.2 One-loop anomalous dimensions . . . 123
7.3.3 Higher-order anomalous dimensions . . . 124

8 Conclusions and outlook **125**

Acknowledgments **127**

Appendices **128**

A Conventions **129**

B $SU(N_c)$ Wilson anomalous dimensions **131**
B.1 Two-loop anomalous dimensions . . . 131
B.2 Three-loop anomalous dimensions . . . 132
B.3 Four-loop anomalous dimensions . . . 133
B.4 Five-loop anomalous dimensions . . . 135

Aan ‘onzen Bompa’,
een nieuwe ster aan de hemel.

List of abbreviations

ADM anomalous dimension matrix

dimreg dimensional regularization

DIS deep-inelastic scattering

DVCS deeply-virtual Compton scattering

GPD generalized parton distribution

LCO local composite operator

NTD next-to-diagonal

OME operator matrix element

OPE operator product expansion

PDF parton distribution function

QCD quantum chromodynamics

QED quantum electrodynamics

QFT quantum field theory

RG renormalization group

TDF transverse distribution function

Abstract

We consider the renormalization of operator matrix elements for exclusive hard scattering processes in the chiral limit in the $\overline{\text{MS}}$-scheme. For such processes, mixing with total derivative operators has to be taken into account. By analyzing the renormalization structure of the operators in the chiral limit, we construct a consistency relation between the elements of the corresponding anomalous dimension matrices, which determine the scale-dependence of non-forward parton distributions. This relation, which is valid to all orders in the strong coupling α_s, then forms the basis for an algorithm to reconstruct the off-diagonal elements of such matrices. We apply the algorithm to multiple cases. In the limit of a large number of quark flavors n_f, we determine the anomalous dimension matrices for Wilson operators to fifth order in the strong coupling. In the same approximation, the anomalous dimensions for the transversity operators are presented to fourth order. Finally, we also apply the algorithm to obtain some low-N results for the Wilson operators in full QCD to fifth order in α_s.

Zusammenfassung

Wir betrachten die Renormierung von Operatormatrixelementen für exklusive harte Streuprozesse im chiralen Limit im $\overline{\text{MS}}$-Schema. Für solche Prozesse muss die Mischung mit totalen Ableitungsoperatoren berücksichtigt werden. Durch die Analyse der Renormierungsstruktur der Operatoren im chiralen Limit konstruieren wir eine Konsistenzrelation zwischen den Elementen der entsprechenden Matrizen der anomalen Dimension, die die Skalenabhängigkeit von nicht-vorwärts gerichteten Partonverteilungen bestimmen. Diese Beziehung, die für alle Ordnungen der starken Kopplung α_s gültig ist, bildet dann die Grundlage für einen Algorithmus zur Rekonstruktion der Nebendiagonalelemente solcher Matrizen. Wir wenden den Algorithmus auf mehrere Fälle an. Im Grenzfall einer großen Anzahl von Quark-Flavors n_f bestimmen wir die anomalen Dimensionsmatrizen für Wilson-Operatoren bis zur fünften Ordnung der starken Kopplung. In der gleichen Näherung werden die anomalen Dimensionen für die Transversaloperatoren bis zur vierten Ordnung dargestellt. Schließlich verwenden wir diesen Algorithmus um einige Ergebnisse für niedrige N für die Wilson-Operatoren in der vollständigen QCD bis zur fünften Ordnung in α_s zu erhalten.

List of publications

The content of this work is based on the following publications

- S. Moch and S. Van Thurenhout, *Renormalization of non-singlet quark operator matrix elements for off-forward hard scattering*, Nucl. Phys. B971 (2021), p. 115536, arXiv: 2107.02470 [hep-ph].

- S. Van Thurenhout and S. Moch, *Renormalization of non-singlet quark operator matrix elements in deep-inelastic scattering*", Acta Phys. Pol. B Proc. Suppl. 15, 2-A4 (2022), arXiv: 2112.01783 [hep-ph].

- S. Van Thurenhout, *Off-forward anomalous dimensions of non-singlet transversity operators*", Nucl. Phys. B980 (2022), p. 115835, arXiv: 2204.02140 [hep-ph].

- S. Van Thurenhout and S. Moch, "*Off-forward anomalous dimensions in the leading-n_f limit*", arXiv: 2206.04517 [hep-ph].

Introduction

An interesting open question in modern particle physics is how the properties of hadrons, like protons and neutrons, are determined by the properties of their constituents, namely the quarks and gluons (or partons, collectively). For example, while the spin of the proton is a well-measured quantity, it is as-of-yet not clear how to theoretically describe this in terms of the angular momenta of quarks and gluons. See e.g. the recent reviews [1–4] on this so-called proton spin puzzle. At the experimental level, one can gain some insight by performing scattering experiments at high energies. This way, one can probe the inner structure of the hadrons. Depending on the kinematics of the scattering process at hand, different properties of the hadronic structure can be extracted. One of the determining characteristics is whether the process is inclusive or exclusive, i.e. whether we simply sum over all final states or identify certain final-state particles.

An important quantity available in scattering experiments is the cross-section. For inclusive processes, this cross-section can be written as a convolution between a hard scattering kernel and a forward distribution function. The hard kernel is typically some partonic sub-cross-section, which can be calculated within the framework of perturbation theory. The forward distribution however is non-perturbative. It encodes information about parton distributions within the proton and can be described in terms of one kinematical parameter, e.g. the momentum fraction of the struck parton. Such forward distributions typically have a simple probabilistic interpretation. For example, the standard parton distribution functions (PDFs), accessible in inclusive deep-inelastic scattering ($ep \to eX$), represent the probability of finding a parton within the proton with a certain momentum. These PDFs characterize the longitudinal hadron structure and have been studied e.g. by data collected from the HERA experiment [5, 6]. They will also be central objects to be studied by the future Electron Ion Collider [7, 8]. The transverse structure of hadrons can be studied by considering e.g. polarized Drell-Yan processes [9–13]. The corresponding forward distribution is the so-called transversity distribution function (TDF). In a transversely polarized hadron, it represents the difference in probabilities of finding a parton polarized in the same direction as the hadronic spin and finding one polarized in the opposite direction. Formally, distributions such as PDFs and TDFs are defined as forward hadronic matrix elements of composite operators. These operators are composed out of the fundamental fields of quantum chromodynamics (QCD), i.e. quarks and gluons. Because of this, the scale-dependence of the distributions is determined by the scale-dependence of these operators, which is set by their anomalous dimensions. Such anomalous dimensions can be calculated perturbatively in the strong coupling α_s by renormalizing the corresponding forward partonic matrix elements of the operators.

In exclusive processes, at least one particle in the final state is explicitly identified. Examples include deeply-virtual Compton scattering ($ep \to ep\gamma$) and vector meson production ($B \to e\nu\rho$).

This means that there will be a non-zero momentum transfer to the target, which complicates parts of the analysis. The hadron structure is again characterized by distributions. This time, however, these distributions are non-forward. As a consequence, they do not have a simple probabilistic interpretation and we need more than one kinematical parameter to describe them. The additional ones are then related to the non-zero momentum transfer to the target. Two types of off-forward distributions are particularly important. The first are the generalized parton distributions (GPDs), accessible e.g. in deeply-virtual Compton scattering. They characterize transverse distributions of partons within hadrons. Furthermore, they also allow for the determination of the contributions of partonic angular momentum to the total hadronic spin [14]. The second are the so-called distribution amplitudes (DAs). These are related to vacuum-to-hadron transitions and are accessible e.g. in ρ-meson production. Extensive reviews of the description of hadron structure in terms of GPDs and DAs can be found e.g. in [14, 15]. At the formal level, GPDs and DAs are related to off-forward hadronic matrix elements of composite operators, meaning that the initial and final hadron have different momenta. The scale-dependence of the distributions is once again set by the anomalous dimensions of the relevant operators. Contrary to the inclusive case, these are now determined by renormalizing off-forward partonic matrix elements, i.e. the initial and final parton have unequal momenta. Furthermore, because of the non-zero momentum transfer, the operators can now mix under renormalization with total derivative operators. This implies that one has to deal with anomalous dimension or mixing matrices. Moreover, one has to choose a basis for the additional operators in order for the discussion to be non-ambiguous.

In this work, our main focus is on the anomalous dimensions in off-forward kinematics. These have been studied for a long time, by different groups using different methods and different operator bases. For explicitness, let us discuss the situation for the flavor non-singlet Wilson operators. For such operators, the three-loop evolution kernel is known [16]. The computation exploited conformal symmetry [17] of the QCD Lagrangian which was first utilized in pioneering work for the two-loop radiative corrections [18, 19]. In $D = 4-2\varepsilon$ dimensions and adopting the modified minimal subtraction ($\overline{\text{MS}}$) scheme conformal symmetry in QCD is exact for a specific number of quark flavors n_f at the critical coupling. In the physical four-dimensional theory the renormalization group equations then inherit a conformal symmetry such that the generators of the conformal transformations and the evolution kernel commute [20]. Consistency relations following from the conformal algebra allow one to restore the L-loop triangular mixing matrix for the off-forward anomalous dimensions from the L-loop forward anomalous dimensions and an $(L-1)$-loop result for a so-called conformal anomaly [16, 21, 22].

Additional calculations exist that do not employ conformal symmetry. The one-loop anomalous dimension matrix was derived in the $\overline{\text{MS}}$ renormalization scheme in [23, 24]. This computation employed a different operator basis than the one used in the conformal one. Finally, there also exist fixed moment calculations of non-singlet quark operator matrix elements (OMEs) at three-loop order. These were performed in the $\overline{\text{MS}}$-scheme as well as in alternative ones, such as the regularization invariant (RI) scheme, which are suitable for a direct application to hadronic structure studies using lattice QCD [25, 26]. The operator basis chosen in these works differs from those introduced above.

As the three branches of literature described above use different operator bases, direct comparisons of the results are not possible. The goals of this thesis are now two-fold. The first is to derive a new method to calculate the operator anomalous dimensions, which is based purely on the renormalization structure of the operators in a specific basis. The second goal of this work is to construct transformation formulae between the possible operator bases. This way, we can connect as-of-yet unrelated results in the literature, which provides valuable cross-checks.

Outline of the thesis

The first three chapters of this work will provide some theoretical background. Chapter 1 provides an overview of relevant concepts in quantum field theory (QFT) and QCD. The first part of this chapter reviews basic concepts of QCD, after which we discuss some general aspects of renormalization. The last part of Chapter 1 deals with the operator product expansion (OPE), which is important in the study of hard scattering processes. The second chapter of this work briefly summarizes some important properties of two such processes, namely inclusive deep-inelastic scattering (DIS) and exclusive deeply-virtual Compton scattering (DVCS). In Chapter 3, we give an overview of important mathematical concepts. After introducing a number of special functions, which frequently show up in QFT calculations, we discuss the concept of the binomial transform. This is a type of transformation which acts on sequences, and will be of importance in later chapters. The final section of Chapter 3 deals with the evaluation of finite sums. After reviewing telescoping algorithms, we discuss the explicit calculation of certain types of single and double sums.

In Chapter 4, we discuss the renormalization of flavor non-singlet spin-N operators in the $\overline{\text{MS}}$-scheme in two kinematic regimes. First we review the renormalization in forward kinematics, which is relevant for the analysis of inclusive processes. This allows one to extract the forward operator anomalous dimensions, which determine the scale-dependence of forward distributions like the PDF. Second we give an overview of the renormalization in the non-forward regime, which is important for the operator analysis of exclusive processes. As in this case the operators can mix with total derivative ones, we first need to choose a basis for the additional operators. Several options will be discussed. After this, we pick a specific basis and implement the renormalization. A detailed analysis will reveal useful relations between the operators, and in turn between their anomalous dimensions. This ultimately leads to a consistency relation between the anomalous dimensions, which forms the basis for a novel algorithm to construct the full off-forward mixing matrices. These mixing matrices characterize the scale-dependence of non-forward parton distributions like the GPD. Applications of this algorithm are discussed in the next two chapters. In Chapter 5, we present the mixing matrices for Wilson operators. In the limit of a large number of quark flavors, we construct these matrices to fifth order in the strong coupling α_s. Beyond this limit, the second order mixing matrix is presented in the limit of a large number of colors, and low-N results to fifth order in α_s in full QCD are derived. Chapter 6 discusses the determination of the mixing matrix for the transversity operators, in the limit of a large number of quark flavors, to fourth order in the strong coupling. Some recent progress, which is part of ongoing research, is collected in Chapter 7 and we present a general conclusion and outlook in Chapter 8.

Chapter 1

Overview of QCD, renormalization and the OPE

Introduction

This chapter contains three main parts. The first one discusses some basic elements of quantum chromodynamics, the non-Abelian gauge theory describing the strong interaction. After giving a qualitative introduction, we introduce the QCD Lagrangian and study its symmetries. Finally, we discuss the concept of factorization, which is of vital importance for the theoretical description of scattering processes involving hadrons.

The second part of the chapter discusses general aspects of renormalization. After arguing why it is necessary to regularize and renormalize quantities in quantum field theories, we discuss the concept and some examples of renormalization schemes. These are important to give a consistent physical definition of parameters such as masses and interaction strengths. Next we introduce the renormalization group, along with the concept of QFT beta-functions and anomalous dimensions. Finally, we say a few things about the renormalization of composite operators, which are important quantities in the description of hadron structure.

In the third and final part of this chapter we take a look at the OPE by Wilson, and apply it to the product of two electromagnetic currents. This is relevant for the calculation of hadronic scattering cross sections.

1.1 QCD

1.1.1 Qualitative introduction

The strong interaction, which binds quarks and gluons inside the nucleon, is very successfully described by QCD, which is a non-Abelian quantum gauge theory based on $\mathrm{SU}(3)$. Before the advent of QCD, the strong interaction was described in terms of the so-called parton model [27]. Here, one assumes that protons are composed of non-interacting particles called partons. While the parton model correctly predicts certain properties of hard scattering processes, like the scaling behaviour of structure functions, there are important deviations which cannot be explained within the model. It is one of the great successes of QCD to solve the issues of the parton model in a consistent way[1].

The fundamental charge of QCD is called the color charge, which affects both quarks *and* gluons. The fact that also the gauge bosons are charged, and hence can have self-interactions, is a consequence of the non-Abelian nature of the theory. In contrast, gauge bosons in Abelian models do not have such self-interactions, as is well known for e.g. the photon. These self-interactions are vital for the property of *asymptotic freedom*, which all non-Abelian gauge theories enjoy [28, 29]. Asymptotic freedom implies that the interaction strength tends to zero for increasing energies. As such, we can use perturbation theory to calculate physical quantities such as cross-sections at high energies. The low-energy regime, however, is fundamentally non-perturbative, meaning that other methods have to be called upon to make meaningful predictions. One successful framework for such non-perturbative calculations is *lattice gauge theory*, which is based on the discretization of spacetime.

An important example of a non-perturbative effect in QCD is *confinement*, which states that color-charged particles (quarks and gluons) cannot be isolated. Instead, the strong interaction works such that, when trying to separate two quarks, it is energetically more favorable to create quark-anti-quark pairs which in turn form bound states with the initial partons. Hence, quarks will always be bound up into colorless hadrons, either as mesons (quark-anti-quark pairs) or baryons (bound states with three quarks). More exotic types of hadrons, such as bound states of five quarks, are also possible [30] and have recently been confirmed to exist by the LHCb experiment [31].

1.1.2 The QCD Lagrangian

To study any quantum field theory, we need to specify the field content and the interactions between the fields. This is neatly summarized in the Lagrange density[2]. The first ingredient for writing down the Lagrange density of full QCD is the Lagrangian of a pure Yang-Mills interaction coupled to fermionic matter

$$\mathcal{L}_{mYM} = -\frac{1}{2}\mathrm{Tr}\, F_{\mu\nu}F^{\mu\nu} + \sum_f \overline{\psi}_f (i\not{D} - m_f)\psi_f. \tag{1.1}$$

Here ψ_f represents a quark of flavor f and $F_{\mu\nu}$ is the gluon field strength defined as

$$F^a_{\mu\nu} = \partial_\mu A^a_\nu - \partial_\nu A^a_\mu + g_s f^{abc} A^b_\mu A^c_\nu. \tag{1.2}$$

The trace in Eq.(1.1) is with respect to the $SU(3)_{\text{color}}$ generators, and we have left the sum over the color degrees of freedom of the quarks implicit ($\psi \equiv \psi_i$, $i = 1,2,3$). The covariant derivative is defined as

$$D_\mu \equiv \partial_\mu - i g_s A_\mu. \tag{1.3}$$

Here and in the following, we will usually suppress the color indices of the gluon fields

$$(A_\mu)_{ij} \equiv A^a_\mu (T^a)_{ij} \to A_\mu. \tag{1.4}$$

[1] In the next chapter, we give a more detailed description of the parton model, its successes and its failures.

[2] As is custom in high-energy physics, we will use the terms Lagrange density and Lagrangian interchangeably.

The generators of $\mathrm{SU}(3)_{\mathrm{color}}$ are written as T^a_{ij} where i and j run from one to three (corresponding to the fundamental representation) and a from one to eight (corresponding to the adjoint representation). These matrices form a basis for the 3×3 Hermitean matrices and constitute a Lie algebra

$$[T^a, T^b] = i f^{abc} T^c. \tag{1.5}$$

f^{abc} are the totally anti-symmetric structure constants, and we use the normalization

$$\mathrm{Tr}(T^a T^b) \equiv T_F \delta^{ab} = \frac{1}{2}\delta^{ab}. \tag{1.6}$$

This implies that the gluonic part of Eq.(1.1) can also be written as

$$\mathcal{L}_{\mathrm{gluon}} = -\frac{1}{4} F^a_{\mu\nu} F^{a,\mu\nu}. \tag{1.7}$$

Instead of g_s, we will often use

$$\alpha_s \equiv \frac{g_s^2}{4\pi} \tag{1.8}$$

or

$$a_s \equiv \frac{\alpha_s}{4\pi} \tag{1.9}$$

for the strong coupling constant.

In many applications it is useful to consider an arbitrary color gauge group $\mathrm{SU}(N_c)$ instead of the physical $\mathrm{SU}(3)_{\mathrm{color}}$. N_c then represents the number of colors. The reason for doing this is that practical calculations simplify in the so-called leading-color limit, $N_c \to \infty$. This is also called the planar limit, as it entails discarding all non-planar Feynman diagrams (i.e. diagrams with line crossings) in a perturbative calculation. In this more general case, the fundamental representation is N_c-dimensional and the adjoint one $(N_c^2 - 1)$-dimensional. A common choice for the normalization of the structure constants is

$$\sum_{c,d} f^{acd} f^{bcd} = N_c \delta^{ab}. \tag{1.10}$$

The quadratic Casimir operators for $\mathrm{SU}(N_c)$, which correspond to the (most common) color factors in QCD calculations, are generally defined as

$$T^a_R T^a_R \equiv C_2(R) \mathbb{1} \tag{1.11}$$

for some representation R. Specifically, we have

$$C_F = \frac{N_c^2 - 1}{2N_c} \tag{1.12}$$

for the fundamental representation and

$$C_A = N_c \tag{1.13}$$

for the adjoint one. In the following, we assume to be working with this more general gauge group unless stated otherwise[3].

[3] The more general $\mathrm{SU}(N_c)$ model will still be referred to as QCD though.

Feynman rules

The QCD Feynman rules can be derived using the standard path integral approach. We do not derive them here, but just list them for completeness[4]. See e.g. [33] for more details.

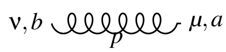

$$= -\frac{i}{p^4}(p^2 g_{\mu\nu} - \xi p_\mu p_\nu)\delta_{ab}$$

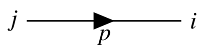

$$= \frac{i\delta^{ij}}{\not{p} - m + i\varepsilon} \xrightarrow{m\to 0} \frac{i\not{p}}{p^2 + i\varepsilon}\delta^{ij}$$

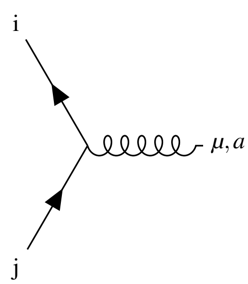

$$= i g_s \gamma^\mu T^a_{ij}$$

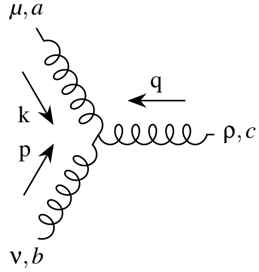

$$= g_s f^{abc}[g^{\mu\nu}(k-p)^\rho + g^{\rho\nu}(p-q)^\mu + g^{\mu\rho}(q-k)^\nu]$$

[4]The Feynman diagrams were drawn using TikZ-Feynman [32].

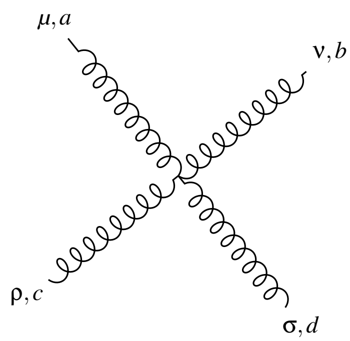

$$= -ig_s^2[f^{abe}f^{cde}(g^{\mu\rho}g^{\nu\sigma} - g^{\mu\sigma}g^{\nu\rho}) + f^{ace}f^{bde}(g^{\mu\nu}g^{\rho\sigma} - g^{\mu\sigma}g^{\nu\rho}) + f^{ade}f^{bce}(g^{\mu\nu}g^{\rho\sigma} - g^{\mu\rho}g^{\nu\sigma})]$$

For the three-gluon vertex, we assumed all momenta to be incoming. The factor ξ in the expression for the gluon propagator is the arbitrary covariant gauge parameter. Note that in the literature one often uses $1-\xi$ in the definition of the propagator. In our conventions, the Feynman gauge corresponds to $\xi = 0$. For the quark propagator, we have given the expressions for the massive and massless cases.

Gauge fixing and ghosts

As is well known, in order to properly define the propagator of a gauge boson, the gauge has to be fixed. The reason for this is that, if we want to determine the propagator of a spin-one gauge boson, we have to solve the following momentum-space equation

$$(-k^2 g_{\mu\nu} + k_\mu k_\nu)A^\mu = J_\nu \tag{1.14}$$

with J_ν some external current to which the gauge field couples. To determine the propagator, we now would have to take the inverse of $-k^2 g_{\mu\nu} + k_\mu k_\nu$. However, this operator is actually non-invertible, as one of its eigenvalues is zero. The origin of the problem can be traced back to gauge invariance. Under the gauge transformation

$$A_\mu \to A_\mu + \partial_\mu \alpha(x), \tag{1.15}$$

with $\alpha(x)$ an arbitrary scalar function, physical quantities remain unchanged. As such, different values of A_μ lead to the same current J_μ. The way to solve this issue is by selecting a particular gauge. This is done by adding a Lagrange multiplier to the Lagrangian density corresponding to the condition we want to impose. For example, if we want to use the Lorenz condition,

$$\partial \cdot A = 0, \tag{1.16}$$

we add the following gauge-fixing piece to the Lagrangian

$$\mathcal{L}_{\text{gauge}} = -\frac{1}{2\xi}(\partial \cdot A)^2. \tag{1.17}$$

In Abelian models like quantum electrodynamics (QED), this is enough to solve the issue unambiguously. However, more work has to be done to obtain a consistent non-Abelian model. The problem is that the gauge-fixing condition makes it possible for the longitudinal component of the gluon field ($\partial \cdot A$), which is unphysical, to interact with the transverse one, which is physical[5]. So, we need to get rid of these unphysical contributions. A consistent way of doing this was found by Fadeev and Popov in the late sixties [34]. The basic idea is to add fictitious fields to the Lagrangian called ghosts. These are anti-commuting, colored scalar fields which transform under the adjoint representation of SU(N_c). Every time a gluon loop appears in a Feynman diagram, one also has to include the same diagram with the gluons replaced by ghosts. This leads to an exact cancellation of the unphysical longitudinal components of the gluons. The Fadeev-Popov ghost part of the QCD Lagrangian can be written as

$$\mathcal{L}_{\text{ghost}} = -\overline{\eta}^a \partial \cdot D^{ac} \eta^c \tag{1.18}$$

with η and $\overline{\eta}$ the ghost fields. We also need two additional Feynman rules describing the ghost propagator and the ghost-ghost-gluon vertex. These are

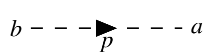

$$= \frac{i\delta^{ab}}{p^2 + i\varepsilon}$$

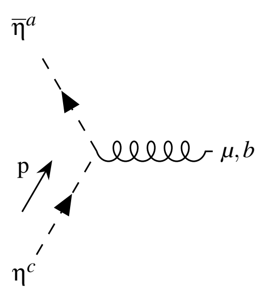

$$= -g_s f^{abc} p^\mu$$

Note that vertices with more than one occurrence of η or $\overline{\eta}$ cannot appear because of their anti-commuting nature. The complete Lagrangian density of QCD is now

$$\mathcal{L}_{\text{QCD}} = \mathcal{L}_{\text{mYM}} + \mathcal{L}_{\text{gauge}} + \mathcal{L}_{\text{ghost}}. \tag{1.19}$$

It should be noted that introducing additional non-physical ghosts is only necessary when working in a covariant gauge. When using physical gauges, like the class of axial gauges, there is no possibility for the non-physical components of the gluon field to propagate, and hence there is no need to introduce ghosts. However, the downside is that the form of the gluon propagator is usually more complicated in such gauges. For this reason, we will always employ a general covariant gauge, including ghosts when necessary.

[5]This does not happen in QED because of the Abelian equations of motion, which tell us that the unphysical components of the photon field obey a free field equation.

1.1.3 Symmetries

QCD possesses a number of interesting symmetries, which we now briefly discuss. In this section we work with physical QCD, based on $SU(3)_{color}$. Obviously, before choosing a particular gauge, the QCD Lagrangian is invariant under $SU(3)_{color}$ gauge transformations. It is this gauge symmetry which determines the interactions of the fields, as we saw in the previous section. Being a relativistic quantum field theory, QCD also enjoys invariance under Poincaré transformations (collection of Lorentz transformations and translations) and under the combined discrete symmetries CPT (charge conjugation, parity and time reversal). However, it is not necessary for the theory to be separately invariant under such discrete symmetries. To see this, consider the effect of adding the so-called θ-term to the Lagrangian

$$\mathcal{L}_\theta = \theta \frac{g_s^2}{64\pi^2} F_{\mu\nu}\tilde{F}^{\mu\nu} \tag{1.20}$$

with $\tilde{F}^{\mu\nu}$ the dual field strength

$$\tilde{F}^{\mu\nu} \equiv \frac{1}{2}\varepsilon^{\mu\nu\rho\sigma}F_{\rho\sigma}. \tag{1.21}$$

As this additional term obeys all the continuous symmetries mentioned above, we can (and should) incorporate it into the QCD Lagrangian. Its inclusion does not influence the classical equations of motion, nor does it have any perturbative effects. The reason for this is that we can write the θ-term as a total derivative. Written as a color trace we have

$$\mathrm{Tr}\, F_{\mu\nu}\tilde{F}^{\mu\nu} = \partial \cdot K \tag{1.22}$$

with

$$K^\mu \equiv 2\,\varepsilon^{\mu\nu\rho\sigma}\mathrm{Tr}\left(A_\nu\partial_\rho A_\sigma - \frac{2ig_s}{3}A_\nu A_\rho A_\sigma\right) \tag{1.23}$$

the Chern-Simons current.

This additional term does not obey all the discrete symmetries. Particularly, it breaks T, P and CP. The physical effect of this term is to give an electric dipole moment (EDM) to the neutron. Remember that electric dipole moments are sensitive probes for P-violation. To see this, recall that the Hamiltonian of a non-relativistic spin-S particle in an electromagnetic field is given by

$$H = -\mu\frac{\vec{B}\cdot\vec{S}}{|\vec{S}|} - d\frac{\vec{E}\cdot\vec{S}}{|\vec{S}|}. \tag{1.24}$$

Now, as the electric field is a vector while the magnetic field and the spin are axial vectors, we have

$$\mathrm{P}(\vec{E}\cdot\vec{S}) = -\vec{E}\cdot\vec{S}, \tag{1.25}$$

$$\mathrm{P}(\vec{B}\cdot\vec{S}) = \vec{B}\cdot\vec{S}. \tag{1.26}$$

From this it follows that the electric dipole moment d characterizes P-violation. The experimental upper limit for the neutron EDM is[6]

$$d_{\mathrm{neutron}} < 2.9\cdot 10^{-26}\ \mathrm{e\ cm} \tag{1.27}$$

[6] For a recent overview of general considerations of EDMs, see e.g. [35].

which in turn requires θ to obey[7]

$$|\theta| < 10^{-10}. \tag{1.28}$$

There is no a priori reason to expect θ to be this small, and the issue has been dubbed the *strong CP-problem*. A possible solution was offered by Peccei and Quinn in 1977 [37]. They proposed to introduce a novel scalar field which is charged under a new global U(1) symmetry, now called Peccei-Quinn (PQ) symmetry. It is also assumed that this U(1) symmetry is anomalous. The scalar field is then supposed to undergo spontaneous symmetry breaking, similarly to the Brout-Englert-Higgs (BEH) field. The associated pseudo-Goldstone boson is called the axion a. After the symmetry is broken, the remaining Lagrangian contains the following two terms

$$\mathcal{L} \sim \frac{g_s^2}{64\pi^2} F_{\mu\nu}\tilde{F}^{\mu\nu}\left(\theta + \chi\frac{a}{f_a}\right). \tag{1.29}$$

We recognize the first term as the one associated to the strong CP-problem. The second one appears because of the assumption that the PQ symmetry is anomalous. The constant χ in this term is related to the PQ charge of the quarks, while f_a is the decay constant of the axion. Analogously to the BEH field, the vacuum expectation value of the axion is non-vanishing. Instead we have

$$\langle a \rangle = -\frac{f_a\theta}{\chi}. \tag{1.30}$$

One can then perform a redefinition of the axion field

$$a \to a + \langle a \rangle \tag{1.31}$$

to cancel the θ parameter, hence solving the strong CP-problem dynamically. While this procedure is very promising from a theoretical standpoint, the axion is yet to be observed[8]. Experiments all over the globe are searching for this elusive particle, including MADMAX [38, 39] and ALPS II [40, 41] at DESY.

Let us now zoom in on the quark sector of the model,

$$\mathcal{L}_\psi = \sum_f \overline{\psi}_f (i\not{D} - m_f)\psi_f. \tag{1.32}$$

It is easy to see that $\mathcal{L}_\psi$ is invariant under a global U(1) symmetry

$$\psi \to e^{i\alpha}\psi \tag{1.33}$$

with associated Noether current

$$j_B^\mu = \frac{1}{3}\overline{\psi}\gamma^\mu\psi. \tag{1.34}$$

[7] In this discussion, we implicitly assumed the quarks to be massless. Otherwise, the physical θ parameter receives contributions from the quark mass matrix. An in-depth discussion of this subject is outside the scope of this text, see e.g. [36] for a more accurate treatment.

[8] Its interaction strength with standard model particles would be very small. While this makes observing it challenging, it also makes it a good candidate for dark matter.

This corresponds to the baryon number, which is conserved in the standard model[9]. It is an example of a so-called *accidental symmetry*, originating from the fact that we do not include operators in the Lagrangian of dimension larger than four. There are no new interactions associated to such accidental symmetries.

Let us now assume that the three lightest quark flavors are actually exactly massless, i.e.

$$m_u = m_d = m_s = 0. \tag{1.35}$$

Defining

$$q \equiv \begin{pmatrix} u \\ d \\ s \end{pmatrix} \tag{1.36}$$

the Lagrangian describing the quark sector of QCD, for these three flavors, reduces to

$$\mathcal{L}_q = \overline{q} i \not{D} q \tag{1.37}$$

and enjoys an additional SU(3) symmetry

$$\begin{pmatrix} u \\ d \\ s \end{pmatrix} \to U \begin{pmatrix} u \\ d \\ s \end{pmatrix}. \tag{1.38}$$

This is called *flavor symmetry*, denoted by $\mathrm{SU}(3)_\mathrm{f}$. Here U represents an arbitrary SU(3) matrix. In reality, the masses of the up- and down-quark are pretty similar ($m_u, m_d \sim 1$ MeV) while the mass of the strange quark is about two orders of magnitude larger, $m_s \sim 100$ MeV. Hence a better approximation would be to only assume the up- and down-quarks to be massless. The corresponding symmetry group is $\mathrm{SU}(2)_f$ and $\mathrm{SU}(2)_f \subset \mathrm{SU}(3)_f$. This is known as *isospin*. It can also be viewed as a symmetry relating the proton and the neutron, in that they can be regarded as two states of one particle dubbed the *nucleon*. Isospin then allows one to distinguish these two states.

Finally, we consider *chiral symmetry*. For this, we introduce the two chiral projection operators

$$P_{R/L} = \frac{\mathbb{1} \pm \gamma_5}{2} \tag{1.39}$$

obeying

$$\begin{aligned} P_{R/L}^2 &= P_{R/L}, \\ P_{R/L} P_{L/R} &= 0. \end{aligned} \tag{1.40}$$

We then form right- and left-handed quarks as

$$\psi_R = P_R \psi,$$

[9]Conservation of baryon number implies that the proton is stable. Conversely, if the conservation law is violated the proton could decay, which is possible according to certain models looking for beyond the standard model physics. An example of this is the class of grand unified theories.

$$\psi_L = P_L \psi. \tag{1.41}$$

Rewriting the quark kinetic term of the QCD Lagrangian in terms of ψ_R and ψ_L yields

$$\overline{\psi} i \not{D} \psi = \overline{\psi}_R i \not{D} \psi_R + \overline{\psi}_L i \not{D} \psi_L, \tag{1.42}$$

which implies that the QCD interactions conserve chirality. Conversely, the left- and right-handed components mix for the mass term,

$$m_\psi \overline{\psi} \psi = m_\psi \overline{\psi}_L \psi_R + m_\psi \overline{\psi}_R \psi_L. \tag{1.43}$$

We now introduce the so-called chiral transformation, which acts on the quark fields as

$$\psi \to e^{i\alpha\gamma_5} \psi, \tag{1.44}$$
$$\overline{\psi} \to \overline{\psi} e^{i\alpha\gamma_5}. \tag{1.45}$$

It is straightforward to see that this transformation leaves the kinetic term invariant, while the mass term transforms as

$$m_\psi \overline{\psi} \psi \to m_\psi \overline{\psi} e^{i\alpha\gamma_5} \psi. \tag{1.46}$$

Hence we only have exact chiral symmetry if all quarks are massless. The Noether current associated with chiral symmetry is

$$j_A^\mu = \overline{\psi} \gamma^\mu \gamma_5 \psi. \tag{1.47}$$

Since the symmetry only holds exactly in the massless limit, the axial current j_A^μ is only conserved in this limit,

$$\partial_\mu j_A^\mu = 2 i m_\psi \overline{\psi} \gamma_5 \psi. \tag{1.48}$$

In QCD, chiral symmetry is spontaneously broken. As per the Goldstone theorem [42, 43], we then expect the appearance of massless (Goldstone) bosons. With chiral symmetry only being an approximate symmetry in the real world, these bosons obtain a relatively low mass, and can be identified with the pions.

Another important property of chiral symmetry is that it is anomalous. While at the classical level the axial current is conserved (assuming exactly massless quarks), the quantum current has a non-vanishing divergence given by

$$\partial \cdot j_A = \frac{g_s^2}{16\pi^2} n_f \mathrm{Tr} F_{\mu\nu} \tilde{F}^{\mu\nu} \tag{1.49}$$

with n_f the number of massless quark flavors. The anomaly, known as the chiral or Adler-Bell-Jackiw (ABJ) anomaly, is generated at the one-loop level by triangle diagrams, see Fig.1.1. Note that it is only present for the flavor singlet axial current, i.e. if the quark fields in Eq.(1.47) are of the same flavor. Adler and Bardeen showed in the late sixties that the ABJ anomaly is one-loop exact, i.e. it does not receive additional radiative corrections [44].

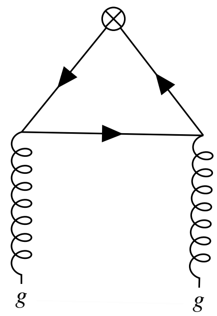

Figure 1.1: Triangle diagram that generates the ABJ anomaly. Note that there is also a second diagram with all fermion arrows reversed. The cross represents an insertion of the axial current operator.

1.1.4 Note on factorization

QCD enjoys the property of *factorization*, which signifies a decoupling of high- and low-energy properties of scattering processes[10]. As a simple illustration, consider the creation of a photon from a pp-collision, cf. Fig.1.2. The cross section for this process can be written as

$$\begin{aligned}
&\sigma[p(p_1)p(p_2) \to \gamma^*] \\
&\qquad = \int \mathrm{d}x_1 \int \mathrm{d}x_2 \sum_{q,q'} f_{p\to q}(x_1,\mu_F^2) f_{p\to \overline{q}'}(x_2,\mu_F^2)\hat{\sigma}[q(x_1p_1)\overline{q}'(x_2p_2) \to \gamma^*] \\
&\qquad \equiv \sum_{q,q'} f_q(\mu_F^2) \otimes f_{q'}(\mu_F^2)\hat{\sigma}[q\overline{q}' \to \gamma^*]
\end{aligned} \tag{1.50}$$

where in the second line we introduced a more compact representation in terms of *convolutions*. $\hat{\sigma}$ represents the hard scattering subprocess of a quark-anti-quark pair going into a virtual photon γ^* and can be calculated using perturbation theory. The function f, representing the PDF, is non-perturbative and depends on the factorization scale μ_F[11]. It represents the probability to find a quark or gluon carrying a certain fraction of the momentum of the parent hadron. We discuss PDFs in more detail in the next chapter in the context of deep-inelastic scattering. At the level of Feynman diagrams, factorization is a consequence of general diagrams having subgraphs with large (perturbative) or low (PDFs) virtuality. One then factorizes the low virtuality parts. The corrections to this procedure scale as inverse powers of the hard scale.

Instead of working with the convolutions in Eq.(1.50), it is often more convenient to work with the *Mellin moments* of the corresponding quantities. The Mellin moment of some function $f(x)$ is defined as

$$\mathcal{M}[f](N) \equiv \int_0^1 \mathrm{d}x\, x^{N-1} f(x). \tag{1.51}$$

[10] See e.g. [45] and references therein.

[11] For simplicity, we have suppressed here the dependence of the PDF on the renormalization scale μ.

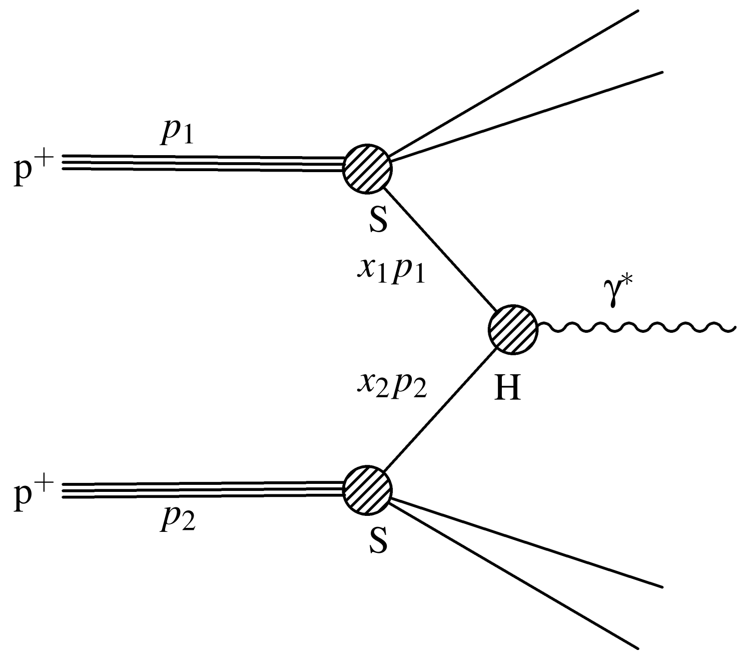

Figure 1.2: Sketch of the production of a photon during a pp-collision. S denotes the non-perturbative region, characterized by the PDF, and H the perturbative one. The latter represents the hard partonic subprocess. The diagram was drawn using FEYNMF *[46].*

The advantage of working in Mellin N-space is that convolutions, such as those appearing in Eq.(1.50), turn into products

$$\mathcal{M}[f_1 \otimes f_2](N) = \mathcal{M}[f_1](N) \cdot \mathcal{M}[f_2](N), \tag{1.52}$$

which are easier to handle.

1.2 Renormalization

This part of the chapter is dedicated to renormalization. After discussing some generalities, we review the renormalization of non-abelian gauge theories and the renormalization of composite operators.

1.2.1 Quantum corrections and infinities

To set the stage, we consider a one-loop self-energy diagram for some scalar particle of mass m.

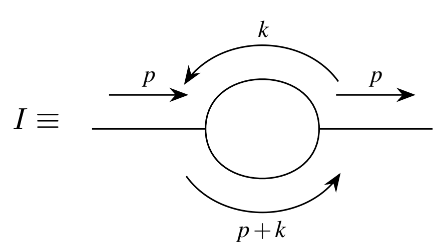

As the momentum k running through the loop is arbitrary, we have to integrate over all possible k-values. Hence

$$I \sim \int \frac{\mathrm{d}^4 k}{(k^2 - m^2 + i\varepsilon)((k+p)^2 - m^2 + i\varepsilon)} \tag{1.53}$$

where we ignore any possible prefactors. For large values of k this becomes, using polar coordinates,

$$I \xrightarrow{k\to\infty} \int_0^\infty \frac{k^3 \mathrm{d}k}{k^4} = \int_0^\infty \frac{\mathrm{d}k}{k} \to \infty. \tag{1.54}$$

We see that our simple one-loop diagram diverges for large energies, and it is said to have a *UV-divergence*. This would naively imply that whatever model it originated from has no physical meaning. Fortunately, this type of issue can be solved by the process of *renormalization*. The basic idea of renormalization is to absorb the infinities associated to quantum corrections in the parameters of the theory. In light of this, a theory is called *renormalizable* if this can be done consistently and using a finite number of parameters. In a *non-renormalizable* theory, one would need an infinite amount of parameters in order to get rid of all divergences[12]. We then distinguish between bare parameters, which are those that appear in the initial expression for the Lagrangian and are divergent (and hence non-physical) and renormalized parameters, which are finite. Suppose for example that our model contains some parameter ϕ. Multiplicative renormalization then entails

$$\phi^b = \left(1 + \frac{\delta\phi}{\phi}\right)\phi \equiv Z_\phi \phi. \tag{1.55}$$

Here and in the following, bare quantities will be denoted with superscript b. $\delta\phi$ represents the counterterm to ϕ, which is how the divergent terms are absorbed in order to make ϕ finite. Z_ϕ is called the renormalization factor or Z-factor of ϕ. When the parameter represents some field of the model, it is common to use the square root of the Z-factor, e.g. for some fermion field ψ we would have

$$\psi^b = \sqrt{Z_2}\psi. \tag{1.56}$$

This way the corresponding propagator, which consists of two fields, only has one power of Z_2. As an aside, note that it is not actually strictly necessary to renormalize the fields if we are only interested in making physical observables, like S-matrix elements, finite. However, the advantage is that field renormalizations also render the Green's functions of the theory UV-finite.

1.2.2 Regularization

Before implementing the renormalization, one first has to *regularize* the model. The purpose of regularization is to transform the divergent integrals, which are mathematically ill-defined, into finite well-defined ones. This is done by introducing a regulator, which is to be removed after renormalization is completed. There is no unique way of doing this, but physical observables should be independent of the regulator. A physically intuitive method for regulating loop integrals is the introduction of a high-energy cut-off Λ,

$$\int_0^\infty \mathrm{d}^4 k \to \int_0^\Lambda \mathrm{d}^4 k. \tag{1.57}$$

[12] This does not mean that non-renormalizable theories have no predictive power, as can be seen within the framework of effective field theories.

After renormalization the limit $\Lambda \to \infty$ is taken. In practical calculations, one often chooses not to regularize using such a cut-off as it breaks certain symmetries like Lorentz and gauge invariance. Nowadays, regularization is often done using a method called *dimensional regularization* or *dimreg* for short [47–50][13]. Dimreg is based on the observation that the divergences in loop integrals are often only present in four dimensions, and disappear for lower values of the spacetime dimension. The central idea of dimreg is then to analytically continue the spacetime dimension from four to $D \equiv 4 - 2\varepsilon$, with ε a small positive constant[14]. The divergences are then translated into terms proportional to $1/\varepsilon$, and after renormalization one takes the limit $\varepsilon \to 0$. While physically less intuitive, dimreg keeps Lorentz and gauge invariance intact. If our model contains some dimensionless coupling parameter α, it is often preferable to keep this coupling dimensionless, also in D dimensions. To achieve this, we introduce an arbitrary mass-parameter μ and redefine

$$\alpha \to \mu^{2\varepsilon}\alpha \tag{1.58}$$

in the D-dimensional theory. As μ is arbitrary, it does not have a direct physical interpretation.

1.2.3 Renormalization schemes

The process of renormalization has two main goals. The first is to absorb infinities coming from quantum corrections into the bare free parameters of the model, rendering it finite. The second is to give a physical meaning to these parameters. Within perturbation theory this has to be repeated order per order. In practice this can be a bit tricky, as the procedure is not unique. The ambiguity arises from the freedom to choose how to deal with finite terms of loop integrals. While the counterterms are enough to fix all the divergent parts, one can choose what to do with the finite pieces. Different choices then amount to different *renormalization schemes*. To illustrate this, let us assume we have some parameter ϕ with a counterterm of the form

$$\delta\phi = \frac{a_1}{\varepsilon} + a_2\varepsilon^0 + O(\varepsilon). \tag{1.59}$$

The terms proportional to ε vanish when we send $D \to 4$, and the $1/\varepsilon$ piece is independent of the renormalization scheme. Hence, the only ambiguity is in how we choose to deal with the terms proportional to ε^0. For the sake of argument, assume the parameter under consideration to be a mass. One possible renormalization scheme is then the *on-shell scheme*, which fixes the finite terms by positing the physical mass to correspond to the pole of the corresponding propagator. If we are to use the on-shell scheme, it has to be checked whether or not there exists an on-shell definition (or if one makes sense). This is not of any concern in QED, but it is an issue in QCD because of the non-existence of free quarks. Alternatively one can use the *minimal subtraction (MS) scheme*, which nullifies the finite piece in the counterterm

$$\delta\phi^{\text{MS}} = \frac{a_1}{\varepsilon}. \tag{1.60}$$

In the *modified minimal subtraction ($\overline{MS}$) scheme*, one also subtracts the Euler-Mascheroni constant γ_E and a factor of $\ln 4\pi$, which commonly appear in the calculation of loop integrals

$$\delta\phi^{\overline{\text{MS}}} = \frac{a_1}{\varepsilon} - \gamma_E + \ln 4\pi. \tag{1.61}$$

[13] An in-depth discussion of all the nitty-gritty details of dimensional regularization is beyond the scope of this text. A good overview is provided in e.g. chapter 4 of [51].

[14] Incidentally, dimreg can also deal with infrared divergences by choosing ε to be a small negative number.

An advantage of the $\overline{\text{MS}}$-scheme is that it is mass-independent, meaning that the renormalization factors do not depend on any of the masses in the model. The price we pay is that renormalized quantities will depend on the arbitrary energy scale μ, called the *renormalization scale*. This dependence is called the *running* of the quantity at hand. So, in QCD, we speak of running masses $m(\mu^2)$ and the running coupling $\alpha_S(\mu^2)$. This means that these parameters are not constant, but that they, due to loop-induced quantum corrections, depend on the energy scale of the process under consideration.

As a final remark we want to emphasize that, while choosing a renormalization scheme boils down to giving a definite physical definition of the parameters in the Lagrangian, it is possible to relate a quantity calculated in scheme A to the same quantity calculated in scheme B. This is of vital importance for the comparison of theoretical predictions with experimental data, and for comparing quantities renormalized on the lattice to the corresponding quantities renormalized in the continuum limit.

1.2.4 The renormalization group

Since the parameter μ is completely arbitrary, physical observables should not depend on it. Hence

$$\mu^2 \frac{\mathrm{d}}{\mathrm{d}\mu^2} \Theta = 0 \tag{1.62}$$

with Θ some observable (e.g. an S-matrix element). This invariance under a change of μ constitutes the so-called *renormalization group (RG)*. Another realization of the RG is the following. Assume we have some bare quantity Γ^b which depends on some bare coupling a^b (e.g. a_s^b in QCD). The corresponding renormalized function is then

$$Z\Gamma(a(\mu^2), \mu^2) = \Gamma^b(a). \tag{1.63}$$

Since the bare quantity on the right-hand side is independent of the renormalization scale, changing μ to μ' should not affect the left-hand side. This leads to the so-called *Callan-Symanzik equation* [52, 53]

$$\left[\mu^2 \frac{\partial}{\partial \mu^2} + \mu^2 \frac{\partial a}{\partial \mu^2} \frac{\partial}{\partial a} + \frac{1}{Z} \mu^2 \frac{\mathrm{d}Z}{\mathrm{d}\mu^2}\right] \Gamma(a(\mu^2), m(\mu^2), \mu^2) = 0. \tag{1.64}$$

The physical content of this equation is that a change in the renormalization scale is accompanied by a change of the parameters of the model, in a way such that physical observables remain the same[15]. We now introduce the RG parameters

$$\mu^2 \frac{\partial a}{\partial \mu^2} \equiv \beta(a), \tag{1.65}$$

$$-\frac{1}{Z} \mu^2 \frac{\mathrm{d}Z}{\mathrm{d}\mu^2} \equiv \gamma(a), \tag{1.66}$$

[15]The distant cousin of Laplace's demon, having access to all-order results, would see no change when the scale μ was changed. Mere humans, however, usually have to work order per order in perturbation theory, in which case there will be residual effects under such changes. These changes are always one order higher than the considered one; e.g. in a calculation at order a there will be a residual of order a^2.

which are characteristic for the model under consideration, and do not depend on specific physical observables. $\beta(a)$ is called the *beta-function* of the model, and encodes how the coupling varies when the energy scale is changed. Hence, it gives us a way of determining when the model can be handled using perturbation theory (small coupling), and when non-perturbative effects become important (large coupling). The β-function can be expanded in powers of the coupling

$$\beta(a) = -\varepsilon a - \beta_0 a^2 - \cdots = -\varepsilon a + \beta^{D=4}. \tag{1.67}$$

We assumed here to be working in dimensional regularization with $D = 4 - 2\varepsilon$. Of note is that the D-dimensional β-function already starts running at order a, while in the physical four-dimensional spacetime it starts running at order a^2. As the beta-function is measurable[16] (as the comparison of the values of the coupling strength at different energy scales), it should not depend on the gauge parameter. If the interaction strength is not scale-dependent, $\beta(a) = 0$, the model under consideration is said to be *conformal*[17]. Let us now briefly compare the properties of the beta-function in QED and QCD. In QED, we write the expansion of the D-dimensional beta-function as

$$\beta^{\mathrm{QED}}(a_e) = -a_e(\varepsilon + \beta_0^{\mathrm{QED}} a_e + \ldots) \tag{1.68}$$

with

$$a_e = \frac{\alpha_e}{4\pi} \tag{1.69}$$

and α_e the fine-structure constant. The one-loop coefficient is

$$\beta_0^{\mathrm{QED}} = -\frac{4}{3} n_f. \tag{1.70}$$

Since n_f is positive, $\beta_0^{\mathrm{QED}} < 0$, meaning that the coupling strength increases with increasing energy scale. So, we expect the low-energy regime to be well-described by perturbation theory, while for high energies non-perturbative effects have to be taken into account. At some finite value of the energy, the coupling strength of QED blows up. This is called the Landau pole of QED, denoted by Λ_{QED}, and its value is

$$\Lambda_{\mathrm{QED}} \sim 10^{280}\mathrm{GeV}. \tag{1.71}$$

At this energy scale, perturbation theory completely breaks down.

In QCD, the beta-function is expanded in the strong coupling as

$$\beta^{\mathrm{QCD}}(a_s) = -a_s(\varepsilon + \beta_0^{\mathrm{QCD}} a_s + \beta_1^{\mathrm{QCD}} a_s^2 + \beta_2^{\mathrm{QCD}} a_s^3 + \ldots). \tag{1.72}$$

Its one-loop coefficient is

$$\beta_0^{\mathrm{QCD}} = \frac{11}{3} C_A - \frac{2}{3} n_f. \tag{1.73}$$

[16]For this, one needs to consider a process which is sensitive to the coupling. For QCD, examples include hadronic decays of the Z-boson and electron-positron annihilation into hadrons.

[17]Note that renormalization also introduces a scale in such conformal models. This phenomenon is called *dimensional transmutation*, and it tells us that generically quantum corrections break conformal invariance. A small number of models is able to retain conformal invariance even after inclusion of quantum corrections. A well-known example is $\mathcal{N} = 4$ super-Yang-Mills theory.

With $C_A = 3$ and $n_f = 6$, $\beta_0^{\rm QCD} > 0$, which implies that the coupling strength decreases for increasing energies. This phenomenon is called *asymptotic freedom*. Hence at high energies, perturbation theory provides an accurate tool to describe the strong interaction in terms of quarks and gluons. Conversely, the low-energy regime is dominated by non-perturbative physics. The scale at which perturbation theory breaks down is the Landau pole of QCD, $\Lambda_{\rm QCD}$, which is of the order of $2 \cdot 10^2$ MeV. The coefficients of the QCD beta-function are known up to five-loop order [28, 29, 54–60]. For further use, we also quote here the two- and three-loop coefficients

$$\beta_1^{\rm QCD} = \frac{34}{3} C_A^2 - 2 C_F n_f - \frac{10}{3} C_A n_f, \tag{1.74}$$

$$\beta_2^{\rm QCD} = \frac{2857}{54} C_A^3 + C_F^2 n_f - \frac{205}{18} C_F C_A n_f - \frac{1415}{54} C_A^2 n_f + \frac{11}{9} C_F n_f^2 + \frac{79}{54} C_A n_f^2. \tag{1.75}$$

The function γ, defined in Eq.(1.66), is called the *anomalous dimension* of Γ and encodes the behaviour Γ when changing the energy scale. Like the beta-function, it is a perturbative function, i.e. we can write

$$\gamma = a\gamma^{(0)} + a^2\gamma^{(1)} + \dots . \tag{1.76}$$

1.2.5 Renormalization in QCD

Let us now focus on the $\overline{\rm MS}$-scheme, which is the scheme we will use for the remainder of this text, in dimensional regularization. In this renormalization scheme, the Z-factors do not depend on any dimensionful parameters and can be written as a series in the coupling constant and inverse powers of ε

$$Z = \delta_{\Gamma,\rm tree} + \sum_i a^i \sum_{j=1}^{i} \frac{z_{ij}}{\varepsilon^j}. \tag{1.77}$$

We introduced here the object $\delta_{\Gamma,\rm tree}$ which is one if Γ has non-trivial tree-level contributions and zero otherwise. In general, the Z-factors can also depend on the gauge parameter ξ. Hence the definition of the anomalous dimensions in the $\overline{\rm MS}$-scheme can be rewritten as

$$\gamma_\alpha = \beta Z^{-1}\frac{{\rm d}Z}{{\rm d}a} + \xi\gamma_3 Z^{-1}\frac{{\rm d}Z}{{\rm d}\xi}. \tag{1.78}$$

In QCD, γ_3 is the anomalous dimension of the gluon field which renormalizes as

$$A_b^\mu = \sqrt{Z_3} A^\mu. \tag{1.79}$$

Also the strong coupling a_s has to be renormalized

$$a_s^b = Z_a a_s. \tag{1.80}$$

The $\frac{1}{\varepsilon}$-poles of Z_a correspond to the expansion parameters of the QCD beta-function, cf. Eq.(1.72). When using a general covariant gauge, the gauge parameter ξ has to be renormalized as well. As the gauge parameter appears through the gluon propagator, it renormalizes with the same Z-factor as the gluon, i.e.

$$(1-\xi)_b = Z_3(1-\xi). \tag{1.81}$$

When combining Eq.(1.78) with the series expansions of the Z-factors and anomalous dimensions, it can be used to derive the explicit expressions for z_{ij} in Eq.(1.77) in terms of RG parameters. For example, the quark wave function renormalization constant,

$$\psi_b = \sqrt{Z_2}\psi, \tag{1.82}$$

can be easily derived. Up to order a_s^3 we find

$$\begin{aligned} Z_2 =& 1+\frac{a_s}{\varepsilon}\gamma_2^{(0)}+\frac{a_s^2}{2\varepsilon}\Big\{\frac{1}{\varepsilon}[(\gamma_2^{(0)}-\beta_0)\gamma_2^{(0)}-\gamma_3^{(0)}(1-\xi)g_{211}]+\gamma_2^{(1)}\Big\} \\ &+\frac{a_s^3}{3\varepsilon}\Big\{\frac{1}{\varepsilon^2}\Big[\Big(\frac{1}{2}\gamma_2^{(0)}-\frac{3}{2}\beta_0\Big)(\gamma_2^{(0)})^2+\beta_0\gamma_2^{(0)} \\ &-\frac{1}{2}\gamma_3^{(0)}[\gamma_3^{(0)}-g_{311}(1-\xi)](1-\xi)g_{211}-\frac{3}{2}\gamma_3^{(0)}(1-\xi)(\gamma_2^{(0)}-\beta_0)g_{211}\Big] \\ &+\frac{1}{\varepsilon}\Big[\frac{3}{2}\gamma_2^{(1)}\gamma_2^{(0)}-\beta_0\gamma_2^{(1)}-\beta_1\gamma_2^{(0)}-\gamma_3^{(1)}(1-\xi)g_{211} \\ &-\frac{1}{2}\gamma_3^{(0)}(1-\xi)(2\xi g_{222}+g_{221})\Big]+\gamma_2^{(2)}\Big\}. \end{aligned} \tag{1.83}$$

Here the quantities g_{ijk} are defined via

$$\gamma_\alpha^{(i)} = \sum_{j=0}^{i+1}\xi^j g_{\alpha ji} \tag{1.84}$$

with $\alpha = 2$ for quarks and $\alpha = 3$ for gluons. The QCD anomalous dimensions are well-known and, up to order a_s^3, their coefficients read

$$\gamma_2^{(0)} = \xi C_F - C_F, \tag{1.85}$$

$$\gamma_2^{(1)} = \frac{3}{2}C_F^2-\frac{17}{2}C_FC_A+C_Fn_f+\frac{5}{2}\xi C_FC_A-\frac{1}{4}\xi^2C_FC_A, \tag{1.86}$$

$$\begin{aligned} \gamma_2^{(2)} =& -\frac{3}{2}C_F^3-C_F^2C_A\left(12\zeta_3-\frac{143}{4}\right)-C_FC_A^2\left(-\frac{15}{2}\zeta_3+\frac{10559}{144}\right) \\ &-\frac{3}{2}C_F^2n_f+\frac{1301}{72}C_FC_An_f-\frac{5}{9}C_Fn_f^2-\xi\left[C_FC_A^2\left(-\frac{3}{2}\zeta_3-\frac{371}{32}\right)\right. \\ &\left.+\frac{17}{8}C_FC_An_f\right]-\xi^2\left(\frac{3}{8}\zeta_3+\frac{69}{32}\right)C_FC_A^2+\frac{5}{16}\xi^3C_FC_A^2 \end{aligned} \tag{1.87}$$

for quarks and

$$\gamma_3^{(0)} = \frac{5}{3}C_A-\frac{2}{3}n_f+\frac{1}{2}C_A\xi, \tag{1.88}$$

$$\gamma_3^{(1)} = \frac{23}{4}C_A^2-2n_fC_F-\frac{5}{2}C_An_f+\frac{15}{8}C_A^2\xi-\frac{1}{4}C_A^2\xi^2, \tag{1.89}$$

$$\gamma_3^{(2)} = -C_A^3\left(\frac{3}{2}\zeta_3-\frac{4051}{144}\right)+n_fC_F^2-C_FC_An_F\left(12\zeta_3+\frac{5}{36}\right)$$

$$
\begin{aligned}
&- n_f C_A^2\left(-9\zeta_3+\frac{875}{36}\right)+\frac{11}{9}n_f^2 C_F+\frac{19}{9}n_f^2 C_A \\
&-\xi\left[C_A^3\left(-\frac{9}{8}\zeta_3-\frac{127}{16}\right)+n_f C_A^2\right]-\xi^2 C_A^3\left(\frac{3}{16}\zeta_3+\frac{27}{16}\right) \\
&+\frac{7}{32}\xi^3 C_A^3
\end{aligned} \tag{1.90}
$$

for gluons.

1.2.6 Renormalization of local composite operators

In particle physics, local composite operators (LCOs) and their matrix elements have an important rôle to play. By a local composite operator, we mean a product of fields and their derivatives, all of which are evaluated at the same spacetime point. A particularly important example is the electromagnetic current

$$
j^\mu(x)=\overline{\psi}(x)\gamma^\mu\psi(x). \tag{1.91}
$$

In the following, the argument x will usually be omitted. We will mainly be interested in gauge invariant LCOs, although it is not hard to imagine non-gauge invariant ones. Examples in non-Abelian gauge theories include LCOs involving ghost fields or partial derivatives acting on the gauge field. There are multiple ways LCOs appear in the context of particle physics. One is in the calculation of cross-sections of processes like deep-inelastic scattering and deeply-virtual Compton scattering, which will be discussed in the next chapter. LCOs can also be used to study hadron structure, i.e. to determine how the properties of quarks and gluons influence hadronic properties like spin, mass, etc.

A priori, one might expect that renormalizing the fundamental fields appearing in the Lagrangian would be enough to also render the matrix elements of LCOs finite. Unfortunately, this is not the case. Instead, we need to introduce a separate renormalization for the operators as well. So, if we have some bare operator O, we have to renormalize it as

$$
O=Z_O[O]. \tag{1.92}
$$

When renormalizing LCOs, we leave out the superscript b for bare operators and put square brackets around the renormalized ones. The scale-dependence of LCOs is determined by their anomalous dimension

$$
\frac{\mathrm{d}}{\mathrm{d}\ln\mu^2}[O]=\gamma[O]. \tag{1.93}
$$

which in turn can be extracted from the Z-factor as

$$
\gamma=-Z_O^{-1}\frac{\mathrm{d}Z_O}{\mathrm{d}\ln\mu^2}. \tag{1.94}
$$

At order a_s^L, the L-loop anomalous dimension can be read off from the $1/\varepsilon$-pole of the Z-factor as

$$
Z_O\sim\frac{a_s^L}{L}\gamma^{(L-1)}+\dots\ . \tag{1.95}
$$

The higher-order poles in ε of the Z-factor are completely determined in terms of lower-order RG-parameters. A particularly straightforward example is the renormalization of conserved currents, like e.g. the electromagnetic one in Eq.(1.91). Because it is conserved, $\partial_\mu j^\mu = 0$, it does not receive any quantum corrections. This implies that its anomalous dimension vanishes to all orders, such that

$$j^\mu = [j^\mu]. \tag{1.96}$$

A complication that can arise when renormalizing composite operators is the issue of *operator mixing*. This becomes relevant when there are multiple operators of the same dimension[18] carrying the same quantum numbers. The renormalization then goes as

$$O = \sum_{O'} Z_{OO'}[O'], \tag{1.97}$$

where the renormalization factors $Z_{OO'}$ will now depend on the anomalous dimensions of all relevant operators. The diagonal elements, Z_{OO}, start with $1 \times a^0$ while the off-diagonal elements only start at $O(a)$, i.e.

$$Z_{OO'} = \delta_{O,O'} + O(a). \tag{1.98}$$

A consistent study now requires one to choose a basis for the operators. In doing so, it is important to make sure that the basis is complete, and that all operators are independent of one another. This can be tricky because of the use of equations of motion or integration by parts when the operators contain derivatives. One way to check the completeness of the selected basis is by analyzing the Lorentz structure of Green's functions, as different operators may lead to different Lorentz structures by their Feynman rules. The full renormalization of all operators is most conveniently written as a matrix equation. For example, if we have two operators O_1 and O_2 their renormalization is written as

$$\begin{pmatrix} O_1 \\ O_2 \end{pmatrix} = \begin{pmatrix} Z_{11} & Z_{12} \\ Z_{21} & Z_{22} \end{pmatrix} \begin{pmatrix} [O_1] \\ [O_2] \end{pmatrix} \tag{1.99}$$

where we abbreviate $Z_{O_i O_j}$ by Z_{ij}. The matrix of Z-factors, which we will denote by $\hat{Z}$, is often called the *mixing matrix*. We can now also define the *anomalous dimension matrix (ADM)* by generalizing Eq.(1.94):

$$\hat{\gamma} \equiv -\hat{Z}^{-1} \left(\frac{\mathrm{d}}{\mathrm{d} \ln \mu^2} \hat{Z} \right). \tag{1.100}$$

Because of this relation between $\hat{\gamma}$ and $\hat{Z}$, we will also use the term mixing matrix when referring to the ADM.

The way to calculate such operator anomalous dimensions in practice is by calculating matrix elements of the operator, e.g. by inserting it into a quark or gluon two-point function. The divergences in these bare matrix elements can then be related to the anomalous dimensions using Eq.(1.92) or Eq.(1.97). This will be discussed in more detail in a later chapter, when we discuss the operators relevant for the analysis of scattering of a lepton off a proton.

[18] When operators are built out of massive fields, they can also mix with lower-dimensional operators under renormalization. The mismatch of the dimension is then fixed by introducing the mass parameter raised to the appropriate power. In this work, we do not consider this case.

1.3 Operator products

Having summarized the basic elements of QCD, renormalization and local operators, we now turn to the topic of evaluating *products* of local operators. These are relevant for the analysis of hard scattering processes. Specifically, suppose we have two local operators O_1 and O_2. The question we want answered is how to evaluate the time-ordered product $\mathcal{T} O_1(x) O_2(y)$ when $x \to y$. The situation is problematic when $x = y$, as then the operator product is ill-defined. The solution, called the *operator product expansion*, was found by Wilson in the late sixties [61], and later proven in perturbation theory by Zimmerman [62]. The main idea of the OPE is that a time-ordered product of two local operators can be expanded in a series of regular (i.e. finite) local operators. These operators are multiplied by functions, called *Wilson coefficients*, encoding the singularity of the operator product as $x \to y$

$$\lim_{x \to y} \mathcal{T} O_1(x) O_2(y) = \sum_{n=0}^{\infty} C_n(x-y) O_n\left(\frac{x-y}{2}\right). \tag{1.101}$$

In order for both sides of the relation to be consistent, the quantum numbers of the O_n have to correspond to those of $O_1 O_2$. Furthermore, if the operators on the left-hand side are invariant under some gauge transformations, the operators on the right should also be invariant. For simplicity but without loss of generality, we can set $y = 0$. The simplest example of such an expansion is the time-ordered product of two scalar fields, $\mathcal{T}\phi(x)\phi(0)$. A straightforward application of Wick's theorem gives

$$\mathcal{T}\phi(x)\phi(0) = \contraction{}{\phi}{(x)}{\phi}\phi(x)\phi(0) + :\phi(x)\phi(0): \tag{1.102}$$

where $:\phi(x)\phi(0):$ denotes the normal-ordered product. The Wick contraction of two fields just corresponds to the propagator

$$\contraction{}{\phi}{(x)}{\phi}\phi(x)\phi(0) = \langle 0|\mathcal{T}\phi(x)\phi(0)|0\rangle, \tag{1.103}$$

such that the first term in Eq.(1.102) is singular as $x \to 0$. So the Wilson coefficient here is just the propagator while the operator is the identity. In the second term, the Wilson coefficient is simply one, multiplied by the normal product which is regular when $x \to 0$.

In practical calculations, one often prefers to work in momentum space, in which case the OPE becomes

$$\int d^4x\, e^{iq\cdot x} O_1(x) O_2(0) = \sum_{n=0}^{\infty} C_n(q) O_n(0). \tag{1.104}$$

An important application of the OPE is to the product of two currents[19],

$$\mathcal{T} j^\mu(x) j^\nu(0) = \mathcal{T}[\overline{\psi}(x)\gamma^\mu\psi(x)][\overline{\psi}(0)\gamma^\nu\psi(0)], \tag{1.105}$$

which is a basic building block in the analysis of hard scattering processes like DIS. In the discussion that follows, we will work to leading order in the strong coupling α_s. This simplifies the analysis while still giving all the relevant operators in the expansion. Note that this means that the

[19] This discussion is heavily influenced by [63].

quarks are effectively free. This approximation is known as the *parton model*, and we will discuss this in some detail in the next chapter. To lighten the notation, we also omit the time-ordering operator $\mathcal{T}$. As in our simple example in Eq.(1.102), we can apply Wick's theorem to the product of currents. Focusing on the most singular terms in the limit of $x \to 0$ we have

$$j^\mu(x)\,j^\nu(0) \sim \,:\overline{\psi}(x)\gamma^\mu \overbracket{\psi(x)\overline{\psi}}(0)\gamma^\nu\psi(0): + :\overbracket{\overline{\psi}(x)\gamma^\mu\psi(x)\overline{\psi}(0)\gamma^\nu\psi}(0):. \tag{1.106}$$

As it will be easier to draw conclusions from a momentum expansion, we now perform a Fourier transformation. Furthermore, as both term in Eq.(1.106) give similar results, we focus on the first one. So we have

$$\int \mathrm{d}^4x\, e^{iq\cdot x} :\overline{\psi}(x)\gamma^\mu \overbracket{\psi(x)\overline{\psi}}(0)\gamma^\nu\psi(0): \,=\, :\overline{\psi}\gamma^\mu \frac{i(i\partial\!\!\!/ + q\!\!\!/)}{(i\partial + q)^2}\gamma^\nu\psi(0):. \tag{1.107}$$

This is of course just the quark propagator with momentum $p+q$, where p is the momentum through the quark line (and identified as $i\partial$) and q comes from the Fourier transform. With an application to hard scattering processes in mind, we now assume that q is much larger than all other scales. Assuming the momentum q to be spacelike, which it will be in DIS, we expand the denominator in Eq.(1.107) for $Q^2 \equiv -q^2 \gg p^2$. This is just a simple application of the geometric series

$$\begin{aligned}\frac{-1}{Q^2 - 2iq\cdot\partial + \partial^2} &= \frac{-1}{Q^2}\frac{1}{1-\frac{2iq\cdot\partial - \partial^2}{Q^2}} \\ &= \frac{-1}{Q^2}\sum_{n=0}^{\infty}\left(\frac{2iq\cdot\partial - \partial^2}{Q^2}\right)^n.\end{aligned} \tag{1.108}$$

In the limit $p^2/Q^2 \ll 1$, we can ignore terms coming from ∂^2/Q^2 such that the expansion simplifies to

$$\frac{-1}{Q^2 - 2iq\cdot\partial + \partial^2} = \frac{-1}{Q^2}\sum_{n=0}^{\infty}\left(\frac{2iq\cdot\partial}{Q^2}\right)^n. \tag{1.109}$$

Hence the product of currents becomes

$$j^\mu(x)\,j^\nu(0) = \frac{-1}{Q^2}\overline{\psi}\gamma^\mu i(i\partial\!\!\!/ + q\!\!\!/)\gamma^\nu \sum_{n=0}^{\infty}\left(\frac{2iq\cdot\partial}{Q^2}\right)^n \psi. \tag{1.110}$$

More simplifications can be introduced if we assume the hard scattering to only include the electromagnetic interaction. In this case, the interaction should be parity conserving and the hadronic tensor, giving rise to the product of currents, should be symmetric in its Lorentz indices. Hence, we can symmetrize Eq.(1.110) to give

$$j^\mu(x)\,j^\nu(0) = \frac{-i}{Q^2}\overline{\psi}[2\gamma^\mu(i\partial^\nu) - g^{\mu\nu}q\!\!\!/]\sum_{n=0}^{\infty}\left(\frac{2iq\cdot\partial}{Q^2}\right)^n \psi. \tag{1.111}$$

We have discarded a term proportional to $\partial\!\!\!/\psi$ on account of the Dirac equation. Now recall the ingredients of the Wilson OPE. On the one hand, we have the Wilson coefficients, which are c-functions incorporating the short-distance physics. On the other hand, we have the operators, which are assumed to be regular. With Q^2 providing a hard scale, it follows from Eq.(1.111) that the Wilson coefficients should be of the form

$$C^{\mu_1 \cdots \mu_n} \sim \frac{2^n}{Q^{2n+1}} q^{\mu_1} \dots q^{\mu_n}. \tag{1.112}$$

To extract the operators, we note that these are expected to be gauge invariant. Hence, any partial derivative should be replaced by a covariant one. The operators are also expected to have n open Lorentz indices. This means that they would have several components that transform differently under Lorentz transformations. Furthermore, these components would behave differently under renormalization. Fortunately, to a good approximation, we can focus on those operators that have spin n, implying that they are fully symmetric in their Lorentz indices and traceless. This is because operators of dimension d and spin s are suppressed by

$$\left(\frac{1}{Q^2}\right)^{d-s} \equiv \left(\frac{1}{Q^2}\right)^{t}. \tag{1.113}$$

Here $t \equiv d - s$ is called the *twist* of the operator [64]. So, the operators with the least amount of suppression are the leading-twist ones, which are those with maximal spin. The lowest value of the twist is two for the present case. Taking all of these considerations into account, the local operators appearing in the expansion of two currents are the *spin-N, twist-two quark operators*[20]

$$O_{\mu_1 \dots \mu_N} \equiv \mathcal{S} \overline{\psi} \gamma_{\mu_1} D_{\mu_2} \dots D_{\mu_N} \psi. \tag{1.114}$$

Here $\mathcal{S}$ denotes symmetrization of the Lorentz indices and subtraction of the traces, which is how we select the leading-twist contributions; see e.g. [23] for more details.

We have focused our discussion on free-field quark contributions which are flavor singlet. However, in the full form of the OPE of two electromagnetic currents, there will be two additional contributions. The first is the set of spin-N twist-2 flavor non-singlet quark operators,

$$O^{\mathrm{NS}}_{\mu_1 \dots \mu_N} \equiv \mathcal{S} \overline{\psi} \lambda^{\alpha} \gamma_{\mu_1} D_{\mu_2} \dots D_{\mu_N} \psi. \tag{1.115}$$

λ^{α} represent the generators of the flavor group SU(n_f) with n_f the number of active quark flavors. The second is the set of spin-N twist-two gluon operators, which appear once we move away from the free-field assumption (i.e. when working in full QCD instead of the parton model)

$$O^{\mathrm{G}}_{\mu_1 \dots \mu_N} \equiv \mathcal{S} F_{\nu \mu_1} D_{\mu_2} \dots D_{\mu_{N-1}} F_{\mu_N}{}^{\nu}. \tag{1.116}$$

As discussed above, Fadeev-Popov ghost fields have to be introduced into non-Abelian gauge theories to avoid propagation of non-physical components of the gauge fields. This implies that, complementary to Eq.(1.116), we also have to take into account ghost operators. However, we shall not need them in this work, and hence do not consider them any further.

[20]Because of the second term in Eq.(1.107) only operators with N even end up contributing to the DIS expansion.

Chapter 2

Scattering experiments

Introduction

If we want to further our understanding of proton structure, we need to perform scattering experiments at energies which are high enough such that the internal degrees of freedom can be resolved. At the LHC, this is done by scattering two proton beams off each other. Since protons are not elementary particles but are composed of quarks and gluons, which feel the strong interaction, starting of with two hadronic states leads to a complicated collection of particles in the detector, which has to be disentangled. A cleaner way of looking inside the proton is by scattering elementary particles, like electrons, off protons. In this chapter, we consider two such processes, namely deep-inelastic scattering and deeply-virtual Compton scattering. Both processes are well-studied and involve probing the proton using the electromagnetic interaction.

In the first part of the chapter, we provide a basic overview of DIS. We start by defining the kinematics of the process, after which we review the calculation of the inclusive cross-section using the OPE. Next, we make a small detour and consider a comparison with the parton model. Historically, the parton model was introduced before the advent of QCD. It assumes the proton to be composed of non-interacting fermions. While it makes some accurate predictions, we will see that deviations arise between parton model predictions and experimental data. The great success of QCD is that it is able to explain away all these discrepancies. Finally, the matrix elements of the operators arising from the OPE are used to define the standard PDFs, whose the scale-dependence is related to that of the operators. As we saw in the previous chapter, the scale-dependence of composite operators is determined by their anomalous dimensions which can be calculated perturbatively in the strong coupling α_s. As most of the content of this chapter can be found in standard QFT textbooks, e.g. [33, 36, 65], an attempt is made to keep the discussion relatively brief.

The second part of the chapter deals with a non-forward extension of DIS, namely DVCS. This is an exclusive process. As such, it gives access to non-forward (off-diagonal) parton distributions, which are not accessible in inclusive processes. The knowledge gained by these new distributions is of vital importance for our understanding of hadronic structure. After defining the process and its kinematics, we argue that the same operators as those in DIS appear in the study of DVCS. As before, a connection is made between these operators and non-perturbative functions describing the inner proton structure, which this time are the GPDs. The content of this part is mostly based

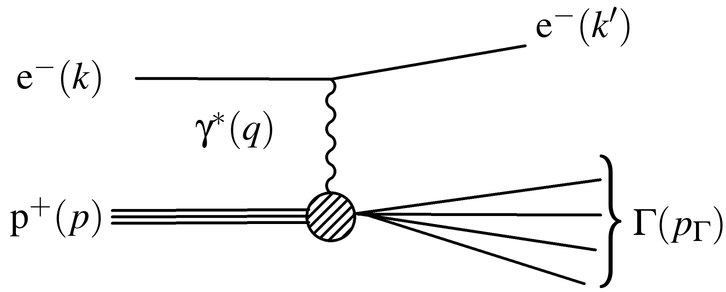

Figure 2.1: Sketch of the DIS process, where the proton structure is probed by a high-energy photon. For inclusive DIS, we sum over all hadronic final states, collectively denoted by Γ*. The diagram was drawn using* FEYNMF *[46].*

on the review [14] and the original paper by Ji [66].

2.1 Deep-inelastic scattering

2.1.1 Kinematics

In DIS,

$$e\,p \to e\,p,$$

an electron is scattered off a proton at high energy, see e.g. Fig.2.1. The proton structure is then probed by the exchanged virtual gauge boson, which we will assume to be a photon[1]. The spacelike momentum of this virtual photon will be denoted by q and corresponds to the electron momentum transfer, $k-k'$. Note that this quantity is experimentally observable; all that needs to be done is measure the momentum and energy of the final-state electron. We will also assume the virtuality to be large, i.e. $Q^2 \equiv -q^2$ is large[2]. This implies that it is able to probe the partonic structure of the proton and hence provide insight into how its properties emerge from those of the constituent quarks and gluons. If the center-of-mass energy of the process is much greater than the proton mass $m_p \sim 1$ GeV, the proton breaks apart, leading to a shower of hadrons ending up in the detector. In this case we have $M_\Gamma \equiv p_\Gamma^2 > m_p$, which leads to the requirement $Q^2 < 2(p\cdot q)$. In inclusive DIS, one is not interested in the specific hadrons appearing in the final state and they are simply summed. We denote this generic collection of hadronic final states by Γ.

To describe the DIS process, we need to introduce two invariants (i.e. Lorentz invariant quantities). One obvious choice is the virtuality Q^2. For the second variable one could e.g. choose

$$\nu \equiv \frac{p\cdot q}{m_p}. \tag{2.1}$$

In the rest frame of the proton, ν corresponds to the energy difference between the initial and final state electrons, $E-E^{'}$. In practice though, it is more common to use

$$x \equiv \frac{Q^2}{2\nu m_p} \tag{2.2}$$

[1]It could also be a Z- or W-boson, where in the latter case the final-state electron should be replaced by a final-state neutrino.

[2]Note that for a real photon $Q^2 = 0$.

instead of ν. This is the so-called Bjorken-x variable. For physical processes one has $0 \leq x \leq 1$, where $x = 1$ corresponds to elastic scattering. In the parton model, it corresponds to the fraction of the proton's momentum carried by the struck parton.

As the proton is probed by a (virtual) photon, the relevant interaction is simply the electromagnetic one, i.e.

$$\mathcal{L}_{int} = e j^{\mu} A_{\mu} \tag{2.3}$$

with A_{μ} the photon field and j^{μ} the standard electromagnetic current

$$j^{\mu} = \sum_{f} Q_f \overline{\psi}_f \gamma^{\mu} \psi_f. \tag{2.4}$$

We sum over all fermions ψ_f of flavor f and charge Q_f.

2.1.2 The inclusive cross-section

To study inclusive DIS in practise, we need to determine its cross-section, σ_{DIS}. A straightforward calculation shows that the differential cross-section can be written as

$$\frac{\mathrm{d}^2\sigma_{\mathrm{DIS}}}{\mathrm{d}\Omega \mathrm{d}E'} = \frac{\alpha_e^4}{Q^4} \frac{E'}{E} L_{\mu\nu} W^{\mu\nu} \tag{2.5}$$

with α_e the fine-structure constant. The tensors appearing on the right-hand side are the leptonic tensor, $L_{\mu\nu}$, and the hadronic one, $W^{\mu\nu}$. They encode different properties of the process. In order for the representation of the cross-section as a factorized quantity to be valid, we implicitly assumed to be working in the Bjorken limit, i.e. $Q^2, \nu \to \infty$ while x remains constant.

The leptonic tensor $L_{\mu\nu}$ encodes information about the polarization of the initial and final state electrons and of the off-shell photon. With the kinematics as in Fig.(2.1), one can easily convince oneself that it is given by

$$L_{\mu\nu} = \frac{1}{2}\mathrm{Tr}[\not{k}'\gamma_{\mu}\not{k}\gamma_{\nu}] = 2[k'_{\mu}k_{\nu} + k'_{\nu}k_{\mu} - g_{\mu\nu}(k' \cdot k) + i\varepsilon_{\mu\nu\alpha\beta}\, k^{\alpha} q^{\beta}]. \tag{2.6}$$

For unpolarized scattering, the last term in Eq.(2.6) is absent. The hadronic tensor $W^{\mu\nu}$ represents the purely hadronic part of the process, $\gamma^* p \to \Gamma$. It contains useful information about the structure of the proton, encoded in its form factors and structure functions. The amplitude of this sub-process can be shown to be proportional to the matrix element of the electromagnetic current,

$$\mathcal{M}(\gamma^* p \to \Gamma) \sim \langle \Gamma | \, j_{\mu} \, | p \rangle \, . \tag{2.7}$$

The hadronic tensor, written in momentum space, is then

$$W_{\mu\nu} = \int \mathrm{d}^4 x \, e^{iq\cdot x} \langle p | \, j_{\mu}(x) j_{\nu}(0) \, | p \rangle \, , \tag{2.8}$$

in which we used the completeness relation

$$\sum_{\Gamma} |\Gamma\rangle \langle \Gamma| = 1. \tag{2.9}$$

Using general arguments (e.g. Lorentz covariance), one can write down the generic form of the hadronic tensor in terms of structure functions. The spin-independent part is

$$W^S_{\mu\nu} = -W_1\left(g_{\mu\nu} + \frac{q_\mu q_\nu}{Q^2}\right) + \frac{1}{m_p^2}W_2\left(p_\mu + \frac{p\cdot q}{Q^2}q_\mu\right)\left(p_\nu + \frac{p\cdot q}{Q^2}q_\nu\right) \tag{2.10}$$

and the spin-dependent one

$$W^A_{\mu\nu} = \frac{i}{m_p^2}\varepsilon_{\mu\nu\lambda\sigma}q^\lambda\left[s^\sigma\left(G_1 + \frac{\nu}{m_p}G_2\right) - \frac{s\cdot q}{m_p^2}\,p^\sigma G_2\right], \tag{2.11}$$

with s^μ the proton spin vector. Note that the spin-independent hadronic tensor is symmetric in its Lorentz indices, while the spin-dependent one is anti-symmetric. This was to be expected, as $W^S_{\mu\nu}$ corresponds to the purely electromagnetic part of the interaction, which is parity conserving. W^A on the other hand is obtained from polarized scattering, coming from the weak interaction which is parity violating. The structure functions W_i and G_i depend in general on the two invariants Q^2 and x. If we ignore the mass of the electron, which we can do at the high energies we consider here, the terms proportional to q_μ drop out once contracted with the leptonic tensor. To see this, consider first the terms in the hadronic tensor which are proportional to $q_\mu q_\nu$. Contacting with $L_{\mu\nu}$ and using momentum conservation to write $q = k - k'$ this leads to

$$4m_e^2[(k\cdot k') - m_e^2]$$

which vanishes in the limit of $m_e \to 0$. A similar conclusion holds for the terms of the form $p_\mu q_\nu$ which give

$$4m_e^2[(k'\cdot p) - (k\cdot p)].$$

Eq.(2.8) implies that the calculation of the hadronic tensor for inclusive DIS is equivalent to the calculation of a matrix element of a product of two electromagnetic currents, which can be dealt with using the OPE, cf. Section 1.3. There we derived that this product can be written as a sum of spin-N, twist-two quark operators

$$O_{\mu_1\ldots\mu_N} \equiv \mathcal{S}\overline{\psi}\gamma_{\mu_1}D_{\mu_2}\ldots D_{\mu_N}\psi, \tag{2.12}$$

where $\mathcal{S}$ selects the twist-two components. Note however that there is a small caveat in this discussion. The expansion we derived in Chapter 1 was for the *time-ordered* product of two currents. However, the product appearing in the hadronic tensor is not time-ordered. Fortunately this does not prove to be an issue. We can simply apply the optical theorem to relate the rate of $\gamma^* p \to \Gamma$ to the imaginary part of the forward scattering rate of $\gamma^* p \to \gamma^* p$. Specifically we have

$$W_{\mu\nu} = 2\,\mathrm{Im}\,T_{\mu\nu} \tag{2.13}$$

with

$$T_{\mu\nu} = i\int \mathrm{d}^4x\, e^{iq\cdot x}\langle p|\mathcal{T}\, j_\mu(x)\, j_\nu(0)|p\rangle. \tag{2.14}$$

The product of currents in this final equation does allow for an application of the OPE as explained in Chapter 1.

The final step in the calculation of the inclusive DIS cross-section is to sandwich the operators in Eq.(2.12) between two proton states,

$$\langle p|\,O_{\mu_1\ldots\mu_N}\,|p\rangle \sim \mathcal{M}_N(Q)\,p_{\mu_1}\ldots p_{\mu_N}. \tag{2.15}$$

The parton model

Before continuing with our main discussion, we want to briefly comment on the so-called parton model, historically first introduced by Feynman in the late sixties [27]. We still consider the scattering of an electron off a proton in the Bjorken limit, but now assume that the proton (and all other hadrons for that matter) are simply built up from free, non-interacting partons. The expansion of the hadronic tensor in terms of structure functions, Eq.(2.10), remains valid in this simplified model. For convenience, we also introduce the reduced structure functions defined as

$$\begin{aligned} F_1(x,Q^2) &\equiv W_1(x,Q^2), \\ F_2(x,Q^2) &\equiv \frac{\nu}{m_p^2} W_2(x,Q^2). \end{aligned} \tag{2.16}$$

The F_1 structure function is also called the transverse structure function, while the combination

$$F_L \equiv F_2 - 2xF_1 \quad (Q^2 \to \infty) \tag{2.17}$$

is the longitudinal one. They describe the absorption of transversly and longitudinally polarized virtual photons, respectively. Rewriting the decomposition of the (spin-independent) hadronic tensor in terms of the structure functions F_i gives

$$W^S_{\mu\nu} = -F_1 \left(g_{\mu\nu} + \frac{q_\mu q_\nu}{Q^2} \right) + \frac{1}{\nu} F_2 \left(p_\mu + \frac{p \cdot q}{Q^2} q_\mu \right) \left(p_\nu + \frac{p \cdot q}{Q^2} q_\nu \right). \tag{2.18}$$

Within the parton model, these structure functions F_i can be written in terms of the parton distribution functions $f_q(x)$, which can be interpreted to give the probability to find a parton of type q inside the proton with momentum xp $(0 \leq x \leq 1)$. We omit writing here the dependence of the PDFs on the factorization scale μ_F. The F_2 structure function then becomes

$$F_2(x,Q^2) = x \sum_q Q_q^2 f_q(x). \tag{2.19}$$

Important to note here is that this only involves electrically charged partons within the proton. Hence we only take into account quarks and anti-quarks, which are assumed to be non-interacting, and ignore gluons. The F_1 structure function can be directly related to the F_2 one using the so-called Callan-Gross relation [67]

$$F_2(x,Q^2) = 2xF_1(x,Q^2), \tag{2.20}$$

which expresses that the partons are spin-1/2 fermions. Experimental data on this is shown in Fig.2.2. For $x \gtrsim 0.2$, we see that the data nicely follow the Callan-Gross relation. However, for lower values of x, discrepancies appear, which the parton model cannot explain. The solution to this conundrum presents itself when combining the parton model with perturbative QCD, leading to the *QCD-improved parton model*. Within this framework, the low-x behaviour of the structure functions is dominated by gluonic contributions.

Written in terms of the longitudinal structure function F_L, the Callan-Gross relation is simply the statement that F_L exactly vanishes in the parton model, which we can interpret as the inability of the spin-1/2 partons to absorb longitudinally polarized virtual photons. When considering the

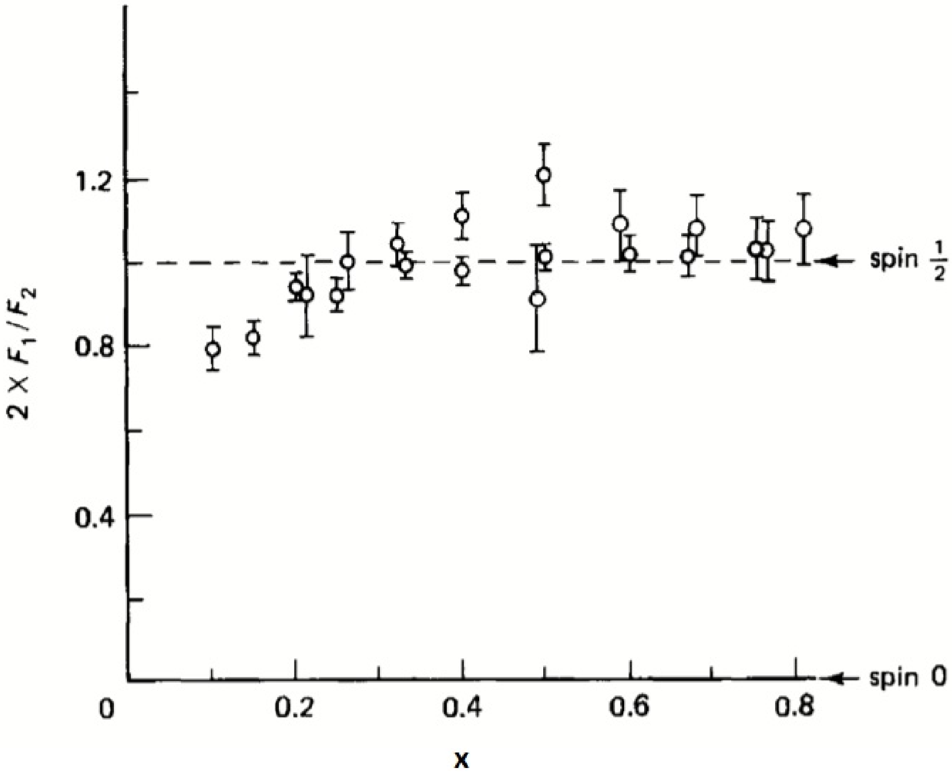

Figure 2.2: Historical plot demonstrating the Callan-Gross relation. Figure taken from [68, 69].

QCD-improved model, higher-order corrections break the Callan-Gross relation, i.e. $F_L \neq 0$ starting from order α_s.

The structure functions F_i have yet another remarkable property. Namely, in the Bjorken limit, they actually become independent of Q^2, i.e.

$$F_i(x, Q^2) \xrightarrow[x \text{ fixed}]{Q^2 \to \infty} F_i(x). \tag{2.21}$$

This behaviour is called *Bjorken scaling* [70]. Some historical measurements that demonstrate this scaling behaviour are shown in Fig.2.3. It demonstrates that the electron scatters off point-like partons within the proton[3].

At low and high values of the Bjorken variable, the scaling behaviour of the structure functions break downs and logarithmic corrections in Q^2 become important. These corrections can be calculated explicitly within the QCD-improved parton model.

2.1.3 Parton distribution functions

The parton distribution functions are non-perturbative functions characterizing long-range physical effects. They are universal, in the sense that they do not depend on the process under consideration,

[3]If the scattering was instead off an extended object, there would be an additional Q^2-dependent form factor.

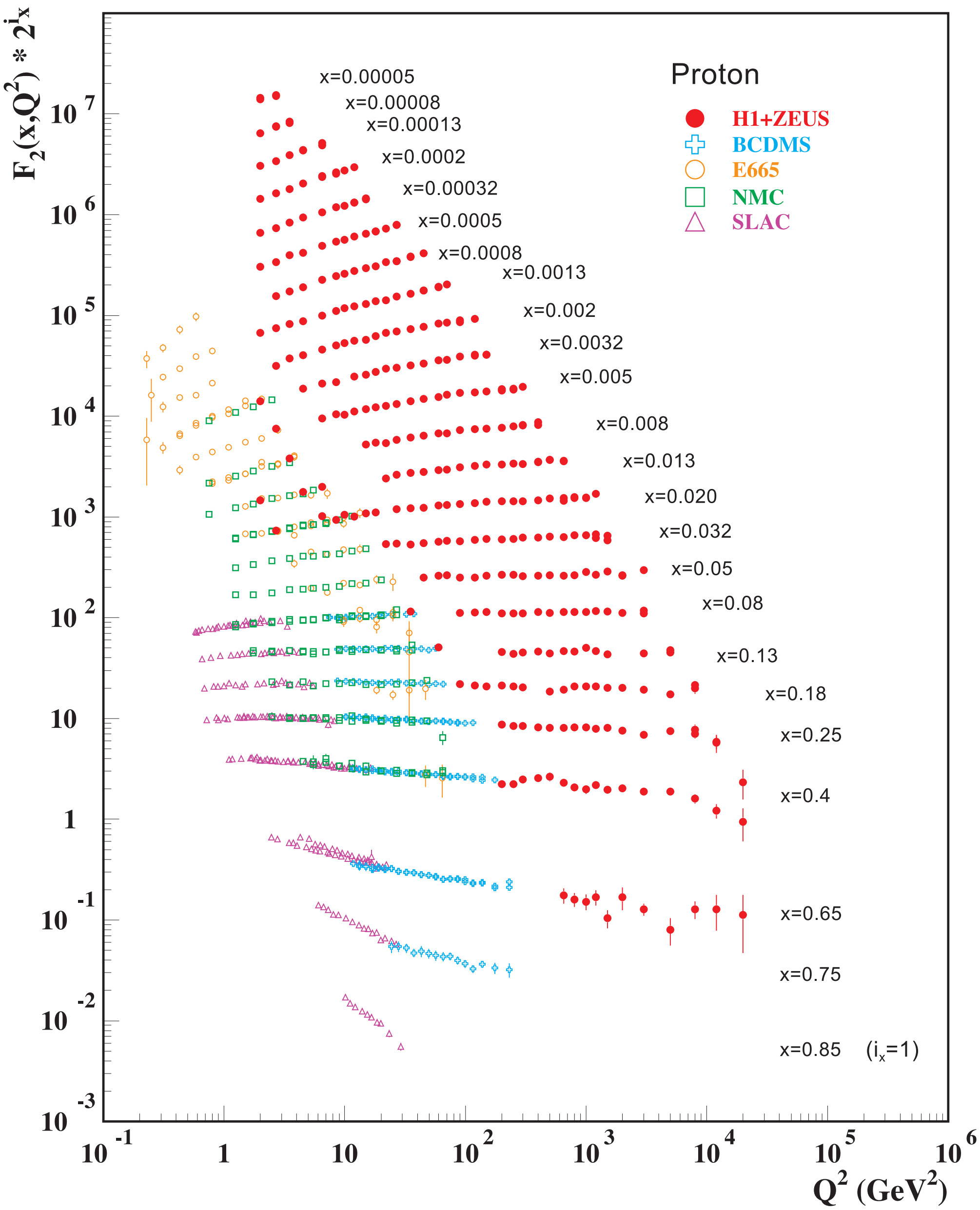

Figure 2.3: Historical plot demonstrating Bjorken scaling in DIS data. Figure taken from [71].

and encode the longitudinal momentum and polarization carried by partons within fast-moving hadrons. They can be related to the hadronic matrix elements in Eq.(2.15) as [36]

$$f_q(x) = \frac{1}{\pi} \sum_n \frac{\text{Im}\, \mathcal{M}_n}{x^n}. \tag{2.22}$$

Non-perturbative techniques have to be employed for their determination, see e.g. [72, 73] and [74–79] for recent progress in lattice QCD. It is also possible to extract them directly from experiment, see e.g. [80]. PDFs have been studied in detail using data gathered by the HERA collider [5, 6], and they are one of the central objects to be studied by the planned Electron Ion Collider (EIC) [7, 8].

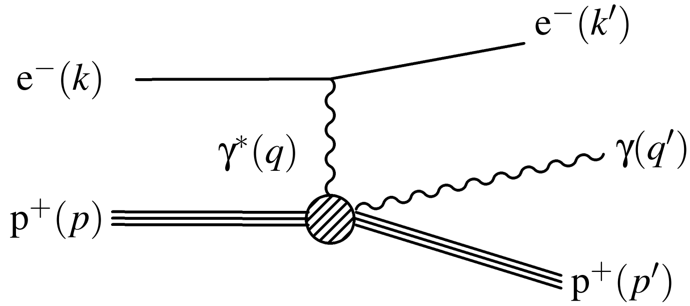

Figure 2.4: Sketch of the DVCS process, where the proton structure is probed by a high-energy virtual photon, which is accompanied by the production of a real photon. The diagram was drawn using FEYNMF *[46].*

Scale-dependence

Besides the PDFs themselves, it is also important to understand how changing the energy scale (say of the experiment) affects the PDFs. The PDF scale-dependence is neatly summarized in the well known DGLAP equation [81–83]

$$\frac{\mathrm{d}f_a(x,\mu^2)}{\mathrm{d}\ln\mu^2} = \int_x^1 \frac{dy}{y} P_{ab}(y) f_b\left(\frac{x}{y},\mu^2\right). \tag{2.23}$$

P_{ab} represent the QCD splitting functions. Because of the direct relation between PDFs and local spin-N operators, cf. Eq.(2.22), the scale-dependence of PDFs is related to the scale-dependence of the operators, the latter being determined by the operator anomalous dimension, cf. Eq.(1.93). For practical purposes we focus on the flavor non-singlet quark operators, cf. Eq.(1.115). The operator anomalous dimension enters the DGLAP equation through the splitting function. Specifically, the two quantities are related through a Mellin transformation

$$\gamma_{\mathrm{NS}}(N) = -\int_0^1 \mathrm{d}x\, x^{N-1} P_{\mathrm{NS}}(x). \tag{2.24}$$

The explicit calculation of operator anomalous dimensions will be discussed in detail in Chapter 4.

2.2 Deeply-virtual Compton scattering

2.2.1 Kinematics

As was the case for DIS, the DVCS process,

$$e\,p \to e\,p\,\gamma,$$

involves studying the structure of the proton by scattering a high-energy electron off it. However, different from DIS, we also take into account the production of a real photon γ. This implies that there has to be a non-zero momentum transfer to the target proton, see Fig.2.4. Another difference with DIS is that the nucleon survives the process, i.e. it is not broken apart.

Because of the non-zero momentum transfer, we need to introduce more invariants to fully describe DVCS. In total, four such invariants are needed:

- The Mandelstam variable t, which corresponds to the invariant momentum transfer

$$t = (p - p')^2, \tag{2.25}$$

- the photon virtuality, $Q^2 = -q^2$, which is again assumed to be large,
- the momentum-fraction x carried by the struck parton and
- the average hadron momentum

$$\chi = \frac{1}{2}(p + p'). \tag{2.26}$$

2.2.2 Cross-section

As before we assume the proton structure to be probed by the electromagnetic interaction, cf. Eq.(2.3). In the Bjorken limit, the DVCS cross-section also factorizes into a leptonic part and a hadronic one. As the expressions for the corresponding leptonic and hadronic tensors are considerably more complex than in the DIS case, and since we do not actually need their exact forms in the following, we do not quote them here. Instead, we refer the interested reader to [66]. Here we will just give a brief overview of some of the similarities and differences with the analysis of DIS.

- The hadronic tensor can again be written as a matrix element of a time-ordered product of electromagnetic currents

$$T_{\mu\nu} = i \int \mathrm{d}^4x \, e^{i(q+q')\cdot x} \left\langle p' \right| \mathcal{T} j_\mu(x) j_\nu(0) \left| p \right\rangle . \tag{2.27}$$

  Note that now the initial and final states do not have the same momentum, and that both the momentum of the virtual photon and of the real one (q') appear in the expression. As the same operator product appears as in DIS, the same spin-N operators, and their anomalous dimensions, have to be considered. The difference with DIS is that these now have to be considered in off-forward kinematics, i.e. between states of unequal momenta. This implies that also operators with external total derivatives can contribute.

- At the end of the calculation, the unpolarized Compton amplitude is written in terms of two off-forward distributions denoted by H and E, depending on the Dirac structure. These are the GPDs and can be interpreted as matrix elements of quark operators. Using lightcone coordinates, cf. Appendix A, we have [14, 66]

$$\begin{aligned} \int \frac{\mathrm{d}z^-}{2\pi} \mathrm{e}^{ix\chi^+ z^-} \left\langle p' \right| \overline{\psi}(-z/2)\gamma^+\psi(z/2) \left| p \right\rangle \sim & \; H(x,\chi,t)\overline{\psi}(p')\gamma^+\psi(p) \\ & + E(x,\chi,t)\overline{\psi}(p')\frac{i\sigma^{+\nu}\tilde{\Delta}_\nu}{2m_p}\psi(p) \\ & + \text{higher twist} \end{aligned} \tag{2.28}$$

  where as before we focus on the leading-twist contributions. The variable $\tilde{\Delta}$ is defined such that

$$t = \tilde{\Delta}^2. \tag{2.29}$$

Note that the operator appearing in Eq.(2.28) is non-local. It is always possible to relate such a non-local operator to local ones by means of a Taylor expansion,

$$O(x;z_1,z_2) = \sum_{m,k} \frac{z_1^m z_2^k}{m!\,k!} [\overline{\psi}(x)(\overleftarrow{D} \cdot n)^m \not{n} (n \cdot \overrightarrow{D})^k \psi(x)], \tag{2.30}$$

see e.g. [16]. Here n is an arbitrary light-like vector.

2.2.3 Properties of GPDs

While the standard PDFs only depend on one kinematic variable, namely x, the off-forward GPDs depend on three such variables, with the additional two being related to the non-zero momentum transfer. It can be shown that in the forward limit, where $p = p'$ (and assuming the initial- and final state protons to have the same helicity), the GPDs reduce to the forward distributions, e.g. $H(x,0,0) = f_q(x)$ for $x > 0$ [14]. Another difference between PDFs and GPDs is their interpretation. As diagonal (i.e. forward) matrix elements, PDFs have a simple probabilistic interpretation. However, since GPDs correspond to non-diagonal (non-forward) matrix elements, this no longer works. Instead, GPDs reflect the *interference* between nucleon amplitudes with different parton configurations. This implies that they form important probes for momentum correlations between partons in the proton [14, 84].

While the finite momentum transfer to the target is dominated by its longitudinal component, it is possible for a small transverse component to appear as well. Information about the transverse structure of the proton will then also be encoded in the GPDs. When combined with the longitudinal information, GPDs hence create the possibility for a *fully three-dimensional* description of proton (or more generally hadron) structure. See e.g. [85] for more details about this exciting application and [86] for an overview of recent progress.

Moments and local operators

Instead of considering the matrix elements themselves, it is also interesting to study the effect of integrating the GPDs over (powers of) x, i.e. calculating their Mellin moments. These moments turn out to be extremely valuable, as they are related to form factors of local quark operators. In the simplest case we just consider

$$\int_{-1}^{1} \mathrm{d}x\, H(x,\chi,t) \;\text{ and }\; \int_{-1}^{1} \mathrm{d}x\, E(x,\chi,t).$$

These are nothing more than the Dirac and Pauli form factors for the standard electromagnetic current

$$\int_{-1}^{1} \mathrm{d}x\, H(x,\chi,t) = F_1(t) \tag{2.31}$$

$$\int_{-1}^{1} \mathrm{d}x\, E(x,\chi,t) = F_2(t) \tag{2.32}$$

defined as

$$\langle p' | \overline{\psi}(0)\gamma^{\mu}\psi(0) | p\rangle = \bar{u}(p')\left[F_1(t)\gamma^{\mu} + F_2(t)\frac{i\sigma^{\mu\alpha}\tilde{\Delta}_{\alpha}}{2m_p}\right]u(p). \tag{2.33}$$

In the same fashion, the higher moments of GPDs are related to form factors of operators with additional covariant derivatives [14]. These are exactly the local spin-N, twist-two operators that also appeared in the analysis of DIS, cf. Eq.(2.12).

Scale-dependence

Like PDFs, GPDs are non-perturbative quantities, meaning that they have to be calculated on the lattice or extracted from experiments. But, as we have just seen, also GPDs are related to spin-N twist-two operators, which implies that their scale-dependence will once again be determined by the scale-dependence of the operators. For example, for the scale-dependence of the generalized distribution H we have

$$\frac{\mathrm{d}}{\mathrm{d}\ln\mu^2}H(x,\chi,t) = \frac{1}{|\chi|}\int_{-1}^{1}\mathrm{d}y\, V(x,y)H(y,\chi,t). \tag{2.34}$$

This is the so-called ERBL evolution equation [87–90]. The evolution kernel $V(x,y)$ is a generalization of the splitting function in the forward limit. As such, it can be related to a Mellin transform of operator anomalous dimensions [91]

$$\int_0^1 \mathrm{d}x\, x^N\, V(x,y) = -\sum_{k=0}^{N}\gamma_{N,k}\, y^k. \tag{2.35}$$

Here $\gamma_{N,k}$ denote the elements of the anomalous dimension matrix $\hat{\gamma}$. They represent the mixing into total derivative operators, which is relevant for off-forward kinematics. The renormalization of the spin-N operators and the extraction of the corresponding anomalous dimensions, both in forward and off-forward kinematics, will be discussed in detail in Chapter 4.

Chapter 3

Mathematical background

Introduction

Before continuing with our main discussion, we first give an overview of mathematical concepts and special functions which will be necessary in the coming chapters. The first section deals with special functions. Here we review the definitions and some properties of harmonic sums, the Euler-Gamma functions and Gegenbauer polynomials. After this, we introduce the binomial transform, which is a special type of transformation acting on sequences. Finally, we review useful concepts and algorithms for the evaluation of finite sums.

3.1 Special functions

3.1.1 Harmonic sums

Harmonic sums at argument N can be defined recursively as [92, 93]

$$\begin{aligned} S_{\pm m}(N) &= \sum_{i=1}^{N} \frac{(\pm 1)^i}{i^m}, \\ S_{\pm m_1,m_2,\ldots,m_d}(N) &= \sum_{i=1}^{N} \frac{(\pm 1)^i}{i^{m_1}} S_{m_2,\ldots,m_d}(i). \end{aligned} \tag{3.1}$$

An associated quantity is the *weight* w of harmonic sums, which is

$$w \equiv \sum_i |m_i|. \tag{3.2}$$

We will also use the concept of weight when dealing with denominators in N. Specifically, we associate a weight ω to denominators of the form

$$\frac{1}{(N+\alpha)^\omega} \quad (\alpha \in \mathbb{N}). \tag{3.3}$$

The harmonic numbers, $S_1(N)$, are known to diverge in the limit of large N. We have

$$S_1(N) \xrightarrow[N\to\infty]{} \ln N + \gamma_E + O\left(\frac{1}{N}\right) \tag{3.4}$$

with γ_E the Euler-Mascheroni constant, $\gamma_E \approx 0.577$. The higher-weight harmonic sums are finite in the limit of large N and correspond to the Riemann-zeta function

$$\zeta_n = \sum_{i=1}^{\infty} \frac{1}{i^n}. \tag{3.5}$$

3.1.2 Euler-Gamma and polygamma functions

The Euler-Gamma function $\Gamma(z)$ can be considered to be the analytical continuation of the factorial to complex numbers. It obeys [94]

$$z\Gamma(z) = \Gamma(z+1) \tag{3.6}$$

and has isolated poles for $z \in \mathbb{Z}^-$. As such, we can define an analytic continuation of binomial coefficients as follows

$$\binom{N}{r} = \frac{\Gamma(N+1)}{\Gamma(r+1)\Gamma(N-r+1)}. \tag{3.7}$$

The Gamma function also has an integral representation,

$$\Gamma(z) = \int_0^{\infty} \mathrm{d}x\, x^{z-1} e^{-x}, \tag{3.8}$$

which is valid for $\mathrm{Re}(z) > 0$. When the argument is a half-integer number, the Gamma function obeys

$$\Gamma\left(N + \frac{1}{2}\right) = \frac{(2N)!}{4^N N!}\sqrt{\pi} \ \ (n \in \mathbb{N}). \tag{3.9}$$

Important associated functions are the *polygamma functions*, which are the logarithmic derivatives of the Gamma function

$$\psi^{(m)} \equiv \frac{\mathrm{d}^{m+1}}{\mathrm{d}z^{m+1}} \ln \Gamma(z). \tag{3.10}$$

When the polygamma functions are evaluated in an argument $N \in \mathbb{N}_0$, they are related to the harmonic sums. We have

$$\psi^{(0)}(N) = -\gamma_E + S_1(N-1) \tag{3.11}$$

and

$$\psi^{(m)}(N) = (-1)^m m! \left[\zeta_{m+1} - S_{m+1}(N-1)\right] \ \ (m > 0). \tag{3.12}$$

The Gamma function often shows up in QFT calculations. This is because, when calculating loop integrals in dimensional regularization, it is a natural object to appear. For example, in D dimensions, the area of the unit-sphere is

$$\int \Omega_D = \frac{2\pi^{D/2}}{\Gamma(D/2)}. \tag{3.13}$$

In dimensional regularization, the poles as $\varepsilon \to 0$ are usually incorporated in the appearing Gamma functions. A typical example of this is

$$\int \frac{\mathrm{d}^D k}{(2\pi)^D} \frac{1}{k^2 + \tilde{\Delta}^2} = \frac{1}{(4\pi)^{D/2}} \frac{\Gamma(2 - D/2)}{\Gamma(2)} \left(\frac{1}{\tilde{\Delta}}\right)^{2-D/2} \tag{3.14}$$

which is singular for $D \to 4$. Hence we need to know how the Gamma function behaves near $z = 0$. We have

$$\Gamma(\varepsilon) = \frac{1}{\varepsilon} - \gamma_E + O(\varepsilon). \tag{3.15}$$

3.1.3 Gegenbauer polynomials

Gegenbauer polynomials can be defined in terms of the hypergeometric function ${}_2F_1$ as [94]

$$C_N^{\nu}(z) = \frac{(2\nu)_N}{N!}{}_2F_1\left(-N, N+2\nu; \nu+\frac{1}{2}; \frac{1}{2}-\frac{z}{2}\right) \tag{3.16}$$

with

$$(x)_N \equiv x(x-1)\dots(x-N+1) \tag{3.17}$$

the rising factorial or Pochhammer symbol. Recall that the generalized hypergeometric function is defined as

$${}_mF_n(a_1,\dots,a_m;b_1,\dots,b_n;z) = \sum_{i=0}^{\infty}\frac{(a_1)_i\dots(a_m)_i}{(b_1)_i\dots(b_n)_i}\frac{z^i}{i!}. \tag{3.18}$$

In the case of a negative first argument, as in Eq.(3.16), the series does not go all the way to infinity. Instead we have

$${}_2F_1(-N,m;a,z) = \sum_{i=0}^{N}(-1)^i\binom{N}{i}\frac{(m)_i}{(a)_i}z^i. \tag{3.19}$$

This then allows one to write down a series representation of the Gegenbauer polynomials in terms of the Gamma function

$$C_N^{\nu}(z) = \frac{\Gamma(\nu+1/2)}{\Gamma(2\nu)}\sum_{l=0}^{N}(-1)^l\frac{\Gamma(2\nu+N+l)}{l!\,(N-l)!\,\Gamma(\nu+1/2+l)}\left(\frac{1}{2}-\frac{z}{2}\right)^l. \tag{3.20}$$

In a QFT context, they appear naturally when analyzing composite operators in the presence of conformal symmetry. Particularly important are then the Gegenbauer polynomial with $\nu = 3/2$, relevant for the description of quark operators

$$C_N^{3/2}(z) = \frac{1}{2N!}\sum_{l=0}^{N}(-1)^l\binom{N}{l}\frac{(N+l+2)!}{(l+1)!}\left(\frac{1}{2}-\frac{z}{2}\right)^l \tag{3.21}$$

and the one with $\nu = 5/2$ for the description of gluon operators

$$C_N^{5/2}(z) = \frac{1}{12N!}\sum_{l=0}^{N}(-1)^l\binom{N}{l}\frac{(N+l+4)!}{(l+2)!}\left(\frac{1}{2}-\frac{1}{2}z\right)^l. \tag{3.22}$$

3.2 The binomial transform

Suppose we have some sequence $\{a_k\}$. Its *binomial transform* b_N is then defined as [95]

$$b_N \equiv \sum_{k=0}^{N}\binom{N}{k}a_k. \tag{3.23}$$

The inverse transformation is

$$a_N = \sum_{k=0}^{N} (-1)^{N-k} \binom{N}{k} b_k. \tag{3.24}$$

To see this, we can substitute Eq.(3.23) into Eq.(3.24)

$$\sum_{k=0}^{N} (-1)^{N-k} \binom{N}{k} b_k = \sum_{k=0}^{N} (-1)^{N-k} \binom{N}{k} \sum_{j=0}^{k} \binom{k}{j} a_j. \tag{3.25}$$

Next we change the order of summation in the right-hand side

$$\sum_{k=0}^{N} (-1)^{N-k} \binom{N}{k} b_k = \sum_{j=0}^{N} (-1)^{N} \binom{N}{j} a_j \sum_{k=j}^{N} (-1)^{k} \binom{N-j}{k-j} \tag{3.26}$$

in which we used the identity

$$\binom{N}{l}\binom{l}{k} = \binom{N}{k}\binom{N-k}{l-k}. \tag{3.27}$$

Changing now the summation indices $k \to k-j$ and $j \to N-j$ we find

$$\sum_{k=0}^{N} (-1)^{N-k} \binom{N}{k} b_k = \sum_{j=0}^{N} (-1)^{j} \binom{N}{j} a_{N-j} \sum_{k=0}^{j} (-1)^{k} \binom{j}{k}. \tag{3.28}$$

Finally using that

$$\sum_{k=0}^{j} (-1)^{k} \binom{j}{k} = \delta_{j,0} \tag{3.29}$$

we obtain the required result. ■

The so-called *symmetric binomial transform* is also quite common. It is defined as

$$b_N \equiv \sum_{k=0}^{N} (-1)^{k} \binom{N}{k} a_k \tag{3.30}$$

with inversion

$$a_N = \sum_{k=0}^{N} (-1)^{k} \binom{N}{k} b_k. \tag{3.31}$$

A variant with $k \to k-1$ is also used sometimes. These equations imply that the (symmetric) binomial transform is a type of *conjugation*; applying the transformation twice is equivalent to the identity transformation. The binomial transform is also closely connected to the finite difference operator $\Delta a_N \equiv a_{N+1} - a_N$. We have

$$(-1)^N \Delta^N a_0 = \sum_{k=0}^{N} (-1)^{k} \binom{N}{k} a_k. \tag{3.32}$$

This can be easily shown by induction. The base case $N = 0$ trivially gives $a_0 = a_0$. Let us then assume that Eq.(3.32) is true for some $N \in \mathbb{N}$. For $N+1$ the left-hand side is

$$\Delta^{N+1} a_0 = \Delta(\Delta^N a_0) = \sum_{k=0}^{N} (-1)^{N-k} \binom{N}{k} (a_{k+1} - a_k). \tag{3.33}$$

The right-hand side is

$$\sum_{k=0}^{N+1}(-1)^{N+1-k}\binom{N+1}{k}a_k. \tag{3.34}$$

Using the identity

$$\binom{N}{k}=\binom{N-1}{k}+\binom{N-1}{k-1} \tag{3.35}$$

we can rewrite this as

$$\sum_{k=0}^{N+1}(-1)^{N+1-k}\binom{N}{k}a_k+\sum_{k=0}^{N+1}(-1)^{N+1-k}\binom{N}{k-1}a_k. \tag{3.36}$$

Next we shift the summation index in the second sum by one, giving

$$\sum_{k=0}^{N+1}(-1)^{N+1-k}\binom{N}{k}a_k+\sum_{k=-1}^{N}(-1)^{N-k}\binom{N}{k}a_{k+1}. \tag{3.37}$$

Noting now that the first sum vanishes for $k=N+1$ and the second one for $k=-1$ this reduces to

$$\sum_{k=0}^{N}(-1)^{N-k}\binom{N}{k}(a_{k+1}-a_k). \tag{3.38}$$

This concludes the proof. ■

Sequences with the property

$$\sum_{k=0}^{N}(-1)^{k}\binom{N}{k}a_k=a_N \tag{3.39}$$

are called *invariant* or *self-conjugate* sequences. For example, using the symmetric binomial transform with the sign factor $(-1)^{k+1}$, the sequence $\left\{\frac{S_1(N)}{(N+1)}\right\}$ is self-conjugate.

Assume we have some polynomial $f(x)$ of maximal degree N. Then the binomial transform of

$$\frac{f(x-k)}{y+k}\ \ (y\neq-\mathbb{N}) \tag{3.40}$$

can be calculated using *Melzak's formula* [96, 97]

$$\sum_{k=0}^{N}(-1)^{k}\binom{N}{k}\frac{f(x-k)}{y+k}=\frac{N!\,f(x+y)}{y(y+1)\dots(y+N)}. \tag{3.41}$$

For example, if $f(x)=1$ we find

$$\sum_{k=0}^{N}(-1)^{k}\binom{N}{k}\frac{1}{y+k}=\frac{1}{y}\binom{N+y}{y}^{-1}. \tag{3.42}$$

The binomial transform also has interesting properties for division by the discrete variable. Assuming $\{b_N\}$ is the transform of $\{a_N\}$ we have [95]

$$\sum_{k=1}^{N} \binom{N}{k} \frac{a_k}{k+\lambda} = \sum_{m=1}^{N} \frac{(m+1)(m+2)\dots N}{(\lambda+m)(\lambda+m+1)\dots(\lambda+N)} b_m. \tag{3.43}$$

For $\lambda = 0,1$ this reduces to

$$\sum_{k=1}^{N} \binom{N}{k} \frac{a_k}{k} = \sum_{m=1}^{N} \frac{b_m}{m} \tag{3.44}$$

and

$$\sum_{k=1}^{N} \binom{N}{k} \frac{a_k}{k+1} = \frac{1}{N+1} \sum_{m=1}^{N} b_m. \tag{3.45}$$

This can be directly related to binomial transforms involving harmonic sums. Starting from

$$\sum_{k=1}^{N} (-1)^{k-1} \binom{N}{k} = 1 \tag{3.46}$$

and applying Eq.(3.44) we find

$$\sum_{k=1}^{N} (-1)^{k-1} \binom{N}{k} \frac{1}{k} = S_1(N). \tag{3.47}$$

In turn, a second application of Eq.(3.44) leads to

$$\sum_{k=1}^{N} (-1)^{k-1} \binom{N}{k} \frac{1}{k^2} = S_{1,1}(N). \tag{3.48}$$

Eqs.(3.43) and (3.47) can be combined to obtain the following general expression

$$\sum_{k=1}^{N} (-1)^{k-1} \binom{N}{k} \frac{S_1(k)}{k+\lambda} = \sum_{m=1}^{N} \frac{(m+1)(m+2)\dots N}{(\lambda+m)(\lambda+m+1)\dots(\lambda+N)m}. \tag{3.49}$$

We can also consider multiplication with the discrete variable, which obeys [95]

$$\sum_{k=0}^{N} \binom{N}{k} k^p a_k = (N\nabla)^p b_N \;\; (p \in \mathbb{N} \text{ and } N \geq p) \tag{3.50}$$

with ∇ the *backward difference operator*

$$\nabla a_k \equiv a_k - a_{k-1}. \tag{3.51}$$

Finally, we consider the binomial transform of the product of two sequences. Assume we have two sequences $\{a_N\}$ and $\{c_N\}$ with binomial transforms $\{b_N\}$ and $\{d_N\}$ respectively. Then the following identity holds [95]

$$\sum_{k=0}^{N} \binom{N}{k} a_k c_k = \sum_{m=0}^{N} \binom{N}{m} d_m \nabla^m b_N. \tag{3.52}$$

A useful consequence involving harmonic numbers is

$$\sum_{k=0}^{N}(-1)^{k-1}\binom{N}{k}S_1(k)c_k = (-1)^{N-1}S_1(N)d_N + \sum_{m=0}^{N-1}\frac{(-1)^m d_m}{N-m}. \tag{3.53}$$

More relations involving binomial transforms can be found in [95] and in Appendices E and F of [92].

3.3 Evaluating finite sums

The problem of evaluating finite sums will show up frequently in the course of this text. This section gives an overview of some important concepts which will be useful. After briefly reviewing the telescoping and creative telescoping algorithms, we comment on the use of the MATHEMATICA package SIGMA [98, 99] to evaluate complicated sums. In the final section of this chapter we discuss the evaluation of some single and double sums which will appear in later chapters.

3.3.1 Telescoping algorithms

The telescoping algorithm is a well-known method for evaluating finite sums. Suppose we want to evaluate the following sum

$$\sum_{k=a}^{N} f(k) \tag{3.54}$$

with $a, N \in \mathbb{N}$ and $a \leq N$. Now, if we can find a function $g(N)$ such that

$$f(k) = \Delta g(k) \equiv g(k+1) - g(k) \tag{3.55}$$

then

$$\begin{aligned}\sum_{k=a}^{N} f(k) &= \sum_{k=a}^{N} g(k+1) - \sum_{k=a}^{N} g(k) \\ &= g(N+1) - g(a).\end{aligned} \tag{3.56}$$

The finite difference operator Δ is similar to the derivative operator in continuum calculus. As such, the telescoping algorithm can be considered to be the discrete version of the fundamental theorem of calculus,

$$g = \mathrm{D}f \equiv \frac{\mathrm{d}}{\mathrm{d}x}f \Rightarrow \int_a^b \mathrm{d}x\, g(x) = f(b) - f(a). \tag{3.57}$$

The telescoping function $g(N)$ in Eq.(3.55) can be found by application of *Gosper's algorithm* [100], which is applicable if

$$\frac{g(N)}{g(N-1)} \tag{3.58}$$

is a rational function of N. The algorithm consists of three main steps. Say we want to calculate the telescoping function for some sequence $\{a_N\}$

$$a_N = \Delta b(N). \tag{3.59}$$

It is assumed that $\{a_N\}$ is a *hypergeometric sequence*, that is

$$\frac{a_{N+1}}{a_N} = q(N) \tag{3.60}$$

with $q(N)$ a rational function of N. The steps of Gosper's algorithm can then be summarized as follows

1. Determine three functions $f(x), g(x)$ and $h(x)$ such that

$$q(x) = \frac{f(x+1)}{f(x)} \frac{g(x)}{h(x+1)} \tag{3.61}$$

   and

$$\gcd[g(x), h(x+n)] = 1 \ \ (n \in \mathbb{N}_0). \tag{3.62}$$

2. Solve the so-called Gosper equation,

$$f(x) = g(x)y(x+1) - h(x)y(x), \tag{3.63}$$

   for the polynomial $y(x)$.

3. If such a polynomial solution does not exist, it means that the sum in question does not have a hypergeometric closed form. Otherwise, the telescoping function is determined by

$$t(x) = \frac{h(x)}{f(x)} y(x) \tag{3.64}$$

   where we introduced $t(x)$ via

$$b(N) = t(N)a(N). \tag{3.65}$$

More details can e.g. be found in [101].

Classical telescoping works when dealing with sequences that depend on one variable only. When we want to determine a closed form for a summation of a sequence depending on two variables, we can use the *creative telescoping algorithm* by Zeilberger [102]. The idea is similar to that of classical telescoping. Suppose we want to calculate a closed form expression for the summation

$$\sum_{k=a}^{b} f(N,k) \equiv S(N). \tag{3.66}$$

The way to go about this is by attempting to find functions $c_0(N), \dots, c_d(N)$ and a function $g(N,k)$ such that

$$g(N,k+1) - g(N,k) = c_0(N) f(N,k) + ... + c_d(N) f(N+d,k). \tag{3.67}$$

Summing both sides, and applying classical telescoping to the left-hand side, then gives

$$g(N,b+1) - g(N,a) = c_0(N) \sum_{k=a}^{b} f(N,k) + ... + c_d(N) \sum_{k=a}^{b} f(N+d,k). \tag{3.68}$$

This leads to an inhomogeneous recursion relation for the original sum of the form

$$q(N) = c_0(N)S(N) + ... + c_d(N)S(N+d). \tag{3.69}$$

Typically, one starts this procedure at $d = 0$, which is equivalent to classical telescoping. The value of d is then increased stepwise until a solution to Eq.(3.68) is found. The creative telescoping algorithm can be applied when the sequence under consideration is *holonomic*. A sequence $\{a_N\}$ is said to be holonomic if there exist polynomials $p_0(x), \ldots, p_r(x)$ such that the following recursion relation is obeyed [101]

$$p_0(N)a_N + p_1(N)a_{N+1} + \cdots + p_r(N)a_{N+r} = 0 \quad (N \in \mathbb{N}, p_r(N) \neq 0). \tag{3.70}$$

For example, the harmonic numbers $\{S_1(N)\}$ form a holonomic sequence since

$$(N+1)S_1(N) - (2N+3)S_1(N+1) + (N+2)S_1(N+2) = 0. \tag{3.71}$$

More details on the summation algorithms reviewed here can e.g. be found in the excellent books [103, 104].

3.3.2 Evaluating sums using SIGMA

The types of sums that will have to be evaluated throughout this text can be dealt with using the MATHEMATICA package SIGMA [98, 99]. The workflow followed by SIGMA can be summarized as follows

- When given a sum to evaluate, SIGMA will generate a recurrence for it using (creative) telescoping, which it subsequently solves.
- In general, the obtained recurrences are inhomogeneous. The corresponding solution is then the set of solutions for the homogeneous recurrence, supplemented by a particular solution.
- For the final closed-form expression of the summation problem at hand, SIGMA determines that particular linear combination of the recurrence solutions that has the same initial values as the given sum.

Let us see how this works in practice. In Chapter 4, a type of sum we will be interested in is

$$\sum_{j=0}^{N-k} (-1)^j \binom{N-k}{j} f(j+k). \tag{3.72}$$

Here the function f contains harmonic sums and denominators in its arguments. In this example we take

$$f(N) = \frac{S_1(N+1)}{N+1}. \tag{3.73}$$

To simplify the input for SIGMA , we define

$$Nk \equiv N - k. \tag{3.74}$$

First, we feed the sum to SIGMA using the SIGMASUM function. SIGMA also has built-in functions for powers and binomials, namely SIGMAPOWER and SIGMABINOMIAL.

in[1] := **sum = SigmaSum[SigmaPower[-1,j]*SigmaBinomial[Nk,j]S[1,k+j+1]/(k+j+1),{j,0,Nk}]**

out[1] := $\sum_{j=0}^{\mathrm{Nk}} \frac{\binom{\mathrm{Nk}}{j} (-1)^{j} \left(\frac{1}{1+j+k}+S[1,j+k]\right)}{1+j+k}$

Next, we generate the corresponding recurrence using GENERATERE. The input required here is the quantity for which we want to generate the recurrence, and the quantity in terms of which the recurrence should be written.

in[2] := **rec = GenerateRE[sum,Nk]**

out[2] := $\{(1+\mathrm{Nk})^2\mathrm{SUM}[\mathrm{Nk}]+\left(-8-3k-8\mathrm{Nk}-2k\mathrm{Nk}-2\mathrm{Nk}^2\right)\mathrm{SUM}[1+\mathrm{Nk}]+(3+k+\mathrm{Nk})^2\mathrm{SUM}[2+\mathrm{Nk}]==0\}$

We see that in this particular case, we find a homogeneous recurrence of second order. Next we solve the recurrence using SOLVERECURRENCE. To simplify the output, we also use TOSPECIALFUNCTION to transform products to factorials and Pochhammer symbols.

in[3] := **solrec = SolveRecurrence[rec[[1]],SUM[Nk]]//ToSpecialFunction**

out[3] := $\left\{\left\{0,\frac{\mathrm{Nk}!}{(2+k)_{\mathrm{Nk}}}\right\},\left\{0,\frac{\mathrm{Nk}!\left(\frac{\sum_{\iota_1=1}^{\mathrm{Nk}}\frac{1}{\iota_1}}{-1-k}-\frac{\sum_{\iota_1=1}^{\mathrm{Nk}}\frac{1}{1+k+\iota_1}}{-1-k}\right)}{(2+k)_{\mathrm{Nk}}}\right\},\{1,0\}\right\}$

Finally, we need to determine the appropriate linear combination of the solutions of the recurrence. This is done using FINDLINEARCOMBINATION.

in[4] := **sol = FindLinearCombination[solrec,sum,2]//ToSpecialFunction**

out[4] := $\frac{\mathrm{Nk}!}{(1+k)^2(2+k)_{\mathrm{Nk}}}+\frac{\mathrm{Nk}!\left(\sum_{\iota_1=1}^{\mathrm{Nk}}\frac{1}{\iota_1}\right)}{(-1-k)(2+k)_{\mathrm{Nk}}}-\frac{\mathrm{Nk}!\left(\sum_{\iota_1=1}^{\mathrm{Nk}}\frac{1}{1+k+\iota_1}\right)}{(-1-k)(2+k)_{\mathrm{Nk}}}+\frac{\mathrm{Nk}!\,S[1,k]}{(1+k)(2+k)_{\mathrm{Nk}}}$

The output can be simplified further using SIGMAREDUCE, and the remaining sums can be expressed in terms of harmonic numbers using the TOWER command. This leads to

in[5] := **Sol = SigmaReduce[sol,Nk,Tower→{S[1,Nk],S[1,Nk+k]}]/.Nk→N-k**

out[5] := $\frac{(-k+N)!\left(\frac{1}{(1+k)(1+N)}-\frac{S[1,N]}{-1-k}+\frac{S[1,-k+N]}{-1-k}\right)}{(2+k)_{-k+N}}$

Hence, we find that

$$\sum_{j=0}^{N-k}(-1)^j\binom{N-k}{j}\frac{S_1(j+k+1)}{j+k+1}=\frac{(N-k)!}{(k+1)(k+2)_{N-k}}\left(\frac{1}{N+1}-S_1(N-k)+S_1(N)\right). \quad (3.75)$$

3.3.3 Explicit single and double sums

In this section we discuss some explicit single and double sums that will be useful to us throughout this work.

Single sums

As discussed above, the binomial transforms of some simple functions are

$$\sum_{j=0}^{N}(-1)^j\binom{N}{j} = \delta_{N,0} \tag{3.76}$$

$$\sum_{j=0}^{N}(-1)^j\binom{N}{j}\frac{1}{m+j} = \frac{1}{m}\binom{N+m}{m}^{-1} \tag{3.77}$$

$$\sum_{j=0}^{N}(-1)^j\binom{N}{j}S_1(m+j) = -\frac{1}{N}\binom{N+m}{N}^{-1} \tag{3.78}$$

$$\sum_{j=0}^{N}(-1)^j\binom{N}{j}\frac{1}{(m+j)^2} = \frac{1}{m}\binom{N+m}{N}^{-1}[S_1(N+m)-S_1(m-1)] \tag{3.79}$$

$$\sum_{j=0}^{N}(-1)^j\binom{N}{j}S_2(m+j) = -\frac{1}{N}\binom{N+m}{N}^{-1}[S_1(N+m)-S_1(m)], \tag{3.80}$$

see also [95] and appendix F of [92]. Binomial transforms of higher powers of $1/(m+j)$ can be calculated using differentiation. For example, differentiating both sides of Eq.(3.79) with respect to m we find

$$\begin{aligned}&\sum_{j=0}^{N}(-1)^j\binom{N}{j}\frac{1}{(j+m)^3}\\ &= \frac{1}{2m}\binom{N+m}{N}^{-1}\Big(S_2(m+N)-S_2(m+1)+[S_1(m-1)-S_1(m+N)]^2\Big).\end{aligned} \tag{3.81}$$

Binomial transforms of the form $\frac{S_1(N)}{N+m}$ ($m \in \mathbb{N}^+$) can be evaluated using

$$\sum_{j=0}^{N}(-1)^j\binom{N}{j}\frac{S_1(m+j)}{m+j} = \frac{1}{m}\binom{N+m}{N}^{-1}[S_1(N+m)-S_1(N)]. \tag{3.82}$$

To apply this formula, we need to *synchronize* the harmonic sums, meaning that its argument should match the denominator. For example

$$\sum_{j=0}^{N}(-1)^j\binom{N}{j}\frac{S_1(m+j)}{m+j+1} \to \sum_{j=0}^{N}(-1)^j\binom{N}{j}\left(\frac{S_1(m+j+1)}{m+j+1}-\frac{1}{(m+j+1)^2}\right). \tag{3.83}$$

Note that the second sum is just of the type (3.79).

Double sums

In Chapter 4 and beyond, we will be interested in double sums of the form

$$\sum_{j=k}^{N}(-1)^k\binom{j}{k}\sum_{l=j+1}^{N}(-1)^l\binom{N}{l}f(l,j). \tag{3.84}$$

Here $f(l,j)$ represents a function consisting of harmonic sums and denominators in its arguments. Generally, these sums can simply be computed using SIGMA . However, in certain cases the result of the inner sum is already quite complicated, such that the full double sum becomes non-trivial. In such cases, it is advisable to take a closer look at the structure of the summand $f(l,j)$ to see whether simplifications can be made. For example, consider functions of the form

$$f(l,j)=\frac{g(l,j)}{(l-j)^m}\ \ (m\in\mathbb{N}_0 \text{ and } l\neq j). \tag{3.85}$$

$g(l,j)$ is either one or some (product of) harmonic sum(s) with unshifted argument(s)[1]. To evaluate the sum Eq.(3.84) for such a function, we note that this function class closes on itself. By this we mean that, after evaluating the double sum, we do not expect the appearance of shifted denominators. Furthermore, the weight of the result is limited by the weight of the summand. Hence, the number of structures that can appear in the final answers is limited, and we can simply calculate the sum for fixed (N,k)-values and then make a fit using an appropriate basis. This basis is simply the set of functions of type Eq.(3.85), up to the appropriate weight. Let us, as an example, consider the case

$$f(l,j)=\frac{S_1(l-j)}{(l-j)^2}. \tag{3.86}$$

The inner sum is then

$$\sum_{l=j+1}^{N}(-1)^l\binom{N}{l}\frac{S_1(l-j)}{(l-j)^2}\equiv S(N,j). \tag{3.87}$$

To feed this sum to SIGMA , we get rid of the j in the lower limit by shifting $l\to l-j-1$ such that

$$S(N,j)=\sum_{l=0}^{N'}(-1)^{N'+j+1-l}\binom{N'+j+1}{l}\frac{S_1(N'-l+1)}{(N'-l+1)^2}. \tag{3.88}$$

We have defined

$$N'\equiv N-j-1 \tag{3.89}$$

and introduced an additional shift, $l\to N'-l$. The SIGMA result is a complicated expression, including terms such as

$$\sum_{i=1}^{N'}\frac{S_1(i+j)^2}{i}, \tag{3.90}$$

which cannot be simplified further. Instead, if we apply the fitting method described above, we quickly find

$$\sum_{j=k}^{N}(-1)^k\binom{j}{k}\sum_{l=j+1}^{N}(-1)^l\binom{N}{l}\frac{S_1(l-j)}{(l-j)^2}=-\frac{S_2(N-k)}{N-k}. \tag{3.91}$$

[1]By shifted arguments or denominators, we mean arguments or denominators of the type $N+m$ or $k+m$ with $m\in\mathbb{N}_0$.

The basis used to obtain this result was

$$\left\{\frac{S_1(N)}{(N-k)^2}, \frac{S_1(k)}{(N-k)^2}, \frac{S_1(N)^2}{N-k}, \frac{S_1(k)^2}{N-k}, \frac{S_2(N)}{N-k}, \frac{S_2(k)}{N-k}, \frac{S_1(N)S_1(k)}{N-k},\right.$$
$$\frac{S_1(N)}{N-k}, \frac{S_1(k)}{N-k}, \frac{S_1(N-k)}{(N-k)^2}, \frac{S_1(N-k)^2}{(N-k)}, \frac{S_2(N-k)}{(N-k)}, \frac{1}{(N-k)^3}, \tag{3.92}$$
$$\left.\frac{S_1(N-k)}{(N-k)}, \frac{1}{(N-k)^2}, \frac{1}{N-k}\right\}.$$

Another nice application is obtained by choosing

$$f(l,j) = \frac{1}{(l-j)^m} \ \ (m>0). \tag{3.93}$$

The fitting method allows us to derive the following all-m expression

$$\sum_{j=k}^{N}(-1)^k\binom{j}{k}\sum_{l=j+1}^{N}(-1)^l\binom{N}{l}\frac{1}{(l-j)^m} = -\frac{S_{1^m}(N-k)}{N-k} \tag{3.94}$$

with

$$S_{1^m}(N-k) \equiv S_{\underbrace{1,1,\ldots,1}_{m-1}}(N-k) \tag{3.95}$$

and $S_{1^1}(N-k) \equiv 1$.

The fitting method seems to fail however for the following two sums we encounter in Chapter 5

$$\sum_{j=k}^{N}(-1)^k\binom{j}{k}\sum_{l=j+1}^{N}(-1)^l\binom{N}{l}\frac{S_1(l)}{(l-j)^2} \tag{3.96}$$

and

$$\sum_{j=k}^{N}(-1)^k\binom{j}{k}\sum_{l=j+1}^{N}(-1)^l\binom{N}{l}\frac{S_1(j)}{(l-j)^2}. \tag{3.97}$$

Let us consider the sum in Eq.(3.97) in some detail. Because of the appearance of $S_1(j)$, it is simpler to first consider the inner sum over l, i.e.

$$\sum_{l=j+1}^{N}(-1)^l\binom{N}{l}\frac{1}{(l-j)^2}. \tag{3.98}$$

This can be calculated using the standard SIGMA methods. While not giving the full result here, we note that it includes

$$\sum_{i=1}^{N_j}\frac{S_1(i+j)}{i}, \ \ N_j \equiv N-j-1 \tag{3.99}$$

for which no closed form is known. This implies that the final result of the full double sum will include terms proportional to

$$\sum_{j=k}^{N}(-1)^k\binom{j}{k}\sum_{i=1}^{N_j}\frac{S_1(i+j)}{i}, \tag{3.100}$$

which explains why the fitting method did not work in this case[2]. We can now try to continue calculating the outer sum using SIGMA . Unfortunately, this does not work, as SIGMA is not able to find a recursion when terms such as the one in Eq.(3.99) appear. So, we need to find a different method for evaluating Eq.(3.97).

To gain some more insight into the problem, we consider the summation for fixed values of k while leaving N arbitrary:

k	$\sum_{j=k}^{N}(-1)^k\binom{j}{k}\sum_{l=j+1}^{N}(-1)^l\binom{N}{l}\frac{S_1(j)}{(l-j)^2}$
$N-1$	$0-S_1(N-1)$
$N-2$	$1-\frac{3}{4}S_1(N-2)$
$N-3$	$\frac{5}{4}-\frac{11}{18}S_1(N-3)$
$N-4$	$\frac{95}{72}-\frac{25}{48}S_1(N-4)$
$N-5$	$\frac{191}{144}-\frac{137}{300}S_1(N-5)$
$N-6$	$\frac{28259}{21600}-\frac{49}{120}S_1(N-6)$

It is clear that the harmonic number corresponds to $S_1(k)$. Maybe less clear but easy to check is that its coefficient corresponds to $-\frac{S_1(N-k)}{N-k}$. So we have

$$\sum_{j=k}^{N}(-1)^k\binom{j}{k}\sum_{l=j+1}^{N}(-1)^l\binom{N}{l}\frac{S_1(j)}{(l-j)^2}=F(N,k)-\frac{S_1(k)S_1(N-k)}{N-k} \tag{3.101}$$

for some unknown function $F(N,k)$ of N and k. We expect F to only depend on one argument, namely $N-k$, i.e.

$$\sum_{j=k}^{N}(-1)^k\binom{j}{k}\sum_{l=j+1}^{N}(-1)^l\binom{N}{l}\frac{S_1(j)}{(l-j)^2}=F(N-k)-\frac{S_1(k)S_1(N-k)}{N-k}. \tag{3.102}$$

Let us then consider the simpler case of $k=0$,

$$\sum_{j=0}^{N}\sum_{l=j+1}^{N}(-1)^l\binom{N}{l}\frac{S_1(j)}{(l-j)^2}=F(N). \tag{3.103}$$

[2]Note that we have encountered a similar non-reducible sum, Eq.(3.90), when trying to calculate the sum in Eq.(3.87). However, as this non-reducible sum drops out in the final result, the fitting method works. Hence, the break-down of this method points to the non-cancellation of such non-reducible sums.

While the inner sum is still the same, the outer one is much easier to handle and can be calculated with SIGMA , up to one small caveat. During the calculation, one encounters terms of the form

$$A \equiv \sum_{j=0}^{N} \frac{g_1(N,j)}{N-j} \tag{3.104}$$

and

$$B \equiv \sum_{j=0}^{N} \frac{g_2(N,j)}{j(N-j)} \tag{3.105}$$

for some functions g_1 and g_2. While the poles at $j=0$ and $j=N$ are known to be spurious, SIGMA does not seem to interpret them as such and gives an "Infinite expression $\frac{1}{0}$ encountered" error. This is easily fixed by changing the summation limits as to exclude the spurious poles, and then re-adding the (finite) limits,

$$\begin{aligned} A &= \sum_{j=0}^{N-1} \frac{g_1(N,j)}{N-j} + \lim_{j\to N}\Big[\frac{g_1(N,j)}{N-j}\Big] \\ B &= \sum_{j=1}^{N-1} \frac{g_2(N,j)}{j(N-j)} + \lim_{j\to 0}\Big[\frac{g_2(N,j)}{j(N-j)}\Big] + \lim_{j\to N}\Big[\frac{g_2(N,j)}{j(N-j)}\Big]. \end{aligned} \tag{3.106}$$

Finally we have all we need to calculate Eq.(3.103). The result is

$$\begin{aligned} F(N) =& \frac{1}{N^3}[-4-2(-1)^N] + \frac{1}{N^2}[2-2(-1)^N S_1(N) - S_1(N)] \\ &+ \frac{1}{N}[-(-1)^N S_1(N)^2 + 2S_{-2}(N) - S_1(N) + S_1(N)^2 + S_2(N)] \\ &+ (-1)^N S_1(N)^2 + S_{-3}(N) + 2S_{-2,1}(N) - S_{2,1}(N) + 4S_3(N) \\ &- N\sum_{j=0}^{N}(-1)^j \binom{N-1}{j} \frac{S_1(j)}{N-j} \sum_{i=1}^{N-j-1} \frac{S_1(j+i)}{i+1}. \end{aligned} \tag{3.107}$$

Remember that the expression for $F(N)$ is valid for $k=0$, and originates from $F(N-k)$. Hence, in order to calculate the full double sum in Eq.(3.97) we started with, all we have to do is take the expression for $F(N)$ we just calculated, replace N by $N-k$ and substitute back into Eq.(3.102). This finally leads to

$$\begin{aligned} &\sum_{j=k}^{N}(-1)^k\binom{j}{k}\sum_{l=j+1}^{N}(-1)^l\binom{N}{l}\frac{S_1(j)}{(l-j)^2} = \frac{1}{(N-k)^3}[-4-2(-1)^{N-k}] + \frac{1}{(N-k)^2}[2 \\ &-2(-1)^{N-k}S_1(N-k) - S_1(N-k)] + \frac{1}{N-k}[-(-1)^{N-k}S_1(N-k)^2 + 2S_{-2}(N-k) \\ &-S_1(N-k) + S_1(N-k)^2 + S_2(N-k)] + (-1)^{N-k}S_1(N-k)^2 + S_{-3}(N-k) \\ &+2S_{-2,1}(N-k) - S_{2,1}(N-k) + 4S_3(N-k) - \frac{S_1(k)S_1(N-k)}{N-k} \\ &-(N-k)\sum_{j=0}^{N-k}(-1)^j\binom{N-k-1}{j}\frac{S_1(j)}{N-k-j}\sum_{i=1}^{N-k-j-1}\frac{S_1(j+i)}{i+1}. \end{aligned} \tag{3.108}$$

This expression was tested for a large set of (N,k)-values. Note that, in contrast to the other sums discussed so far, negative-index harmonic sums appear in the final result. Let us now briefly discuss the other double sum for which the fitting method did not work, Eq.(3.96). Again analyzing fixed k-values while keeping N arbitrary, we find that the following rewriting holds

$$\sum_{j=k}^{N}(-1)^k\binom{j}{k}\sum_{l=j+1}^{N}(-1)^l\binom{N}{l}\frac{S_1(l)}{(l-j)^2}=F(N-k)-\frac{S_1(N)S_1(N-k)}{N-k} \tag{3.109}$$

with $F(N-k)$ exactly the same function as before. Hence we can immediately write down the result:

$$\begin{aligned}\sum_{j=k}^{N}(-1)^k\binom{j}{k}\sum_{l=j+1}^{N}(-1)^l\binom{N}{l}\frac{S_1(l)}{(l-j)^2}&=\frac{1}{(N-k)^3}[-4-2(-1)^{N-k}]+\frac{1}{(N-k)^2}[2\\
&-2(-1)^{N-k}S_1(N-k)-S_1(N-k)]+\frac{1}{N-k}[-(-1)^{N-k}S_1(N-k)^2+2S_{-2}(N-k)\\
&-S_1(N-k)+S_1(N-k)^2+S_2(N-k)]+(-1)^{N-k}S_1(N-k)^2+S_{-3}(N-k)\\
&+2S_{-2,1}(N-k)-S_{2,1}(N-k)+4S_3(N-k)-\frac{S_1(N)S_1(N-k)}{N-k}\\
&-(N-k)\sum_{j=0}^{N-k}(-1)^j\binom{N-k-1}{j}\frac{S_1(j)}{N-k-j}\sum_{i=1}^{N-k-j-1}\frac{S_1(j+i)}{i+1}.\end{aligned} \tag{3.110}$$

Again we tested this expression for a large set of (N,k)-values.

Chapter 4

Renormalization of non-singlet spin-N operators

Introduction

In this chapter, we investigate the renormalization of the spin-N non-singlet quark operators appearing in the OPEs of DIS and DVCS. Throughout this chapter, we work in the leading-twist approximation. As was discussed before, this works well at high energies, as higher-twist contributions are suppressed by inverse powers of the hard scale. Furthermore, we explicitly assume all quarks to be massless, i.e. we work in the chiral limit. Renormalizing the relevant operators will give access to their anomalous dimensions, which characterize the scale-dependence of (generalized) parton distributions. As such, they form an important input parameter for past and future experiments and lattice calculations.

While the operators relevant for the calculation of cross-sections in DIS and DVCS are the same, there exist important differences at the level of their renormalization. These are a direct consequence of the difference in kinematics between the two processes. In DIS, we need to consider forward kinematics, meaning that there is no momentum transfer to the target proton. At the level of the operator renormalization, the consequence of this is that the matrix elements to be calculated involve operator vertices with zero momentum flow. In turn, this implies a simple multiplicative renormalization, and the extraction of the anomalous dimensions is straightforward. These anomalous dimensions then determine the scale-dependence of the PDF. In DVCS however, the kinematics is off-forward. As we explicitly take into account the production of a real photon, the momenta of the initial and final state proton necessarily differ. In this case, we have to consider matrix elements that involve operator vertices with a non-zero momentum flow. This complicates the extraction of the anomalous dimensions, as now the operators mix with total derivative operators. In this case, the anomalous dimensions are related to the scale-dependence of the off-forward parton distributions, i.e. GPDs.

We first set up the notation for the operator matrix elements and discuss their calculation. Next we review the renormalization of the operators in forward and off-forward kinematics. Because of the operator mixing in the latter case, we first have to choose a particular operator basis. Several options will be discussed. After this, we implement the operator renormalization in a specific basis and show that, in this basis, useful relations exist between the operators. These in turn lead to a consistency relation between the corresponding anomalous dimensions, which can be used to construct the mixing matrix when the forward anomalous dimensions and the bare matrix elements of the relevant operators are known.

4.1 Calculation of operator matrix elements

To calculate the anomalous dimensions of the operators, we consider the following partonic Green's function

$$\mathcal{A}_{ij} \equiv \langle j(p_1)|O_i(p_3)|j(p_2)\rangle. \tag{4.1}$$

We focus our attention in this chapter on the Wilson flavor non-singlet quark operators $O^{\rm NS}_{\mu_1\ldots\mu_N}$, cf. Eq.(1.115). As such, we only need to take quarks as external fields, $j = q$. The general form of the relevant Green's function is then

$$\langle \psi(p_1)|O^{\rm NS}_{\mu_1\ldots\mu_N}(p_3)|\overline{\psi}(p_2)\rangle, \tag{4.2}$$

cf. Fig.4.1.

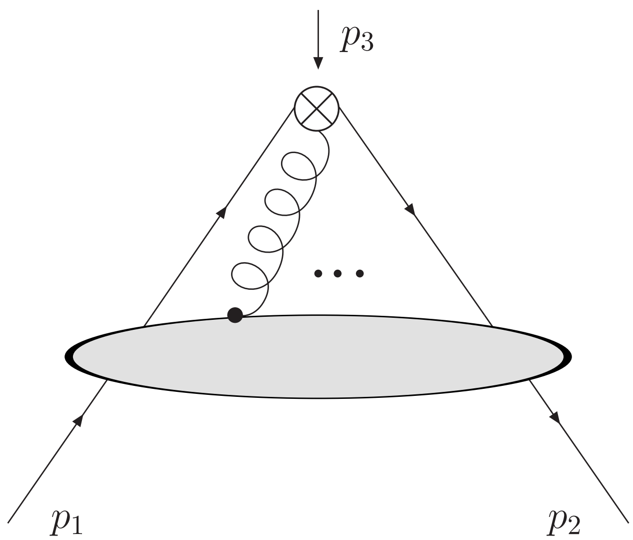

Figure 4.1: General form of the Green's functions to determine the operator anomalous dimensions.

As mentioned above, we will consider two kinematic regions, namely forward and off-forward kinematics. In forward kinematics, relevant for DIS, we identify the momenta of the external quarks such that there is no net momentum flow through the operator vertex. That is, in the forward limit we consider the Green's functions

$$\langle \psi(p_1)|O^{\rm NS}_{\mu_1\ldots\mu_N}(0)|\overline{\psi}(-p_1)\rangle. \tag{4.3}$$

In off-forward kinematics, there should be a non-zero momentum flow through the operator vertex. A priori, this requires us to consider the general three-point function depicted in Fig.4.1. However, we can simplify the calculation by nullifying one of the external momenta. This way, the three-point functions effectively reduce to two-point ones[1]. The Green's functions are then of the form

$$\langle \psi(p) | O^{\mathrm{NS}}_{\mu_1 \ldots \mu_N}(-p) | \overline{\psi}(0) \rangle . \tag{4.4}$$

In practical calculations, we contract the operators $O^{\mathrm{NS}}_{\mu_1 \ldots \mu_N}$ with a tensor constructed out of lightlike vectors

$$O_N \equiv \Delta^{\mu_1} \ldots \Delta^{\mu_N} O^{\mathrm{NS}}_{\mu_1 \ldots \mu_N} \tag{4.5}$$

with $\Delta^2 = 0$. This has two advantages. The first is that it gets rid of all open Lorentz indices, which simplifies the calculation of the loop integrals. The second is that this contraction automatically projects out the leading-twist contributions. In this notation, the conserved vector current is represented by O_1.

The calculation of the Green's functions in Eqs.(4.3) and (4.4) is completely automated, and follows a well-established workflow. First, the Feynman diagrams are generated using *QGRAF* [105]. *QGRAF* allows for the generation of topologies based on a given list of propagators and interaction vertices. The propagators and vertices we use are the standard QCD ones, cf. Section 1.1.2, with the addition of the relevant operator vertices. It should be noted that, while we deal exclusively with quark operators, the operators can still have gluons attached to them. These come from the covariant derivatives inside the operators and are necessarily connected to internal vertices. From the perturbative expansion of the operators it is easy to see that, at the L-loop level, operator vertices with at most L gluons have to be included. For example, at one-loop, we need to include two operator vertices, cf. Fig.4.2.

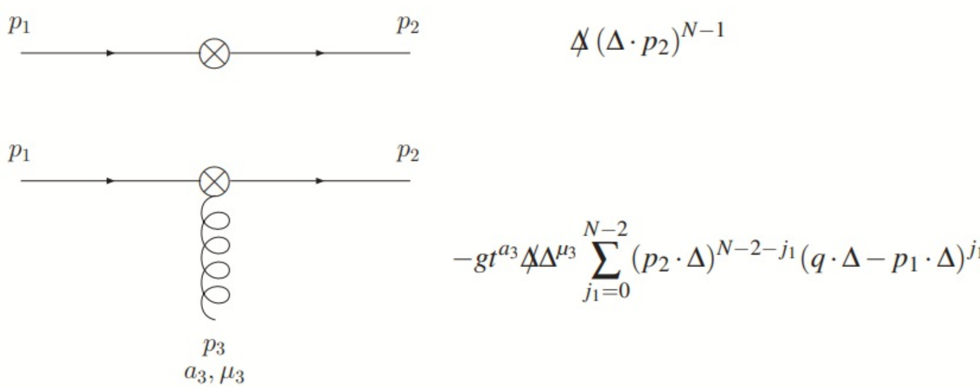

Figure 4.2: Operator vertices appearing at one loop, along with their Feynman rules [106]. All momenta are taken to be incoming and $q = \sum_i p_i$.

In *QGRAF*, the operator vertices can be included by introducing an associated field, with the requirement that this 'operator field' cannot appear as an internal line. Since in both kinematic regimes under consideration the external quarks are off-shell, we in principle also have to include

[1]Two-point functions are easier to deal with than three-point ones, as they lead to simpler loop integrals. However, working with the more general three-point functions would mean having access to the full result and its Lorentz structure, which makes it easier to check completeness of the operator basis in the case of mixing.

diagrams with self-energy corrections on the external legs. However, it is possible to discard such diagrams and instead multiply the result with the quark wave function renormalization factor Z_2 during renormalization. The advantage of this is that the remaining Feynman diagrams are one-particle-irreducible.

When the diagrams are generated, the next step is to actually calculate them. There are many packages and programs available for such calculations; we will employ the *FORM* [107, 108] program *FORCER* [109]. *FORCER* allows for the efficient calculation of massless propagator-type diagrams up to the four-loop level. It does this by reducing the loop integrals to a combination of master integrals within the framework of *integration by parts* (IBP). One of the reasons *FORCER* is efficient is that it automatically tries to reduce topologies to simpler ones, like one-loop integrals. Efficient solutions are known for these, and hence it is not necessary to explicitly solve IBP equations. Another important property of *FORCER* is that it, like its three-loop cousin *MINCER* [110, 111], works in the so-called G-scheme [112]. To explain this, we note that in both programs the general solution of one-loop massless propagator-type diagrams is written in terms of the G-function [113], which is defined in terms of the Euler-Gamma function as

$$G(\alpha,\beta,n,\sigma) \sim \frac{\Gamma(\alpha+\beta-\sigma-D/2)\Gamma(D/2-\alpha+n-\sigma)\Gamma(D/2-\beta+\sigma)}{\Gamma(\alpha)\Gamma(\beta)\Gamma(D-\alpha-\beta+n)}. \tag{4.6}$$

Here $D = 4-2\varepsilon$ denotes the spacetime dimension in dimensional regularization. In loop calculations, it is often convenient to then factor out a power of $\varepsilon G(1,1,0,0)$ per momentum integration. In turn, this factor can be set to one by redefining the surface of the D-dimensional unit sphere. This defines the G-scheme. At the end of the calculation, the results should then be transformed to a renormalization scheme of choice. For us this will be the $\overline{\text{MS}}$-scheme. Before we can use *FORCER*, however, we first have to properly massage the output we get from *QGRAF*. This is done in a *FORM* program called *convdia*, whose original form is due to P. Nogueira and J. Vermaseren [114, 115]. Its main duties can be summarized as follows.

- Identify the topologies of the diagrams and discard tadpoles[2].
- When considering higher-order corrections, a large number of diagrams is obtained by inserting lower-loop propagators into a diagram. For example, at the two-loop level, diagrams of the following type appear

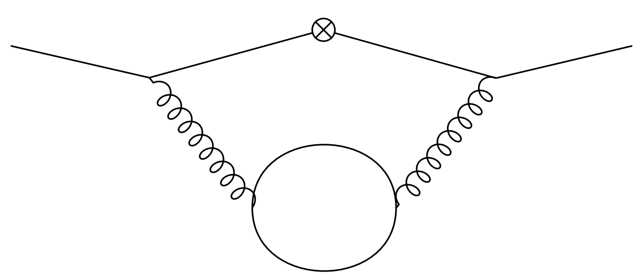

  Instead of calculating such diagrams from scratch, one can just insert the gluon propagator to the appropriate order. This has the form of the standard gluon propagator, with the mo-

[2]These lead to scaleless integrals and hence vanish in dimensional regularization.

mentum in the denominator now being ε-dependent (i.e. the expression is proportional to $k^{-2\varepsilon}$). The recognition of this type of diagram is done in *convdia*.

- Determination of the color factor associated to each diagram. This is based on the algorithms presented in [116].

Once all this is done, *convdia* collects diagrams with the same topology and color factor into so-called *meta-diagrams*. This is done for computational efficiency. More details on the use of *FORM* for the calculation of Feynman diagrams can be found in [115]. The handling of these meta-diagrams is performed with the database program *MINOS* [117], which creates a database of diagrams before the calculation and a database of computed integrals afterwards. The final step of the process consists in substituting the Feynman rules and letting *FORCER* do its magic. We perform all diagram calculations using a general covariant gauge ξ. While this does increase the complexity of the computations, it also provides us with a cross-check, as the operator anomalous dimensions should be gauge-independent.

In the discussion above, we explicitly assumed to be working in Mellin N-space, cf. Section 1.1.4. In the leading-twist approximation, the Mellin moment N of the operators just corresponds to their Lorentz spin. The results from the procedure above are then fixed moments of the bare OME under consideration. In particular, this means that the operator anomalous dimensions will also be written as a function of the Mellin moment N. Note that the corresponding variable in momentum space would be the momentum fraction x carried by the struck parton. In the case of off-forward kinematics, an additional parameter will be necessary. We will generically denote this new parameter by k, and in N-space it counts the number of total derivatives acting on the operator. A possible corresponding momentum variable is the skewedness, which gives a measure for the momentum transfer to the target.

When the Feynman diagram computation is completed, we need to implement the renormalization in order to render the matrix elements finite and to extract the anomalous dimensions. We will employ the $\overline{\text{MS}}$-renormalization scheme. First, the bare interaction strength and gauge parameter have to be replaced by their renormalized versions, cf. Eqs.(1.80) and (1.81). Next, the operator renormalization has to be implemented. This will be the topic of the remainder of this chapter.

It will be useful to have a running example throughout this chapter to illustrate the calculations and concepts we introduce. The one-loop calculation provides a natural candidate to this end. Hence, before moving on to the operator renormalization, let us briefly consider the calculation of the one-loop matrix elements. The relevant Feynman diagrams are shown in Fig.4.3. In the case of forward kinematics the result for the bare matrix element is

$$\langle\psi(p_1)|O_N(0)|\overline{\psi}(-p_1)\rangle = 1 + \frac{a_s C_F}{\varepsilon}\left(4S_1(N) + \frac{2}{N+1} - 4 + \xi\right) + \dots \tag{4.7}$$

The dots represent finite terms and higher-order corrections. Note the appearance of the gauge parameter ξ.

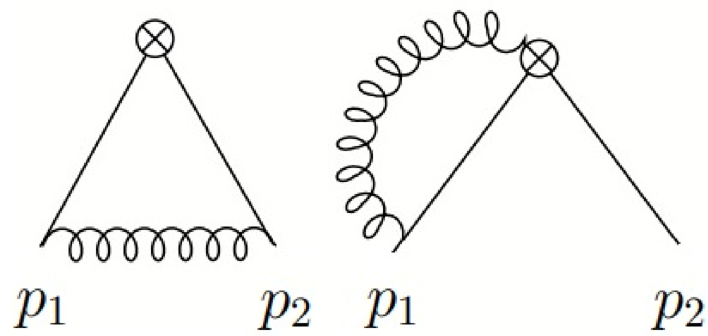

Figure 4.3: One-loop Feynman diagrams. In the forward limit, $p_2 = -p_1$, and one should include the second diagram with the gluon closing on the other quark line. In the off-forward limit we set $p_2 = 0$. As explained before, diagrams with self-energy corrections on the external lines are not included. The Feynman diagrams were drawn using TIKZ-FEYNMAN *[32].*

In off-forward kinematics, with $p_2 = 0$, we find

$$\langle \psi(p_1) | O_N(-p_1) | \overline{\psi}(0) \rangle = 1 + \frac{a_s C_F}{\varepsilon} \left(2S_1(N) - \frac{2}{N+1} - 2 + \xi \right) + \dots \tag{4.8}$$

4.2 Operator renormalization I: Forward limit

In the forward limit, the operators simply renormalize multiplicatively

$$O_{N+1} = Z_2 Z_{N,N} [O_{N+1}]. \tag{4.9}$$

Renormalized operators are written with square brackets. As explained above, we include the quark wave function renormalization factor to account for the self-energy corrections on the off-shell external lines. The derivation of the renormalization factors in terms of anomalous dimensions and the QCD beta-function follows the same procedure as described in Chapter 1. Up to order a_s^3 we find[3]

$$\begin{aligned} Z_{N,N} = 1 &+ \frac{a_s}{\varepsilon} \gamma^{(0)}_{N,N} + \frac{a_s^2}{2\varepsilon} \left\{ \frac{1}{\varepsilon} (\gamma^{(0)}_{N,N} - \beta_0) \gamma^{(0)}_{N,N} + \gamma^{(1)}_{N,N} \right\} \\ &+ \frac{a_s^3}{6\varepsilon} \left\{ \frac{1}{\varepsilon^2} (\gamma^{(0)}_{N,N} - \beta_0)(\gamma^{(0)}_{N,N} - 2\beta_0) \gamma^{(0)}_{N,N} + \frac{1}{\varepsilon} (3\gamma^{(0)}_{N,N} - 2\beta_0) \gamma^{(1)}_{N,N} \right. \\ &\left. - \frac{2}{\varepsilon} \beta_1 \gamma^{(0)}_{N,N} + 2\gamma^{(2)}_{N,N} \right\}. \end{aligned} \tag{4.10}$$

[3]Comparing with Eq.(2.24), we have $\gamma_{\mathrm{NS}}(N) = \gamma_{N-1,N-1}$.

A special case of Eq.(4.9) occurs when $N = 0$,

$$O_1 = Z_2 Z_{0,0}[O_1]. \tag{4.11}$$

Since O_1 is simply the conserved vector current, $O_1 = \overline{\psi}\lambda^\alpha \not{\Delta}\psi$, it is finite to all orders in a_s, i.e. $Z_{0,0} = 1$ and

$$O_1 = Z_2[O_1]. \tag{4.12}$$

In general, the application of the renormalization equation Eq.(4.9) to the one-loop bare OME in Eq.(4.7) leads to

$$\gamma^{(0)}_{N,N} = C_F\left(4S_1(N) + \frac{2}{N+1} + \frac{2}{N+2} - 3\right). \tag{4.13}$$

Note that the dependence on the gauge parameter ξ has dropped out, as expected. Beyond one-loop order, quite a lot is known about these forward anomalous dimensions. Up to the three-loop level, they are completely determined, see [118–121]. At four loops, there exist complete results in the limit of large n_f [122, 123] and some low fixed moments in full QCD [124–126]. Fixed moments, up to $N = 16$, are also known for a general gauge theory SU(N_c) in the planar limit ($N_c \to \infty$) [106]. Finally, even at the five-loop level there is partial information available concerning the large-n_f limit[4] [122] and low fixed moments [127].

Because of this relatively large set of known moments in forward kinematics, some general statements can be made about the anomalous dimensions at L loops. The basic building blocks of the L-loop anomalous dimension are harmonic sums and denominators of weight up to $w = 2L-1$. A more detailed analysis reveals that there is also a relation between the structure of the expression and the color factor and powers of n_f multiplying it. In particular, if we have some term proportional to powers of C_F and C_A, the maximum weight of the multiplying factor will be $2L-1$. However, for every factor of n_f, the maximal weight reduces with one, down to weight L for the leading-n_f terms. The maximal weight also reduces in the presence of the Riemann-zeta function ζ_n; to $2L-n-1$ in general and to $L-n$ for the leading-n_f terms. The reason for these simplifications in the leading-n_f limit is that, when considering a Feynman diagram expansion, the leading-n_f terms originate from those L-loop diagrams that have the maximal amount of one-loop insertions.

As the anomalous dimension in Mellin space is a function of harmonic sums, the corresponding splitting function in x-space, cf. Eq.(2.24), can be written in terms of *harmonic polylogarithms* (HPLs). These are recursively defined as [128]

$$H_0(x) = \ln x, \quad H_{\pm 1}(x) = \mp \ln(1 \mp x) \tag{4.14}$$

$$H_{m_1 \ldots m_w}(x) = \begin{cases} \frac{1}{w!}\ln^w x & \text{if } m_i = 0 \\ \int_0^x \mathrm{d}z\, f_{m_1}(z) H_{m_2 \ldots m_w}(z) & \text{otherwise} \end{cases} \tag{4.15}$$

$$f_0(x) = \frac{1}{x}, \quad f_{\pm 1}(x) = \frac{1}{1 \mp x}. \tag{4.16}$$

[4] In fact, [122] presents the *all-order* result for the anomalous dimensions in the large-n_f limit.

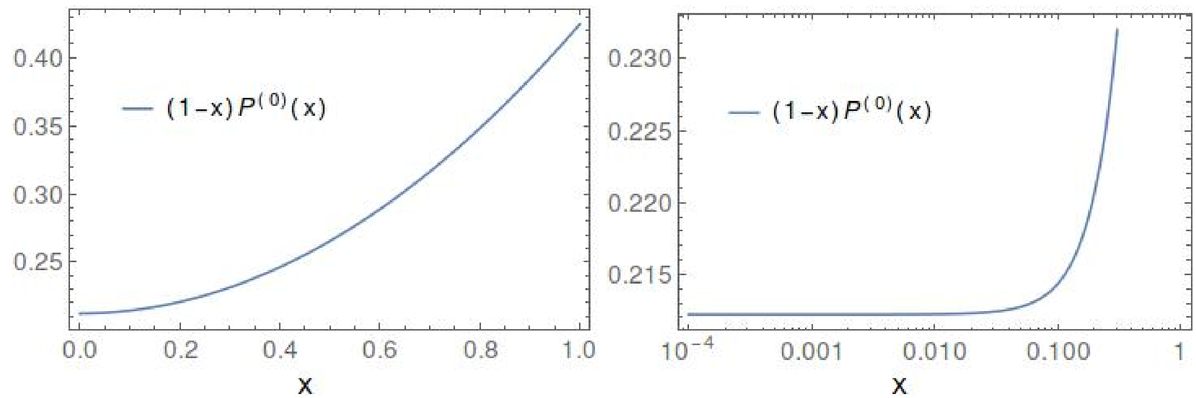

Figure 4.4: The one-loop splitting function on a normal scale and on a logarithmic one. We have introduced a normalization of $\frac{1}{4\pi}$.

For example at one-loop order, the splitting function is given by

$$P^{(0)}(x) = 2C_F \left[\frac{1+x^2}{(1-x)_+} + \frac{3}{2}\delta(1-x) \right]. \tag{4.17}$$

The plus-prescription for some test function $f(x)$ is defined as

$$\int_0^1 \mathrm{d}x \, \frac{f(x)}{(1-x)_+} \equiv \int_0^1 \mathrm{d}x \, \frac{f(x)-f(1)}{1-x}. \tag{4.18}$$

It cancels the divergence at $x=1$ if $f(1)$ is sufficiently smooth. This $x=1$ divergence of the splitting function is associated to soft gluon emissions. The x-space behaviour of the splitting function is depicted in Fig.4.4.

4.3 Operator renormalization II: Off-forward limit

We now discuss the operator renormalization for off-forward kinematics. As mentioned before, this allows for the possibility of mixing with total derivative operators. A consequence of this mixing is that now we have to consider *anomalous dimension matrices*. Hence, before we can discuss the actual renormalization, we first have to choose an appropriate basis for the additional operators. Several options exist in the literature, and we will discuss three of them in some detail. The first, which is predominantly used in calculations that involve conformal symmetry [16, 19, 87], is based on an expansion of the operators in terms of Gegenbauer polynomials. The other two bases select the operators based on the number of (total) derivatives, and are commonly used to connect continuum quantities to lattice ones for non-perturbative studies, see e.g. [25, 72].

4.3.1 Operator bases

The Gegenbauer basis

We start our discussion by introducing renormalized non-local light-ray operators $[O]$. These act as generating functions for local operators as [16]

$$[O](x;z_1,z_2) = \sum_{m,k} \frac{z_1^m z_2^k}{m!\,k!} [\overline{\psi}(x)(\overleftarrow{D}\cdot\Delta)^m \not{\Delta}(\Delta\cdot\vec{D})^k \psi(x)]. \tag{4.19}$$

Here, Δ is an arbitrary light-like vector. For simplicity, the x-dependence will be omitted in the following, writing $O(z_1,z_2) \equiv O(0;z_1,z_2)$. The evolution of these light-ray operators under RG-flow can be written as

$$\Big(\mu^2\partial_{\mu^2} + \beta(a_s)\partial_{a_s} + \mathcal{H}(a_s)\Big)[O](z_1,z_2) = 0 \tag{4.20}$$

with μ the renormalization scale and $\mathcal{H}(a_s)$ the so-called evolution operator. This is an integral operator, which acts on the light-cone coordinates of the fields [129]

$$\mathcal{H}(a_s)[O](z_1,z_2) = \int_0^1 d\alpha \int_0^1 d\beta\, h(\alpha,\beta)[O](z_{12}^{\alpha}, z_{21}^{\beta}) \tag{4.21}$$

with $z_{12}^{\alpha} \equiv z_1(1-\alpha)+z_2\alpha$. $h(\alpha,\beta)$ represents the evolution kernel, the moments of which correspond to the anomalous dimensions of the local operators in Eq.(4.19),

$$\gamma_{N,N} = \int_0^1 d\alpha \int_0^1 d\beta (1-\alpha-\beta)^{N-1} h(\alpha,\beta). \tag{4.22}$$

N represents the total number of covariant derivatives appearing in the operator.

The non-local light-ray operators in Eq.(4.19) can be expanded in a basis of local operators in terms of the Gegenbauer polynomials, see e.g. [19, 87]

$$O_{N,k}^{\mathcal{G}} = (\Delta\cdot\partial)^k \overline{\psi}(x)\not{\Delta} C_N^{3/2}\left(\frac{\overleftarrow{D}\cdot\Delta - \Delta\cdot\vec{D}}{\overleftarrow{\partial}\cdot\Delta + \Delta\cdot\vec{\partial}}\right)\psi(x). \tag{4.23}$$

Here, $k \geq N$ is the total number of derivatives, and we use the superscript $\mathcal{G}$ to emphasize that the operators belong to the Gegenbauer basis. Expanding the Gegenbauer polynomial with the differential operators then gives, cf. Eq.(3.21)

$$(\partial_{z_1}+\partial_{z_2})^k C_N^{3/2}\Big(\frac{\partial_{z_1}-\partial_{z_2}}{\partial_{z_1}+\partial_{z_2}}\Big) = \frac{1}{2N!}\sum_{l=0}^{N}(-1)^l \binom{N}{l} \frac{(N+l+2)!}{(l+1)!} \sum_{j=0}^{k-l} \binom{k-l}{j} (\partial_{z_1})^{k-l-j}(\partial_{z_2})^{l+j} \tag{4.24}$$

with $k \geq N$, such that the local operators become

$$O_{N,k}^{\mathcal{G}} = \frac{1}{2N!}\sum_{l=0}^{N}(-1)^l \binom{N}{l} \frac{(N+l+2)!}{(l+1)!} \sum_{j=0}^{k-l} \binom{k-l}{j} \overline{\psi}(x)\not{\Delta}(\overleftarrow{D}\cdot\Delta)^{k-l-j}(\Delta\cdot\vec{D})^{l+j}\psi(x). \tag{4.25}$$

The evolution equation for the renormalized operators $[O^{\mathcal{G}}_{N,k}]$ is

$$\left(\mu^2\partial_{\mu^2} + \beta(a_s)\partial_{a_s}\right)[O^{\mathcal{G}}_{N,k}] = \sum_{j=0}^{N} \gamma^{\mathcal{G}}_{N,j}[O^{\mathcal{G}}_{j,k}]. \tag{4.26}$$

The mixing of the operators manifests itself in the appearance of the sum on the right-hand side. The mixing matrix[5], denoted by $\hat{\gamma}_{N+1}$, is triangular in the Gegenbauer basis, $\gamma^{\mathcal{G}}_{N,j} = 0$ if $j > N$. Furthermore, its diagonal elements correspond to the forward anomalous dimensions, $\gamma_{N,N}$. Note that $\gamma_{N,N}$ do not depend on the chosen basis for total derivative operators. Hence we can simply write

$$\gamma^{\mathcal{B}}_{N,N} \equiv \gamma_{N,N} \tag{4.27}$$

in any basis for derivative operators $\mathcal{B}$. The Gegenbauer mixing matrix is currently known completely up to the three-loop level [16].

The total derivative basis

Another approach is to identify the operators by counting powers of derivatives. To this end we write

$$O^{\mathcal{D}}_{p,q,r} = (\Delta\cdot\partial)^p\left\{(\Delta\cdot D)^q\overline{\psi}\,\not{\Delta}(\Delta\cdot D)^r\psi\right\}, \tag{4.28}$$

see e.g. [130, 131]. Here we have already selected the leading-twist contributions by contracting all Lorentz indices with light-like Δ. The indices p, q and r count the powers of the respective derivatives, and the superscript $\mathcal{D}$ denotes that the operators are written in the total derivative basis. Because of the chiral limit, the partial derivatives act as

$$O^{\mathcal{D}}_{p,q,r} = O^{\mathcal{D}}_{p-1,q+1,r} + O^{\mathcal{D}}_{p-1,q,r+1}. \tag{4.29}$$

This defines a recursion for the bare operators, which is solved by

$$O^{\mathcal{D}}_{p,q,r} = \sum_{i=0}^{p}\binom{p}{i} O^{\mathcal{D}}_{0,p+q-i,r+i}. \tag{4.30}$$

Another consequence of the chiral limit is that left and right derivative operators renormalize with the same renormalization constants

$$\begin{aligned} O^{\mathcal{D}}_{k,0,N} &= \sum_{j=0}^{N} Z^{\mathcal{D}}_{N,N-j}[O_{k+j,0,N-j}], \\ O^{\mathcal{D}}_{k,N,0} &= \sum_{j=0}^{N} Z^{\mathcal{D}}_{N,N-j}[O_{k+j,N-j,0}]. \end{aligned} \tag{4.31}$$

Note that these statements do not hold beyond the chiral limit, as in that case left- and right-handed fermions obey different equations of motion. This would lead to corrections proportional to the

[5] We denote the elements of the ADM for spin-$(N+1)$ operators as $\gamma_{N,k}$ and the matrix itself as $\hat{\gamma}_{N+1}$.

quark masses. As usual, the operator anomalous dimensions are derived from the renormalization factors as

$$\gamma^{\mathcal{D}}_{N,k} = -(Z^{\mathcal{D}}_{N,j})^{-1} \frac{\mathrm{d}\, Z^{\mathcal{D}}_{j,k}}{\mathrm{d}\ln\mu^2}. \tag{4.32}$$

The mixing matrix is also triangular in the total derivative basis ($\gamma^{\mathcal{D}}_{N,k} = 0$ if $k > N$), with the diagonal elements being the standard forward anomalous dimensions. When considering the actual renormalization in the following sections, we will mainly use this basis for the derivative operators.

It is possible to relate the operator bases introduced so far. For this, we first note that Eq.(4.19) can be written as

$$O(z_1, z_2) = \sum_{m,k} \frac{z_1^m z_2^k}{m!\,k!} O^{\mathcal{D}}_{0,m,k}. \tag{4.33}$$

Using Eqs.(4.23), (4.24) and (4.30) this becomes

$$O^{\mathcal{G}}_{N,k} = \frac{1}{2N!} \sum_{l=0}^{N} (-1)^l \binom{N}{l} \frac{(N+l+2)!}{(l+1)!} O^{\mathcal{D}}_{k-l,0,l}. \tag{4.34}$$

The evolution equation for the operators $[O^{\mathcal{G}}_{N,k}]$, Eq.(4.26), then leads to a relation between the mixing matrices in the two bases

$$\sum_{j=0}^{N} \gamma^{\mathcal{G}}_{N,j} [O^{\mathcal{G}}_{j,N}] = \frac{1}{2N!} \sum_{l=0}^{N} (-1)^l \binom{N}{l} \frac{(N+l+2)!}{(l+1)!} \sum_{j=0}^{l} \gamma^{\mathcal{D}}_{l,l-j} [O^{\mathcal{D}}_{N-l+j,0,l-j}], \tag{4.35}$$

where we have also used the renormalization equation Eq.(4.31). Using Eq.(4.34) for renormalized operators this becomes

$$\begin{aligned} &\sum_{j=0}^{N} \gamma^{\mathcal{G}}_{N,j} \left(\frac{1}{2j!} \sum_{l=0}^{j} (-1)^l \binom{j}{l} \frac{(j+l+2)!}{(l+1)!} [O^{\mathcal{D}}_{N-l,0,l}] \right) \\ &\qquad = \frac{1}{2N!} \sum_{j=0}^{N} (-1)^j \binom{N}{j} \frac{(N+j+2)!}{(j+1)!} \sum_{l=0}^{j} \gamma^{\mathcal{D}}_{j,l} [O^{\mathcal{D}}_{N-l,0,l}]. \end{aligned} \tag{4.36}$$

Upon comparing the coefficients of the operators $[O^{\mathcal{D}}_{N-l,0,l}]$, we finally find

$$\sum_{j=0}^{N} (-1)^j \frac{(j+2)!}{j!} \gamma^{\mathcal{G}}_{N,j} = \frac{1}{N!} \sum_{j=0}^{N} (-1)^j \binom{N}{j} \frac{(N+j+2)!}{(j+1)!} \sum_{l=0}^{j} \gamma^{\mathcal{D}}_{j,l}. \tag{4.37}$$

To get the expression on the left-hand side, we evaluated the sum

$$\sum_{l=0}^{j} (-1)^l \binom{j}{l} \frac{(j+l+2)!}{(l+1)!} = (-1)^j (j+2)!\,. \tag{4.38}$$

Note that this is *not* a relation between specific elements of the ADMs in both bases. E.g., it is not enough to know $\gamma^{\mathcal{G}}_{2,0}$ to determine $\gamma^{\mathcal{D}}_{2,0}$. It can, however, be used as a consistency condition and cross-check. By the first point we mean that, if the ADM is known in one basis, we can use Eq.(4.37) to constrain its functional form in the other basis. This type of consistency check allows us to connect previously unrelated results in the literature.

The Geyer basis

The third and final basis for derivative operators we discuss is due to B. Geyer and friends [23, 24]. The local operators are defined as

$$O_{N,k}^{\text{Geyer}} \equiv \overline{\psi}\not{\Delta}(\overleftarrow{D}+\overrightarrow{D})^{N-k}(\overleftarrow{D}-\overrightarrow{D})^{k}\psi \tag{4.39}$$

with N and k odd. The contraction with an arbitrary light-like vector Δ is understood, i.e.

$$D \equiv \Delta^{\mu} D_{\mu} \tag{4.40}$$

with $\Delta^2 = 0$.

The ADM in this basis shares the same properties as those in the previous two bases, i.e. it is triangular and its diagonal elements are the forward anomalous dimensions. As we did for the Gegenbauer basis, we want to relate the operators, and correspondingly their anomalous dimensions, in the Geyer basis to those in the total derivative one. To accomplish this we first use[6]

$$O^{\mathcal{D}}_{0,N-k,k} = (-1)^k \sum_{j=0}^{k} (-1)^j \binom{k}{j} O^{\mathcal{D}}_{j,N-j,0}, \tag{4.41}$$

which can be derived in the same way as Eq. (4.30). It is then straightforward to see that, for $k=0$, the operators defined above correspond to total derivatives of the vector current, i.e.

$$O_{N,0}^{\text{Geyer}} = O^{\mathcal{D}}_{N,0,0}. \tag{4.42}$$

For arbitrary k-values, we can apply the binomial theorem (twice) together with Eq.(4.41). This leads to the following relation between the bare operators

$$O_{N,k}^{\text{Geyer}} = \sum_{i=0}^{N-k} \sum_{j=0}^{k} (-1)^i \binom{N-k}{i} \binom{k}{j} \sum_{l=0}^{i+j} (-1)^l \binom{i+j}{l} O^{\mathcal{D}}_{l,N-l,0}. \tag{4.43}$$

The corresponding relation for the renormalized operators reads

$$\begin{aligned}
[O_{N,k}^{\text{Geyer}}] = &\sum_{i=0}^{N-k} \sum_{j=0}^{k} (-1)^i \binom{N-k}{i} \binom{k}{j} \sum_{l=0}^{i+j} (-1)^l \binom{i+j}{l} \sum_{m=0}^{N-l} (-1)^m \gamma^{\mathcal{D}}_{N-l,m} \\
&\times \sum_{n=0}^{m} (-1)^n \binom{m}{n} [O^{\mathcal{D}}_{N-m+n,0,m-n}].
\end{aligned} \tag{4.44}$$

In the following, we focus on diagonal operators $O_{N,N}^{\text{Geyer}}$, the evolution equation for which is

$$\mu^2 \frac{\mathrm{d}}{\mathrm{d}\mu^2} O_{N,N}^{\text{Geyer}} = \sum_{k=0}^{N} \frac{1-(-1)^k}{2} \gamma_{N,k}^{\text{Geyer}} [O_{k,N}^{\text{Geyer}}] \tag{4.45}$$

[6] Note that there is a factor of $(-1)^j$ missing in Eq.(2.25) in [132].

with N odd. Furthermore, specializing to the one-loop case[7] we find, using Eq. (4.44) for $k = N$,

$$\gamma_{N,N}^{(0)} + \sum_{j=0}^{N-1} \frac{1-(-1)^j}{2} \gamma_{N,j}^{\text{Geyer},(0)} = (-1)^{N-1} \sum_{l=0}^{N} 2^l (-1)^l \binom{N}{l} \gamma_{l,0}^{\mathcal{D},(0)} \tag{4.46}$$

for odd N. A similar relation can be derived for even values of N, corresponding to the anomalous dimensions of odd-spin operators,

$$\gamma_{N,N}^{(0)} + \sum_{j=0}^{N-1} \frac{1+(-1)^j}{2} \gamma_{N,j}^{\text{Geyer},(0)} = (-1)^{N} \sum_{l=0}^{N} 2^l (-1)^l \binom{N}{l} \gamma_{l,0}^{\mathcal{D},(0)}. \tag{4.47}$$

These are the sought-after relations between the Geyer and total derivative bases.

4.3.2 Renormalization in the total derivative basis

Having discussed some possible bases for total derivative operators, we are now in a position to actually implement the operator renormalization in off-forward kinematics. This is important for operator analyses of hard exclusive processes. The corresponding anomalous dimensions characterize the scale-dependence of the generalized parton distributions. Throughout this section, we will employ the total derivative basis.

The renormalization of the spin-$(N+1)$ operator obeys

$$O_{N+1}^{\mathcal{D}} = Z_2 \left(Z_{N,N} [O_{N+1}^{\mathcal{D}}] + Z_{N,N-1}^{\mathcal{D}} [\partial O_N^{\mathcal{D}}] + \cdots + Z_{N,0}^{\mathcal{D}} [\partial^N O_1^{\mathcal{D}}] \right) \tag{4.48}$$

such that, for the full set of spin-$(N+1)$ operators, we now find a matrix equation

$$\begin{pmatrix} O_{N+1}^{\mathcal{D}} \\ \partial O_N^{\mathcal{D}} \\ \vdots \\ \partial^N O_1^{\mathcal{D}} \end{pmatrix} = Z_2 \begin{pmatrix} Z_{N,N} & Z_{N,N-1}^{\mathcal{D}} & \dots & Z_{N,0}^{\mathcal{D}} \\ 0 & Z_{N-1,N-1} & \dots & Z_{N-1,0}^{\mathcal{D}} \\ \vdots & \vdots & \dots & \vdots \\ 0 & 0 & \dots & 1 \end{pmatrix} \begin{pmatrix} [O_{N+1}^{\mathcal{D}}] \\ [\partial O_N^{\mathcal{D}}] \\ \vdots \\ [\partial^N O_1^{\mathcal{D}}] \end{pmatrix}. \tag{4.49}$$

Note that the $n \times n$ bottom-right submatrix is equivalent to the complete mixing matrix for the renormalization of spin-n operators. For example, the bottom-right 2×2 submatrix is

$$\begin{pmatrix} Z_{1,1} & Z_{1,0}^{\mathcal{D}} \\ 0 & 1 \end{pmatrix} \tag{4.50}$$

which exactly corresponds to the mixing matrix for the spin-two operators $\{O_2^{\mathcal{D}}, \partial O_1^{\mathcal{D}}\}$.

The derivation of the renormalization factors in terms of the RG-parameters is similar to the forward case, with some important differences. As before, the basis for this is the formal definition of the anomalous dimensions in terms of the Z-factors, cf. Eq.(4.32). However, this is now a matrix equation, such that the calculation requires us to determine the inverse matrix of renormalization

[7] The higher-order anomalous dimensions in the Geyer basis have not been calculated.

factors. It is helpful to consider a simple example before tackling the general problem. As such, we focus on the renormalization of the spin-two operators,

$$\begin{pmatrix} O_2^{\mathcal{D}} \\ \partial O_1^{\mathcal{D}} \end{pmatrix} = \begin{pmatrix} Z_{1,1} & Z_{1,0}^{\mathcal{D}} \\ 0 & 1 \end{pmatrix} \begin{pmatrix} [O_2^{\mathcal{D}}] \\ [\partial O_1^{\mathcal{D}}] \end{pmatrix}. \tag{4.51}$$

The equation to solve is then

$$\frac{\beta}{Z_{1,1}} \begin{pmatrix} 1 & -Z_{1,0}^{\mathcal{D}} \\ 0 & Z_{1,1} \end{pmatrix} \begin{pmatrix} \frac{\partial Z_{1,1}}{\partial a_s} & \frac{\partial Z_{1,0}^{\mathcal{D}}}{\partial a_s} \\ 0 & 0 \end{pmatrix} = \begin{pmatrix} \gamma_{1,1} & \gamma_{1,0}^{\mathcal{D}} \\ 0 & 0 \end{pmatrix}. \tag{4.52}$$

Substituting the relevant expansions, up to $O(a_s^3)$, it is straightforward to solve this matrix equation. The results are

$$\begin{aligned} Z_{1,1} =& 1 + \frac{a_s}{\varepsilon}\gamma_{1,1}^{(0)} + \frac{a_s^2}{2\varepsilon}\Big[\frac{1}{\varepsilon}(\gamma_{1,1}^{(0)} - \beta_0)\gamma_{1,1}^{(0)} + \gamma_{1,1}^{(1)}\Big] + \frac{a_s^3}{3\varepsilon}\Big[\frac{1}{2\varepsilon^2}[2\beta_0^2\gamma_{1,1}^{(0)} \\ &- 3\beta_0(\gamma_{1,1}^{(0)})^2 + (\gamma_{1,1}^{(0)})^3] + \frac{1}{2\varepsilon}[-2\beta_1\gamma_{1,1}^{(0)} - 2\beta_0\gamma_{1,1}^{(1)} + 3\gamma_{1,1}^{(0)}\gamma_{1,1}^{(1)}] + \gamma_{1,1}^{(2)}\Big], \end{aligned} \tag{4.53}$$

$$\begin{aligned} Z_{1,0}^{\mathcal{D}} =& \frac{a_s}{\varepsilon}\gamma_{1,0}^{\mathcal{D},(0)} + \frac{a_s^2}{2\varepsilon}\Big[\frac{1}{\varepsilon}(\gamma_{1,1}^{(0)} - \beta_0)\gamma_{1,0}^{\mathcal{D},(0)} + \gamma_{1,0}^{\mathcal{D},(1)}\Big] + \frac{a_s^3}{3\varepsilon}\Big[\frac{1}{2\varepsilon^2}[2\beta_0^2\gamma_{1,0}^{\mathcal{D},(0)} \\ &- 3\beta_0\gamma_{1,0}^{\mathcal{D},(0)}\gamma_{1,1}^{(0)} + (\gamma_{1,1}^{(0)})^2\gamma_{1,0}^{\mathcal{D},(0)}] + \frac{1}{2\varepsilon}[-2\beta_1\gamma_{1,0}^{\mathcal{D},(0)} - 2\beta_0\gamma_{1,0}^{\mathcal{D},(1)} \\ &+ 2\gamma_{1,1}^{(0)}\gamma_{1,0}^{\mathcal{D},(1)} + \gamma_{1,1}^{(1)}\gamma_{1,0}^{\mathcal{D},(0)}] + \gamma_{1,0}^{\mathcal{D},(2)}\Big]. \end{aligned} \tag{4.54}$$

As expected, Eq.(4.53) agrees with the previously derived result for the Z-factors in the forward limit, cf. Eq.(4.10). One can relatively easily repeat this exercise for higher moments. The only difference is that the matrix equations become bigger and more tedious to solve. In general we find, up to $O(a_s^3)$,

$$\begin{aligned} Z_{N,k}^{\mathcal{D}} =& \frac{a_s}{\varepsilon}\gamma_{N,k}^{\mathcal{D},(0)} + \frac{a_s^2}{2\varepsilon}\left\{(\gamma_{N,N} + \gamma_{k,k}^{(0)} - \beta_0)\gamma_{N,k}^{\mathcal{D},(0)} + \frac{1}{\varepsilon}\sum_{i=k+1}^{N-1}\gamma_{N,i}^{\mathcal{D},(0)}\gamma_{i,k}^{\mathcal{D},(0)} + \gamma_{N,k}^{\mathcal{D},(1)}\right\} \\ &+ \frac{a_s^3}{6\varepsilon}\left\{\frac{2}{\varepsilon^2}\beta_0^2\gamma_{N,k}^{\mathcal{D},(0)} - \frac{3}{\varepsilon^2}\beta_0\left(\gamma_{N,k}^{\mathcal{D},(0)}(\gamma_{N,N}^{(0)} + \gamma_{k,k}^{(0)}) + \sum_{i=k+1}^{N-1}\gamma_{N,i}^{\mathcal{D},(0)}\gamma_{i,k}^{\mathcal{D},(0)}\right)\right. \\ &+ \frac{1}{\varepsilon^2}\sum_{i=k}^{N}\sum_{j=1}^{i}\gamma_{N,i}^{\mathcal{D},(0)}\gamma_{i,j}^{\mathcal{D},(0)}\gamma_{j,k}^{\mathcal{D},(0)} - \frac{2}{\varepsilon}\beta_1\gamma_{N,k}^{\mathcal{D},(0)} - \frac{2}{\varepsilon}\beta_0\gamma_{N,k}^{\mathcal{D},(1)} \\ &\left.+ \frac{1}{\varepsilon}\sum_{i=1}^{N}(2\gamma_{N,i}^{\mathcal{D},(0)}\gamma_{i,k}^{\mathcal{D},(1)} + \gamma_{N,i}^{\mathcal{D},(1)}\gamma_{i,k}^{\mathcal{D},(0)}) + 2\gamma_{N,k}^{\mathcal{D},(2)}\right\} \end{aligned} \tag{4.55}$$

with $k \neq N$. The operator mixing manifests itself in the appearance of sums of anomalous dimensions, starting at $O(a_s^2)$.

Let us now take a look at what happens at one-loop order. Recall that in Section 4.1 we calculated the bare OME to be

$$\langle\psi(p_1)|O_N(-p_1)|\overline{\psi}(0)\rangle = 1 + \frac{a_s C_F}{\varepsilon}\left(2S_1(N) - \frac{2}{N+1} - 2 + \xi\right) + \ldots. \tag{4.56}$$

In the forward limit, this was enough to fix the one-loop anomalous dimension for all values of N, cf. Eq.(4.13). This is not the case however in the off-forward limit because of mixing. For simplicity, we start with the spin-two operators, cf. Eq.(4.51). The singular part of the one-loop OME is

$$\frac{a_s C_F}{\varepsilon}\left(\frac{1}{3}+\xi\right). \tag{4.57}$$

According to Eq.(4.48), this has to match

$$Z_2\Big(Z_{1,1}[O_2^{\mathcal{D}}]+Z_{1,0}^{\mathcal{D}}[\partial O_1^{\mathcal{D}}]\Big). \tag{4.58}$$

At the one-loop level, the renormalized operators can just be replaced by one, $[O]=1$. Hence we find

$$\frac{a_s C_F}{\varepsilon}\left(\frac{1}{3}+\xi\right)=\gamma_2^{(0)}+\gamma_{1,1}^{(0)}+\gamma_{1,0}^{\mathcal{D},(0)}. \tag{4.59}$$

With $\gamma_2^{(0)}=C_F(\xi-1)$ and $\gamma_{1,1}^{(0)}=8/3C_F$ this leads to

$$\gamma_{1,0}^{\mathcal{D},(0)}=-\frac{4}{3}C_F. \tag{4.60}$$

A similar calculation for the spin-three operators yields

$$\gamma_{2,1}^{\mathcal{D},(0)}+\gamma_{2,0}^{\mathcal{D},(0)}=-2C_F. \tag{4.61}$$

So, we do not seem to have enough information to disentangle $\gamma_{2,1}^{\mathcal{D},(0)}$ from $\gamma_{2,0}^{\mathcal{D},(0)}$. Obviously the situation gets worse for higher-spin operators. We will see in the next section that this issue can be resolved because of relations between the anomalous dimensions in the total derivative basis.

4.3.3 Constraints on the anomalous dimensions

As we saw in the previous section, a naive implementation of the renormalization in off-forward kinematics is not enough to disentangle the anomalous dimensions. In this section, we discuss certain relations that exist between the operators in the total derivative basis, which lead to corresponding relations between the anomalous dimensions. This will culminate in an algorithm to construct the full (N,k) dependence of the anomalous dimensions, with the required input being the bare matrix elements of the operators *without* total derivatives and the forward anomalous dimensions. As before, we will use the one-loop calculations as a running example throughout this section.

Successive application of Eq.(4.29) to $O_{N,0,0}^{\mathcal{D}}$ allows us to derive the following relation between bare operators

$$O_{0,N,0}^{\mathcal{D}}-(-1)^N\sum_{j=0}^{N}(-1)^j\binom{N}{j}O_{j,0,N-j}^{\mathcal{D}}=0. \tag{4.62}$$

Upon using the renormalization equations, Eq.(4.31), this leads to a connection between the renormalized operators

$$\sum_{k=0}^{N}\sum_{j=k}^{N}\left[(-1)^k\binom{j}{k}Z^{\mathcal{D}}_{N,j}-(-1)^j\binom{N}{j}Z^{\mathcal{D}}_{j,k}\right][O^{\mathcal{D}}_{N-k,0,k}]=0. \tag{4.63}$$

Now, since the coefficient of $[O^{\mathcal{D}}_{N-k,0,k}]$ has to vanish for each value of k, this is equivalent to a relation between the renormalization constants

$$\forall k:\sum_{j=k}^{N}\left[(-1)^k\binom{j}{k}Z^{\mathcal{D}}_{N,j}-(-1)^j\binom{N}{j}Z^{\mathcal{D}}_{j,k}\right]=0 \tag{4.64}$$

which in turn implies a relation between the anomalous dimensions

$$\forall k:\sum_{j=k}^{N}\left[(-1)^k\binom{j}{k}\gamma^{\mathcal{D}}_{N,j}-(-1)^j\binom{N}{j}\gamma^{\mathcal{D}}_{j,k}\right]=0. \tag{4.65}$$

This is a general statement, valid to all orders in a_s.

We can now discover useful dependencies between the anomalous dimensions by choosing specific values for k in Eq.(4.65). Consider for example $k=N-1$. In the mixing matrix, this corresponds to the next-to-diagonal (NTD) elements $\{\gamma^{\mathcal{D}}_{1,0},\gamma^{\mathcal{D}}_{2,1},\ldots,\gamma^{\mathcal{D}}_{N,N-1}\}$. From our general relation, it follows that these NTD elements can be directly related to the forward anomalous dimensions[8]

$$\gamma^{\mathcal{D}}_{N,N-1}=\frac{N}{2}(\gamma_{N-1,N-1}-\gamma_{N,N}). \tag{4.66}$$

At one-loop order, using the expression for the forward anomalous dimensions Eq.(4.13), we find

$$\gamma^{\mathcal{D},(0)}_{N,N-1}=2C_F\left(\frac{1}{N+2}-1\right). \tag{4.67}$$

This reproduces the value for $\gamma^{\mathcal{D},(0)}_{1,0}$ we calculated in the previous section. For the spin-three sector, it gives

$$\gamma^{\mathcal{D},(0)}_{2,1}=-\frac{3}{2}C_F. \tag{4.68}$$

Combined with the condition we found for the renormalization of spin-three operators at one loop, Eq.(4.61), this leads to

$$\gamma^{\mathcal{D},(0)}_{2,0}=-\frac{1}{2}C_F. \tag{4.69}$$

Hence with the inclusion of the relation for the NTD elements, we are able to fix the one-loop spin-three mixing matrix completely. It is not enough however to fix the matrices for higher spins. For example, at spin-four we end up with

$$\gamma^{\mathcal{D},(0)}_{3,1}+\gamma^{\mathcal{D},(0)}_{3,0}=-\frac{13}{15}C_F. \tag{4.70}$$

[8] This relation was pointed out to us for low-N operators by J. Gracey in a private correspondence.

Another interesting choice for k in Eq.(4.65) is $k = 0$,

$$\sum_{j=0}^{N} \left[\gamma^{\mathcal{D}}_{N,j} - (-1)^j \binom{N}{j} \gamma^{\mathcal{D}}_{j,0} \right] = 0. \tag{4.71}$$

With a bit of algebra we can rewrite this as

$$\gamma^{\mathcal{D}}_{N,0} = (-1)^N \Big[\sum_{i=0}^{N} \gamma^{\mathcal{D}}_{N,i} - \sum_{j=1}^{N-1} (-1)^j \binom{N}{j} \gamma^{\mathcal{D}}_{j,0} \Big]. \tag{4.72}$$

Hence, for moment N, we can write $\gamma^{\mathcal{D}}_{N,0}$ in terms of $\gamma^{\mathcal{D}}_{M,0}$ ($M < N$) and the sum of the elements in the N-th row of the mixing matrix. Now, from the renormalization equation, Eq.(4.48), it can be seen that this sum is related to the $1/\varepsilon$-pole of the bare[9] matrix element of $O^{\mathcal{D}}_{N+1}$. We will denote this by $\mathcal{B}(N+1)$. Hence we have

$$\gamma^{\mathcal{D}}_{N,0} = (-1)^N \Big[\mathcal{B}(N+1) - \sum_{j=1}^{N-1} (-1)^j \binom{N}{j} \gamma^{\mathcal{D}}_{j,0} \Big]. \tag{4.73}$$

Using now that the binomial transform acts as a conjugation, cf. Section 3.2, we can rewrite this as

$$\gamma^{\mathcal{D}}_{N,0} = \sum_{i=0}^{N} (-1)^i \binom{N}{i} \mathcal{B}(i+1), \tag{4.74}$$

This relation implies that, whenever we are able to calculate the bare matrix elements of O_{N+1} (which does *not* have total derivatives acting on it), we can use these to recursively determine the last column of the mixing matrix. We again emphasize that this is an all-order statement. Although one might expect similar relations to hold for different values of k, this unfortunately is not the case, since for $k \neq 0$ the corresponding expression does not involve the sum of the anomalous dimensions by itself, but instead a weighted version of this. For example, the $k = 1$ relation involves

$$\sum_{i=0}^{N} i \gamma^{\mathcal{D}}_{N,i}, \tag{4.75}$$

which we cannot relate to the bare OMEs.

Let us again apply our findings to the one-loop case. At this order, the singular part of the bare matrix elements corresponds to

$$\sum_{i=0}^{N} \gamma^{\mathcal{D},(0)}_{N,i} + \gamma^{(0)}_{2} = \mathcal{B}^{(0)}(N+1) + \gamma^{(0)}_{2}. \tag{4.76}$$

Comparing with Eq.(4.56) then leads to

$$\mathcal{B}^{(0)}(N+1) = C_F \Big(2S_1(N+1) - \frac{2}{N+2} - 1 \Big). \tag{4.77}$$

[9]But the bare coupling constant and gauge parameter should already be replaced by their renormalized versions.

Hence, according to Eq.(4.74), the last column of the mixing matrix is determined by

$$\gamma^{\mathcal{D},(0)}_{N,0} = C_F \sum_{i=0}^{N} (-1)^i \binom{N}{i} \Big(2S_1(i+1) - \frac{2}{i+2} - 1 \Big). \tag{4.78}$$

These sums are easily evaluated using the results of Chapter 3, and we find

$$\gamma^{\mathcal{D},(0)}_{N,0} = 2C_F \left(\frac{1}{N+2} - \frac{1}{N} \right). \tag{4.79}$$

This agrees with the previously found expressions in the spin-two and spin-three sectors. Furthermore for the spin-four sector it implies

$$\gamma^{\mathcal{D},(0)}_{3,0} = -\frac{4}{15} C_F \tag{4.80}$$

and hence, cf. Eq.(4.70),

$$\gamma^{\mathcal{D},(0)}_{3,1} = -\frac{3}{5} C_F. \tag{4.81}$$

So, with the relations we derived for the elements in the NTD and the last column, we can completely fix the one-loop mixing matrix of spin-four operators. Of course, this statement is also valid *beyond* one-loop. Starting from the spin-five sector, there is not enough information to disentangle the anomalous dimensions.

Before continuing with our discussion, we want to mention that Eq.(4.71) can be used to derive an alternative relation between the anomalous dimensions in the Gegenbauer and total derivative bases. For, if we substitute Eq.(4.71) into Eq.(4.37) we obtain

$$\sum_{j=0}^{N} (-1)^j \frac{(j+2)!}{j!} \gamma^{\mathcal{G}}_{N,j} = \frac{1}{N!} \sum_{j=0}^{N} (-1)^j \binom{N}{j} \frac{(N+j+2)!}{(j+1)!} \sum_{l=0}^{j} (-1)^l \binom{j}{l} \gamma^{\mathcal{D}}_{l,0}. \tag{4.82}$$

Let us now have a closer look at the general consequences of Eq.(4.74). Because the binomial transform works as a conjugation, we have

$$\sum_{j=0}^{N} (-1)^j \binom{N}{j} \gamma^{\mathcal{D}}_{j,0} = \sum_{j=0}^{N} (-1)^j \binom{N}{j} \sum_{i=0}^{j} (-1)^i \binom{j}{i} \mathcal{B}(i+1) = \mathcal{B}(N+1) \tag{4.83}$$

and hence

$$\mathcal{B}(N+1) = \sum_{j=0}^{N} (-1)^j \binom{N}{j} \gamma^{\mathcal{D}}_{j,0}. \tag{4.84}$$

This is just Eq.(4.65) for $k=0$, see Eq.(4.71). Using this conjugation, we can repeat what we did for $k=0$ in the previous section for arbitrary k. The result is

$$\gamma^{\mathcal{D}}_{N,k} = \sum_{l=k}^{N} (-1)^l \binom{N}{l} \sum_{j=k}^{l} (-1)^k \binom{j}{k} \gamma^{\mathcal{D}}_{l,j}. \tag{4.85}$$

It will be useful to split off the diagonal piece of the mixing matrix, since this is known (at least in certain limits as discussed above)

$$\begin{aligned}\gamma^{\mathcal{D}}_{N,k} = &\binom{N}{k}\sum_{j=0}^{N-k}(-1)^j\binom{N-k}{j}\gamma_{j+k,j+k} \\ &+\sum_{j=k}^{N}(-1)^k\binom{j}{k}\sum_{l=j+1}^{N}(-1)^l\binom{N}{l}\gamma^{\mathcal{D}}_{l,j}.\end{aligned} \tag{4.86}$$

This is a very powerful relation. The only assumption made in its derivation was that we work in the chiral limit. In this limit, the relation is a direct consequence of the renormalization structure of the operators. This means that it can be used as an *order-independent* consistency check. Namely, if the mixing matrix in the total derivative basis has been obtained using some different method, its elements have to obey Eq.(4.86). Alternatively, it can be used to construct the full mixing matrix. To explicitly see this, let us put all the terms on the same side

$$\gamma^{\mathcal{D}}_{N,k} - \binom{N}{k}\sum_{j=0}^{N-k}(-1)^j\binom{N-k}{j}\gamma_{j+k,j+k} - \sum_{j=k}^{N}(-1)^k\binom{j}{k}\sum_{l=j+1}^{N}(-1)^l\binom{N}{l}\gamma^{\mathcal{D}}_{l,j} = 0. \tag{4.87}$$

Now, assuming we know the forward anomalous dimensions, we can, at least in principle, calculate the first sum. Then, based on the structure of the result, we can construct an Ansatz for the off-diagonal elements. The self-consistency of this Ansatz can then be checked by substituting it back into Eq.(4.87). The next-to-diagonal and the last column elements serve as boundary conditions in this procedure. This leads to the following 4-step algorithm for the determination of the mixing matrix:

1. Starting from the diagonal elements and the bare OMEs in Eq.(4.56), determine the all-N expressions for the elements in the NTD and last column of the mixing matrix.

2. Next, calculate the sum
$$\binom{N}{k}\sum_{j=0}^{N-k}(-1)^j\binom{N-k}{j}\gamma_{j+k,j+k}. \tag{4.88}$$
Based on the structure of the result, we can construct an Ansatz for the off-diagonal elements.

3. Calculate the double sum
$$\sum_{j=k}^{N}(-1)^k\binom{j}{k}\sum_{l=j+1}^{N}(-1)^l\binom{N}{l}\gamma^{\mathcal{D}}_{l,j} \tag{4.89}$$
of the Ansatz and collect everything into Eq.(4.87). This leads to a system of equations in the unknown coefficients of the Ansatz. The system is furthermore subject to the condition that the final result for $\gamma^{\mathcal{D}}_{N,k}$ should reduce to the previously found expressions for $k = N-1$ and $k = 0$. This ensures uniqueness of the result.

4. If the system of equations can be solved consistently, we have found the final expression for the elements of the mixing matrix. If not, there will be some remaining terms in Eq.(4.87). We can then use the structure of these terms to adapt the Ansatz, leading us back to step 3.

In the next chapters we will apply this algorithm to the calculation of the off-forward anomalous dimensions of non-singlet quark operators.

So far we only considered flavor non-singlet Wilson operators, which appear in the OPEs of DIS and DVCS. However, the concepts and methods introduced in this chapter do not actually depend on the Dirac structure of the operators. That is, Eq.(4.87) is valid for the mixing of any quark operator of the type

$$O = \overline{\psi}\lambda^{\alpha}\Gamma D_{\mu_1}\ldots D_{\mu_N}\psi \tag{4.90}$$

into total derivative operators. This will be illustrated in Chapter 6, where we will calculate the mixing matrix for the transversity operator, for which Γ is identified with a commutator of two Dirac matrices.

Chapter 5

Anomalous dimensions of Wilson operators[1]

Introduction

We now apply the algorithm derived in the previous chapter to calculate the anomalous dimensions of the non-singlet quark operators appearing in the OPE of DIS and DVCS. The anomalous dimensions will be presented in the total derivative basis. When possible, these results will be connected to results in the Gegenbauer and Geyer bases. For most of this chapter we work in the leading-n_f limit, $n_f \to \infty$, which introduces some simplifications in the structure of the mixing matrix. In this limit, we calculate the mixing matrix up to the five-loop level. Beyond the leading-n_f limit, we present the two-loop mixing matrix in the leading-color limit. For the sake of explicitness, we will always accompany the general expressions with the mixing matrix for spin-five operators. Finally, we present fixed moments up to order a_s^5 in full QCD.

The calculations of the anomalous dimensions in off-forward kinematics have a long history. In the Gegenbauer basis, the evolution kernel for the conformal calculation is known up to order a_s^3 [16–20]. The main bottleneck in this type of calculations is the determination of the *conformal anomaly*. For the total derivative basis, only low fixed moment results up to order a_s^3 were known before the advent of the algorithm discussed in this text. These calculations were done in the $\overline{\text{MS}}$-scheme as well as in the *regularization invariant* (RI) scheme [25, 26]. The latter renormalization scheme is well suited for direct comparisons with lattice results. Finally, in the Geyer basis, the mixing matrix is known to order a_s [23, 24].

5.1 The leading-n_f limit

Before discussing the results, we want to briefly comment on the leading-n_f limit. As was discussed in Section 4.2, the L-loop forward anomalous dimensions contain harmonic sums and denominators up to weight $2L-1$. This maximum weight reduces to L for the leading-n_f terms. Moreover, the leading-n_f part of the anomalous dimensions will only contain positive-index harmonic sums. Negative-index sums are generated when the set of Feynman diagrams to be considered also contains non-planar ones, i.e. diagrams with line crossings. However, as the leading-n_f limit only considers diagrams with a maximum number of one-loop insertions, such non-planar

[1] The results of this chapter were originally presented in [132].

diagrams are absent. Because of the form of the conjugation relation, Eq.(4.87), and its connection to the forward anomalous dimensions, we expect these simplifications to also hold for the off-diagonal elements of the ADM. This implies two simplifications for the application of our algorithm:

1. the number of possible structures in the off-diagonal part decreases considerably compared to the generic case,
2. in the absence of negative-index harmonic sums, the complexity of the sums we need to evaluate in Eq.(4.87) is greatly reduced.

5.2 One-loop anomalous dimensions

Let us first apply the algorithm to the one-loop OMEs. The corresponding expressions for the elements in the NTD and the last column have already been determined in the previous chapter, cf. Eqs.(4.67) and (4.79). For step two of the algorithm, we need to calculate

$$\begin{aligned}&\binom{N}{k}\sum_{j=0}^{N-k}(-1)^j\binom{N-k}{j}\gamma^{(0)}_{j+k,j+k}\\&=C_F\binom{N}{k}\sum_{j=0}^{N-k}(-1)^j\binom{N-k}{j}\left\{4S_1(j+k)+\frac{2}{j+k+2}+\frac{2}{j+k+1}-3\right\}.\end{aligned} \tag{5.1}$$

Using the expressions presented in Chapter 3 we find

$$\binom{N}{k}\sum_{j=0}^{N-k}(-1)^j\binom{N-k}{j}\gamma^{(0)}_{j+k,j+k}=C_F\left(\frac{-2(k+1)}{N+2}+\frac{2(k+2)}{N+1}-\frac{4}{N-k}\right). \tag{5.2}$$

Based on this result, we can now posit an Ansatz for the off-diagonal part of the mixing matrix. The simplest possibility is

$$\gamma^{\mathcal{D},(0)}_{N,k}=C_F\left(\frac{a_1}{N+2}+\frac{a_2}{N+1}+\frac{a_3}{N-k}\right) \tag{5.3}$$

with $a_i\in\mathbb{Q}$. Next we calculate the double sum in Eq.(4.89) for this Ansatz, giving

$$\begin{aligned}\frac{1}{C_F}\sum_{j=k}^{N}(-1)^k\binom{j}{k}\sum_{l=j+1}^{N}(-1)^l\binom{N}{l}\gamma^{\mathcal{D},(0)}_{l,j}&=a_1\left[\frac{-2-k}{N+1}+\frac{2+k}{N+2}\right]\\&\quad-\frac{a_2}{N+1}-\frac{a_3}{N-k}.\end{aligned} \tag{5.4}$$

Substituting into the conjugation relation, Eq.(4.87), leads to

$$\left(\frac{a_1}{N+2}+\frac{a_2}{N+1}+\frac{a_3}{N-k}\right)=\left(\frac{-2(k+1)}{N+2}+\frac{2(k+2)}{N+1}-\frac{4}{N-k}\right)$$

$$+a_1\left[\frac{-2-k}{N+1}+\frac{2+k}{N+2}\right]-\frac{a_2}{N+1}-\frac{a_3}{N-k}. \tag{5.5}$$

Solving for the unknowns and matching to the NTD and last column finally yields[2]

$$\gamma_{N,k}^{\mathcal{D},(0)}=C_F\left(\frac{2}{N+2}-\frac{2}{N-k}\right). \tag{5.6}$$

Hence the mixing matrix for the spin-five operators is of the following form

$$\hat{\gamma}_{N=5}^{\mathcal{D},(0)}=C_F\begin{pmatrix}\frac{91}{15} & -\frac{5}{3} & -\frac{2}{3} & -\frac{1}{3} & -\frac{1}{6}\\ 0 & \frac{157}{30} & -\frac{8}{5} & -\frac{3}{5} & -\frac{4}{15}\\ 0 & 0 & \frac{25}{6} & -\frac{3}{2} & -\frac{1}{2}\\ 0 & 0 & 0 & \frac{8}{3} & -\frac{4}{3}\\ 0 & 0 & 0 & 0 & 0\end{pmatrix}. \tag{5.7}$$

This agrees with the fixed moments calculated in [25]. In the Gegenbauer basis, the one-loop mixing matrix is simply diagonal [87, 133], i.e.

$$\gamma_{N,k}^{\mathcal{G},(0)}=0. \tag{5.8}$$

This means that at one-loop, the operators do not mix and hence simply renormalize multiplicatively. The spin-five mixing matrix is then

$$\hat{\gamma}_{N=5}^{\mathcal{G},(0)}=C_F\begin{pmatrix}\frac{91}{15} & 0 & 0 & 0 & 0\\ 0 & \frac{157}{30} & 0 & 0 & 0\\ 0 & 0 & \frac{25}{6} & 0 & 0\\ 0 & 0 & 0 & \frac{8}{3} & 0\\ 0 & 0 & 0 & 0 & 0\end{pmatrix}. \tag{5.9}$$

Combining this information with the expression in the total derivative basis, we have checked that the consistency relation connecting both bases, cf. Eq.(4.82), holds. Finally, at the one-loop level, we can also cross-check Eq.(5.6) with the corresponding expression in the Geyer basis. The result in the Geyer basis is [23, 24][3]

$$\gamma_{N,k}^{G,(0)}=-2C_F\left[\frac{1}{(N+1)(N+2)}+2\frac{k+1}{(N-k)(N+1)}\right]. \tag{5.10}$$

With our one-loop expression, the consistency relations for the Geyer basis, cf. Eqs.(4.46) and (4.47), are obeyed. For completeness, we also quote the mixing matrix for spin-five operators in

[2]Here and in the following, it is understood that $\gamma_{N,k}$ implies $k \neq N$.

[3]The expression presented here has an additional factor of -2 compared to [23, 24]. This is a consequence of different conventions used in defining the anomalous dimensions.

this basis

$$\hat{\gamma}^{G,(0)}_{N=5} = C_F \begin{pmatrix} \frac{91}{15} & -\frac{49}{15} & -\frac{19}{15} & -\frac{3}{5} & -\frac{4}{15} \\ 0 & \frac{157}{30} & -\frac{31}{10} & -\frac{11}{10} & -\frac{13}{30} \\ 0 & 0 & \frac{25}{6} & -\frac{17}{6} & -\frac{5}{6} \\ 0 & 0 & 0 & \frac{8}{3} & -\frac{7}{3} \\ 0 & 0 & 0 & 0 & 0 \end{pmatrix}. \tag{5.11}$$

5.3 Two-loop anomalous dimensions

Beyond order a_s in perturbation theory, also the mixing matrix in the Gegenbauer basis gets non-trivial off-diagonal elements. The general expression is [16, 18]

$$\hat{\gamma}^{\mathcal{G}}(a_s) = \mathbf{G}\left\{[\hat{\gamma}^{\mathcal{G}}(a_s), \hat{b}]\left(\frac{1}{2}\hat{\gamma}^{\mathcal{G}}(a_s) + \beta(a_s)\right) + [\hat{\gamma}^{\mathcal{G}}(a_s), \hat{w}(a_s)]\right\}. \tag{5.12}$$

Here $[\cdot,\cdot]$ represents the usual matrix commutator. The quantity $\mathbf{G}$ is defined as

$$\mathbf{G}\{\hat{\mathbf{M}}\}_{N,k} = -\frac{M_{N,k}}{a(N,k)}. \tag{5.13}$$

Finally we have

$$a(N,k) = (N-k)(N+k+3), \tag{5.14}$$

$$b_{N,k} = -2k\delta_{N,k} - 2(2k+3)\vartheta_{N,k} \tag{5.15}$$

with ϑ the discrete step-function,

$$\vartheta_{N,k} \equiv \begin{cases} 1 & \text{if } N-k>0 \text{ and even} \\ 0 & \text{else.} \end{cases} \tag{5.16}$$

The appearance of the step-function is a consequence of the fact that only CP-even operators are considered in the Gegenbauer basis. The matrix $\hat{w}(a_s)$ is the so-called *conformal anomaly*, and can be calculated perturbatively in the strong coupling

$$\hat{w}(a_s) = a_s\hat{w}^{(0)} + a_s^2\hat{w}^{(1)} + \ldots. \tag{5.17}$$

It represents the fact that, for physical QCD, conformal symmetry is broken by quantum corrections. If one is interested in the ADM at order a_s^L, the conformal anomaly is only needed up to order a_s^{L-1} [21]. Currently its analytic expression in Mellin (N,k)-space is known up to order a_s^2 [22].

At two-loop order, the general expression Eq.(5.12) reduces to [16]

$$\gamma^{\mathcal{G},(1)}_{N,k} = -\frac{\gamma^{(0)}_{N,N} - \gamma^{(0)}_{k,k}}{a(N,k)}\left\{-2(2k+3)\left(\beta_0 + \frac{1}{2}\gamma^{(0)}_{k,k}\right)\vartheta_{N,k} + w^{(0)}_{N,k}\right\} \tag{5.18}$$

for the off-diagonal elements of the mixing matrix. Since we concentrate on the leading-n_f contributions, we only have to take into account the terms proportional to β_0. The corresponding spin-five mixing matrix is then

$$\hat{\gamma}^{\mathcal{G},(1)}_{N=5} = -n_f C_F \begin{pmatrix} \frac{7783}{1350} & 0 & \frac{133}{135} & 0 & \frac{13}{15} \\ 0 & \frac{13271}{2700} & 0 & \frac{11}{9} & 0 \\ 0 & 0 & \frac{415}{108} & 0 & \frac{5}{3} \\ 0 & 0 & 0 & \frac{64}{27} & 0 \\ 0 & 0 & 0 & 0 & 0 \end{pmatrix}. \tag{5.19}$$

Let us now discuss the application of our algorithm in the total derivative basis. The leading-n_f piece of the two-loop forward anomalous dimension is

$$\begin{aligned} \gamma^{(1)}_{N,N} = \frac{4}{3} n_f C_F \Bigg[& \frac{1}{4} + \frac{11}{3}\left(\frac{1}{N+1}\right) - \left(\frac{1}{N+1}\right)^2 - \frac{11}{3}\left(\frac{1}{N+2}\right) \\ & + \left(\frac{1}{N+2}\right)^2 - \frac{10}{3} S_1(N+1) + 2 S_2(N+1) \Bigg]. \end{aligned} \tag{5.20}$$

Applying Eq.(4.66) leads to the following expression for the elements of the NTD

$$\gamma^{\mathcal{D},(1)}_{N,N-1} = \frac{4}{3} n_f C_F \left(\frac{1}{(N+2)^2} - \frac{25}{6}\frac{1}{N+2} + \frac{2}{N+1} - \frac{1}{2N} + \frac{5}{3} \right). \tag{5.21}$$

According to the renormalization pattern of the quark operators, Eq.(4.48), the $1/\varepsilon$-pole of the bare matrix elements should correspond to

$$\frac{1}{2}\left(\mathcal{B}^{(1)}(N+1) + \gamma^{(1)}_2 \right) \tag{5.22}$$

where we recall that

$$\mathcal{B}^{(L)}(N+1) \equiv \sum_{i=0}^{N} \gamma^{(L)}_{N,i}. \tag{5.23}$$

A calculation of the leading-n_f Feynman diagrams gives

$$\mathcal{B}^{(1)}(N+1) = \frac{2}{3} S_2(N+1) - \frac{10}{9} S_1(N+1) - \frac{2}{3}\frac{1}{(N+2)^2} - \frac{16}{9}\frac{N+1}{N+2} + 2. \tag{5.24}$$

Using Eq.(4.74) and the methods described in Chapter 3 we then find

$$\begin{aligned} \gamma^{\mathcal{D},(1)}_{N,0} = & \frac{4}{3}\left(\frac{1}{N+2} - \frac{1}{N+1} \right) S_1(N+2) + \frac{4}{3}\frac{1}{N+1} S_1(N+1) \\ & - \frac{4}{3}\frac{1}{N} S_1(N) - \frac{44}{9}\frac{1}{N+2} + \frac{8}{3}\frac{1}{N+1} + \frac{20}{9}\frac{1}{N}. \end{aligned} \tag{5.25}$$

Next we calculate the sum of the diagonal elements, Eq.(4.88),

$$
\begin{aligned}
&\binom{N}{k}\sum_{j=0}^{N-k}(-1)^j\binom{N-k}{j}\gamma^{(1)}_{j+k,j+k} \\
=&n_fC_F\Bigg[-\frac{4}{3}\frac{1}{(N+2)^2}(k+1)+\frac{1}{(N+1)^2}(2+k)+\frac{4}{3}\frac{1}{N+2}\Bigg(\frac{14}{3}+\frac{11}{3}k \\
&+(k+1)[S_1(k)-S_1(N)]\Bigg)-\frac{4}{3}\frac{1}{N+1}\Bigg(\frac{13}{9}+\frac{11}{9}k+(k+2)[S_1(k) \\
&-S_1(N)]\Bigg)+\frac{8}{3}\frac{1}{N-k}\Bigg(\frac{5}{3}+[S_1(k)-S_1(N)]\Bigg)\Bigg].
\end{aligned}
\tag{5.26}
$$

Based on this result, we choose the following basis for the off-diagonal elements

$$
\begin{aligned}
&\Bigg\{\frac{1}{(N+2)^2},\frac{1}{(N+1)^2},\frac{S_1(N)}{N+2},\frac{S_1(k)}{N+2},\frac{S_1(N)}{N+1},\frac{S_1(k)}{N+1},\frac{S_1(N)}{N-k},\frac{S_1(k)}{N-k}, \\
&\frac{1}{N+2},\frac{1}{N+1},\frac{1}{N-k}\Bigg\}.
\end{aligned}
\tag{5.27}
$$

The corresponding double sums can be evaluated using SIGMA . Solving the system of equations following from the conjugation relation then leads to the following expression for the two-loop anomalous dimensions

$$
\begin{aligned}
\gamma^{\mathcal{D},(1)}_{N,k} = \frac{4}{3}n_fC_F\Bigg\{&\Big(S_1(N)-S_1(k)\Big)\Big(\frac{1}{N+2}-\frac{1}{N-k}\Big) \\
&+\frac{5}{3}\frac{1}{N-k}+\frac{2}{N+1}-\frac{11}{3}\frac{1}{N+2}+\frac{1}{(N+2)^2}\Bigg\}.
\end{aligned}
\tag{5.28}
$$

We have tested the consistency of this expression with the Gegenbauer moments using Eq.(4.82). Furthermore, we find agreement with the results for spin-two and -three operators presented in [25]. The spin-five ADM is

$$
\hat{\gamma}^{\mathcal{D},(1)}_{N=5} = n_fC_F\begin{pmatrix}
-\frac{7783}{1350} & \frac{17}{10} & \frac{82}{135} & \frac{23}{90} & \frac{43}{540} \\
0 & -\frac{13271}{2700} & \frac{362}{225} & \frac{13}{25} & \frac{106}{675} \\
0 & 0 & -\frac{415}{108} & \frac{53}{36} & \frac{13}{36} \\
0 & 0 & 0 & -\frac{64}{27} & \frac{32}{27} \\
0 & 0 & 0 & 0 & 0
\end{pmatrix}.
\tag{5.29}
$$

It is instructive to also express the Gegenbauer anomalous dimensions in terms of harmonic sums and denominators. Such an expression can be easily found using our conjugation relation. As we checked that our result in the total derivative basis is consistent with the Gegenbauer moments using Eq.(4.82), we can now use the same relation to write down the general (N,k) expression in the Gegenbauer basis. The procedure is the following. First, we construct an Ansatz of the appropriate weight. Then we can feed this Ansatz and the last column in the total derivative basis to the consistency relation connecting both bases, Eq.(4.82). This fixes most, but not all, of the unknown coefficients in the Ansatz. A unique expression is obtained by matching the result to a low number of fixed moments, which can be calculated using Eq.(5.12). We find

$$\begin{aligned}\gamma_{N,k}^{\mathcal{G},(1)} &= \frac{8}{3}\frac{n_f C_F}{a(N,k)}\vartheta_{N,k}\Bigg\{-2\Big(S_1(N)-S_1(k)\Big)(2k+3) \\ &\quad -(2k+3)\Big(\frac{1}{N+1}+\frac{1}{N+2}\Big)+4+\frac{1}{k+1}-\frac{1}{k+2}\Bigg\}.\end{aligned} \tag{5.30}$$

5.4 Three-loop anomalous dimensions

The Gegenbauer anomalous dimensions are again determined by Eq.(5.12). Explicitly we have

$$\begin{aligned}\hat{\gamma}^{\mathcal{G},(2)} &= \mathbf{G}\Bigg\{[\hat{\gamma}^{\mathcal{G},(1)},\hat{b}]\Big(\frac{1}{2}\hat{\gamma}^{\mathcal{G},(0)}+\beta_0\Big)+[\hat{\gamma}^{\mathcal{G},(1)},\hat{w}^{(0)}]+[\hat{\gamma}^{\mathcal{G},(0)},\hat{b}]\Big(\frac{1}{2}\hat{\gamma}^{\mathcal{G},(1)}+\beta_1\Big) \\ &\quad +[\hat{\gamma}^{\mathcal{G},(0)},\hat{w}^{(1)}]\Bigg\}.\end{aligned} \tag{5.31}$$

As mentioned above, the three-loop Mellin space expression for the conformal anomaly is currently not known. Moreover, in the literature only implicit expressions like Eq.(5.31) are given. The expansions presented in this work in terms of harmonic sums are new.

As before, in the leading-n_f limit it suffices to take into account only the term proportional to β_0. In terms of harmonic sums we then find

$$\begin{aligned}\gamma_{N,k}^{\mathcal{G},(2)} &= \frac{32}{9}\frac{n_f^2 C_F}{a(N,k)}\vartheta_{N,k}\Bigg\{-\Big(S_1(N)-S_1(k)\Big)^2(2k+3) \\ &\quad +\Big(S_1(N)-S_1(k)\Big)(2k+3)\Big(\frac{5}{3}-\frac{1}{N+1}-\frac{1}{N+2}\Big) \\ &\quad +\Big(S_1(N)-S_1(k)\Big)\Big(4+\frac{1}{k+1}-\frac{1}{k+2}\Big)+(2k+3)\Big(-\frac{1}{6}\frac{1}{N+1}-\frac{1}{2}\frac{1}{(N+1)^2} \\ &\quad +\frac{11}{6}\frac{1}{N+2}-\frac{1}{2}\frac{1}{(N+2)^2}\Big)-\frac{10}{3}+\frac{2}{N+1}+\frac{1}{N+1}\frac{1}{k+1}-\frac{5}{6}\frac{1}{k+1}-\frac{1}{2}\frac{1}{(k+1)^2} \\ &\quad +\frac{2}{N+2}-\frac{1}{N+2}\frac{1}{k+2}+\frac{5}{6}\frac{1}{k+2}+\frac{1}{2}\frac{1}{(k+2)^2}\Bigg\}.\end{aligned} \tag{5.32}$$

For the spin-five operators this implies

$$\hat{\gamma}^{\mathcal{G},(2)}_{N=5} = n_f^2 C_F \begin{pmatrix} -\frac{215621}{121500} & 0 & \frac{10339}{12150} & 0 & \frac{329}{1350} \\ 0 & -\frac{384277}{243000} & 0 & \frac{793}{810} & 0 \\ 0 & 0 & -\frac{2569}{1944} & 0 & \frac{59}{54} \\ 0 & 0 & 0 & -\frac{224}{243} & 0 \\ 0 & 0 & 0 & 0 & 0 \end{pmatrix} . \tag{5.33}$$

Consider now the operators in the total derivative basis. The three-loop forward anomalous dimensions are, in the leading-n_f limit

$$\begin{aligned} \gamma^{(2)}_{N,N} = \frac{8}{9} n_f^2 C_F \Bigg(& -\frac{2}{3} S_1(N) - \frac{10}{3} S_2(N) + 2 S_3(N) + \frac{1}{(N+1)^3} \\ & + \frac{1}{3}\frac{1}{(N+1)^2} - \frac{14}{3}\frac{1}{N+1} + \frac{1}{(N+2)^3} - \frac{11}{3}\frac{1}{(N+2)^2} \\ & + \frac{4}{N+2} + \frac{17}{8} \Bigg). \end{aligned} \tag{5.34}$$

Applying Eq.(4.66) then leads to

$$\begin{aligned} \gamma^{\mathcal{D},(2)}_{N,N-1} = \frac{8}{9} n_f^2 C_F \Bigg(& \frac{1}{(N+2)^3} - \frac{1}{2N^2} + \frac{2}{(N+1)^2} - \frac{25}{6}\frac{1}{(N+2)^2} \\ & + \frac{11}{6}\frac{1}{N} - \frac{19}{3}\frac{1}{N+1} + \frac{35}{6}\frac{1}{N+2} + \frac{1}{3} \Bigg). \end{aligned} \tag{5.35}$$

Next we determine the last column of the mixing matrix. From the calculation of the bare matrix elements and Eq.(4.74) we find

$$\begin{aligned} \gamma^{(2)}_{N,0} = \frac{8}{9} n_f^2 C_F \Bigg(& \frac{1}{(N+2)^3} + \frac{S_1(N+1)}{(N+2)^2} + \frac{S_{1,1}(N)}{N+2} - \frac{S_{1,1}(N)}{N} \\ & + \frac{2 S_1(N+1)}{N+1} + \frac{1}{(N+2)^2} - \frac{11}{3}\frac{S_1(N+2)}{N+2} \\ & + \frac{5}{3}\frac{S_1(N)}{N} - \frac{5}{3}\frac{1}{N+1} + \frac{4}{3}\frac{1}{N+2} + \frac{1}{3}\frac{1}{N} \Bigg). \end{aligned} \tag{5.36}$$

Using the remaining steps of our algorithm fixes the final form of the off-diagonal entries to be

$$\begin{aligned} \gamma^{\mathcal{D},(2)}_{N,k} = \frac{4}{9} n_f^2 C_F \Bigg\{ & \Big(S_1(N) - S_1(k)\Big)^2 \Big(\frac{1}{N+2} - \frac{1}{N-k}\Big) + 2\Big(S_1(N) - S_1(k)\Big)\Big(\frac{5}{3}\frac{1}{N-k} \\ & + \frac{2}{N+1} - \frac{11}{3}\frac{1}{N+2} + \frac{1}{(N+2)^2}\Big) + \Big(S_2(N) - S_2(k)\Big)\Big(\frac{1}{N+2} - \frac{1}{N-k}\Big) \\ & + \frac{2}{3}\frac{1}{N-k} - \frac{26}{3}\frac{1}{N+1} + \frac{4}{(N+1)^2} + \frac{8}{N+2} - \frac{22}{3}\frac{1}{(N+2)^2} + \frac{2}{(N+2)^3} \Bigg\}. \end{aligned} \tag{5.37}$$

Hence for spin five we have

$$\hat{\gamma}^{\mathcal{D},(2)}_{N=5} = n_f^2 C_F \begin{pmatrix} -\frac{215621}{121500} & \frac{3131}{8100} & \frac{1312}{6075} & \frac{1181}{8100} & \frac{4841}{48600} \\ 0 & -\frac{384277}{243000} & \frac{3947}{10125} & \frac{734}{3375} & \frac{4411}{30375} \\ 0 & 0 & -\frac{2569}{1944} & \frac{259}{648} & \frac{151}{648} \\ 0 & 0 & 0 & -\frac{224}{243} & \frac{112}{243} \\ 0 & 0 & 0 & 0 & 0 \end{pmatrix}. \tag{5.38}$$

It was checked that the three-loop expressions presented here obey the consistency relation in Eq.(4.82). Additionally, the results in the total derivative basis agree with the analytical calculation of the spin-two matrix in [25] and a numerical calculation of the spin-three one in [26].

5.5 Four-loop anomalous dimensions

We begin our discussion in the total derivative basis. Starting at this order in perturbation theory, factors of the Riemann-zeta function start contributing, cf. Eq.(3.5). In particular, at order a_s^4 we expect ζ_3 to appear. Now, since the zeta-function carries its own weight, the remaining factor multiplying it will be of lower weight. At four loops, the leading-n_f term has $w_{\max} = 4$, such that the factor multiplying ζ_3 in this approximation will only have $w_{\max} = 1$. Hence, using our algorithm the determination of such a term has the complexity of a one-loop calculation. We quickly find

$$\gamma^{\mathcal{D},(3)}_{N,k}\bigg|_{\zeta_3} = \frac{32}{27} n_f^3 C_F \zeta_3 \left(\frac{1}{N+2} - \frac{1}{N-k} \right) \tag{5.39}$$

and for the spin-five operators

$$\hat{\gamma}^{\mathcal{D},(3)}_{N=5}\bigg|_{\zeta_3} = n_f^3 C_F \zeta_3 \begin{pmatrix} \frac{1456}{405} & -\frac{80}{81} & -\frac{32}{81} & -\frac{16}{81} & -\frac{8}{81} \\ 0 & \frac{1256}{405} & -\frac{128}{135} & -\frac{16}{45} & -\frac{64}{405} \\ 0 & 0 & \frac{200}{81} & -\frac{8}{9} & -\frac{8}{27} \\ 0 & 0 & 0 & \frac{128}{81} & -\frac{64}{81} \\ 0 & 0 & 0 & 0 & 0 \end{pmatrix}. \tag{5.40}$$

For the terms without ζ_3 our algorithm yields

$$
\begin{aligned}
\gamma_{N,k}^{\mathcal{D},(3)} = \frac{8}{27} n_f^3 C_F \Bigg\{ & \frac{1}{3}\Big(S_1(N)-S_1(k)\Big)^3 \Big(\frac{1}{N+2}-\frac{1}{N-k}\Big) + \Big(S_1(N)-S_1(k)\Big)^2 \Big(\frac{5}{3}\frac{1}{N-k} \\
& + \frac{2}{N+1} - \frac{11}{3}\frac{1}{N+2} + \frac{1}{(N+2)^2}\Big) + \Big(S_1(N)-S_1(k)\Big)\Big(S_2(N)-S_2(k)\Big)\Big(\frac{1}{N+2} \\
& - \frac{1}{N-k}\Big) + 2\Big(S_1(N)-S_1(k)\Big)\Big(\frac{1}{3}\frac{1}{N-k} - \frac{13}{3}\frac{1}{N+1} + \frac{2}{(N+1)^2} + \frac{4}{N+2} \\
& - \frac{11}{3}\frac{1}{(N+2)^2} + \frac{1}{(N+2)^3}\Big) + \Big(S_2(N)-S_2(k)\Big)\Big(\frac{5}{3}\frac{1}{N-k} + \frac{2}{N+1} - \frac{11}{3}\frac{1}{N+2} \\
& + \frac{1}{(N+2)^2}\Big) + \frac{2}{3}\Big(S_3(N)-S_3(k)\Big)\Big(\frac{1}{N+2} - \frac{1}{N-k}\Big) + \frac{2}{3}\frac{1}{N-k} + \frac{2}{N+1} \\
& - \frac{26}{3}\frac{1}{(N+1)^2} + \frac{4}{(N+1)^3} - \frac{8}{3}\frac{1}{N+2} + \frac{8}{(N+2)^2} - \frac{22}{3}\frac{1}{(N+2)^3} + \frac{2}{(N+2)^4} \Bigg\},
\end{aligned}
\tag{5.41}
$$

such that

$$
\hat{\gamma}_{N=5}^{\mathcal{D},(3)} = n_f^3 C_F \begin{pmatrix}
-\frac{10064827}{10935000} & \frac{154397}{729000} & \frac{30097}{273375} & \frac{18049}{243000} & \frac{285967}{4374000} \\
0 & -\frac{17813699}{21870000} & \frac{191989}{911250} & \frac{32683}{303750} & \frac{237557}{2733750} \\
0 & 0 & -\frac{23587}{34992} & \frac{2401}{11664} & \frac{1477}{11664} \\
0 & 0 & 0 & -\frac{1024}{2187} & \frac{512}{2187} \\
0 & 0 & 0 & 0 & 0
\end{pmatrix}. \tag{5.42}
$$

Let us now turn to the mixing matrix in the Gegenbauer basis. At this order in perturbation theory, the Gegenbauer anomalous dimensions are not given in the literature. However, they can be calculated in the same way as the lower-order ones. In particular, they are calculable in terms of the one-loop beta function and the three-loop forward anomalous dimensions. Since these quantities do not depend on ζ_3, we can immediately conclude that

$$
\gamma_{N,k}^{\mathcal{G},(3)}\Big|_{\zeta_3} = 0. \tag{5.43}
$$

As in the total derivative basis, this parallels the one-loop expressions. For the spin-five operators this means that we simply have

$$
\hat{\gamma}_{N=5}^{\mathcal{G},(3)}\Big|_{\zeta_3} = n_f^3 C_F \zeta_3 \begin{pmatrix}
\frac{1456}{405} & 0 & 0 & 0 & 0 \\
0 & \frac{1256}{405} & 0 & 0 & 0 \\
0 & 0 & \frac{200}{81} & 0 & 0 \\
0 & 0 & 0 & \frac{128}{81} & 0 \\
0 & 0 & 0 & 0 & 0
\end{pmatrix}. \tag{5.44}
$$

For the determination of the ζ_3-independent terms as a function of harmonic sums we follow the same procedure as in the previous sections, leading to

$$\begin{aligned}
\gamma_{N,k}^{\mathcal{G},(3)} &= \frac{64}{27}\frac{n_f^3 C_F}{a(N,k)}\vartheta_{N,k}\Bigg\{-\frac{2}{3}\Big(S_1(N)-S_1(k)\Big)^3(2k+3)+\Big(S_1(N)-S_1(k)\Big)^2(2k+3)\Big(\frac{5}{3}\\
&\quad -\frac{1}{N+1}-\frac{1}{N+2}\Big)+\Big(S_1(N)-S_1(k)\Big)^2\Big(4+\frac{1}{k+1}-\frac{1}{k+2}\Big)+\Big(S_1(N)\\
&\quad -S_1(k)\Big)(2k+3)\Big(\frac{1}{3}-\frac{1}{3}\frac{1}{N+1}-\frac{1}{(N+1)^2}+\frac{11}{3}\frac{1}{N+2}-\frac{1}{(N+2)^2}\Big)+\Big(S_1(N)\\
&\quad -S_1(k)\Big)\Big(-\frac{20}{3}+\frac{4}{N+1}+\frac{2}{N+1}\frac{1}{k+1}-\frac{5}{3}\frac{1}{k+1}-\frac{1}{(k+1)^2}+\frac{4}{N+2}\\
&\quad -\frac{2}{N+2}\frac{1}{k+2}+\frac{5}{3}\frac{1}{k+2}+\frac{1}{(k+2)^2}\Big)+(2k+3)\Big(\frac{7}{3}\frac{1}{N+1}-\frac{1}{6}\frac{1}{(N+1)^2}\\
&\quad -\frac{1}{2}\frac{1}{(N+1)^3}-\frac{2}{N+2}+\frac{11}{6}\frac{1}{(N+2)^2}-\frac{1}{2}\frac{1}{(N+2)^3}-\frac{1}{3}\Big(S_3(N)-S_3(k)\Big)\Big)-\frac{2}{3}\\
&\quad +\frac{2}{3}\frac{1}{N+1}+\frac{2}{(N+1)^2}+\frac{1}{(N+1)^2}\frac{1}{k+1}-\frac{5}{3}\frac{1}{N+1}\frac{1}{k+1}-\frac{1}{N+1}\frac{1}{(k+1)^2}\\
&\quad -\frac{8}{3}\frac{1}{k+1}+\frac{5}{6}\frac{1}{(k+1)^2}+\frac{1}{2}\frac{1}{(k+1)^3}-\frac{22}{3}\frac{1}{N+2}+\frac{2}{(N+2)^2}-\frac{1}{(N+2)^2}\frac{1}{k+2}\\
&\quad +\frac{5}{3}\frac{1}{N+2}\frac{1}{k+2}+\frac{1}{N+2}\frac{1}{(k+2)^2}+\frac{5}{3}\frac{1}{k+2}-\frac{5}{6}\frac{1}{(k+2)^2}-\frac{1}{2}\frac{1}{(k+2)^3}\Bigg\}
\end{aligned} \tag{5.45}$$

and

$$\hat{\gamma}_{N=5}^{\mathcal{G},(3)} = n_f^3 C_F \begin{pmatrix} -\frac{10064827}{10935000} & 0 & \frac{394793}{1093500} & 0 & \frac{65923}{121500} \\ 0 & -\frac{17813699}{21870000} & 0 & \frac{36491}{72900} & 0 \\ 0 & 0 & -\frac{23587}{34992} & 0 & \frac{797}{972} \\ 0 & 0 & 0 & -\frac{1024}{2187} & 0 \\ 0 & 0 & 0 & 0 & 0 \end{pmatrix}. \tag{5.46}$$

5.6 Discussion of the results in the total derivative basis

Having presented the leading-n_f anomalous dimensions up to order a_s^4, we can make some general statements for the ζ-independent terms of the L-loop off-diagonal elements of the mixing matrix. For this discussion it is convenient to define

$$b_0 \equiv -\beta_0\Big|_{n_f} = \frac{2}{3}n_f. \tag{5.47}$$

- The leading-n_f anomalous dimensions are simple combinations of harmonic sums and denominators. Denominators in $k+m$ are absent, while the denominators in N come with the shifts $m = 1, 2, -k$. The prefactors of the appearing structures are simple rational numbers, which can be written as

$$\frac{a \cdot 2^b}{3^c} \tag{5.48}$$

with $a \in \mathbb{Z}$ and $b, c \in \mathbb{N}$. Furthermore, the maximum power of denominators in N is $w_{\max} = L$ while the maximum power of denominators in $N-k$ is simply one.

- Except for $\frac{1}{N-k}$, pure functions in $N-k$ are absent. With a pure function we mean a structure of the form

  $$\frac{f(N-k)}{(N-k)^m}. \tag{5.49}$$

  A nice consequence of this is that, when considering $k = N-1$, the only way a constant can appear is through a denominator $\frac{1}{N-k}$ in the full (N,k) expression. Explicitly, we can identify

  $$\alpha \cdot \text{ constant in NTD } \iff \frac{\alpha}{N-k} \text{ in } \gamma^{\mathcal{D}}_{N,k}. \tag{5.50}$$

  A similar reasoning applies to the $\frac{1}{N}$ term in $\gamma^{\mathcal{D}}_{N,0}$.

- The prefactor of $\frac{1}{(N+2)^L}$ can be written as

  $$2C_F b_0^{L-1}. \tag{5.51}$$

- Starting at order a_s^2 a term of the form $S_{L-1}(N) - S_{L-1}(k)$ appears with prefactor

  $$\frac{b_0^{L-1}}{L-1}\gamma^{\mathcal{D},(0)}_{N,k} \quad (L > 1). \tag{5.52}$$

  Similarly we also find a term of the form $[S_1(N) - S_1(k)]^{L-1}$ with prefactor

  $$\frac{b_0^{L-1}}{(L-1)!}\gamma^{\mathcal{D},(0)}_{N,k} \quad (L > 1). \tag{5.53}$$

- The prefactors of the differences $[S_1(N) - S_1(k)]^{\alpha}$, with $0 < \alpha < L-1$ can be determined as a function of the prefactors of the $[S_1(N) - S_1(k)]^{\alpha-1}$ terms in the $(L-1)$-loop anomalous dimension. Specifically we have

  $$\left.\frac{b_0}{\alpha}\gamma^{\mathcal{D},(L-2)}_{N,k}\right|_{[S_1(N)-S_1(k)]^{\alpha-1}} \quad (0 < \alpha < L-1). \tag{5.54}$$

  This also works for products of differences of harmonic sums. For example, the prefactor of $[S_2(N) - S_2(k)][S_1(N) - S_1(k)]$ at four loops corresponds to b_0 times the prefactor of the $[S_2(N) - S_2(k)]$ term at three loops. It is likely that the prefactors of $[S_{\alpha}(N) - S_{\alpha}(k)]$ follow a similar pattern. However, not enough information is available at this point to make strong claims.

- Finally, we can say something about denominators in N. If at the L-loop level the term

$$\frac{1}{(N+m)^{\delta}} \quad (m=1,2) \tag{5.55}$$

appears, then the $(L+1)$-loop expression will contain the term

$$\frac{b_0}{(N+m)^{\delta+1}} \quad (\delta \neq L). \tag{5.56}$$

From the above considerations it follows that, if the L-loop anomalous dimensions are known, we can predict most of the structures and their prefactors appearing in the $(L+1)$-loop expression. The small number of unknowns that remain can then be fixed using the consistency relation, Eq.(4.87). As the leading-n_f terms of the forward anomalous dimensions are known to all orders in perturbation theory, cf. [122], it is then, in principle, possible to reconstruct the full (N,k) dependence of the ζ-independent terms of the mixing matrix to all orders.

5.6.1 Application: Five-loop anomalous dimensions

To illustrate the discussion presented above, we calculate the ζ-independent part of the leading-n_f terms of the five-loop mixing matrix. To achieve this we also need the five-loop forward anomalous dimension, which is presented in [122]. Following the steps described above, only six terms remain whose prefactors are unknown. These are

$$\begin{aligned}
\Bigg\{ & \frac{1}{N+2}, \frac{1}{N+1}, \frac{1}{N-k}, \\
& [S_2(N)-S_2(k)]\Big(\frac{1}{3}\frac{1}{N-k} - \frac{13}{3}\frac{1}{N+1} + \frac{2}{(N+1)^2} + \frac{4}{N+2} - \frac{11}{3}\frac{1}{(N+2)^2} + \frac{1}{(N+2)^3}\Big), \\
& [S_3(N)-S_3(k)]\Big(\frac{5}{3}\frac{1}{N-k} + \frac{2}{N+1} - \frac{11}{3}\frac{1}{N+2} + \frac{1}{(N+2)^2}\Big), \\
& [S_2(N)-S_2(k)]^2\Big(\frac{1}{N+2} - \frac{1}{N-k}\Big)\Bigg\}.
\end{aligned} \tag{5.57}$$

Evaluating the consistency relation, Eq.(4.87), for (N,k)-pairs up to $N=4$ we then find

$$\begin{aligned}
\gamma^{\mathcal{D},(4)}_{N,k} = \; & \frac{16}{81} n_f^4 C_F \Bigg\{ \frac{1}{12}\Big(S_1(N)-S_1(k)\Big)^4 \Big(\frac{1}{N+2} - \frac{1}{N-k}\Big) \\
& + \frac{1}{3}\Big(S_1(N)-S_1(k)\Big)^3 \Big(\frac{5}{3}\frac{1}{N-k} + \frac{2}{N+1} - \frac{11}{3}\frac{1}{N+2} + \frac{1}{(N+2)^2}\Big) \\
& + \frac{1}{2}\Big(S_1(N)-S_1(k)\Big)^2 \Big(S_2(N)-S_2(k)\Big)\Big(\frac{1}{N+2} - \frac{1}{N-k}\Big) \\
& + \Big(S_1(N)-S_1(k)\Big)^2 \Big(\frac{1}{3}\frac{1}{N-k} - \frac{13}{3}\frac{1}{N+1} + \frac{2}{(N+1)^2} + \frac{4}{N+2} \\
& - \frac{11}{3}\frac{1}{(N+2)^2} + \frac{1}{(N+2)^3}\Big)
\end{aligned}$$

$$
\begin{aligned}
&+\Big(S_1(N)-S_1(k)\Big)\Big(S_2(N)-S_2(k)\Big)\Big(\frac{5}{3}\frac{1}{N-k}+\frac{2}{N+1}-\frac{11}{3}\frac{1}{N+2}+\frac{1}{(N+2)^2}\Big)\\
&+\frac{2}{3}\Big(S_1(N)-S_1(k)\Big)\Big(S_3(N)-S_3(k)\Big)\Big(\frac{1}{N+2}-\frac{1}{N-k}\Big)\\
&+\Big(S_1(N)-S_1(k)\Big)\Big(\frac{2}{3}\frac{1}{N-k}+\frac{2}{N+1}-\frac{26}{3}\frac{1}{(N+1)^2}+\frac{4}{(N+1)^3}-\frac{8}{3}\frac{1}{N+2}\\
&+\frac{8}{(N+2)^2}-\frac{22}{3}\frac{1}{(N+2)^3}+\frac{2}{(N+2)^4}\Big)+\frac{1}{4}\Big(S_2(N)-S_2(k)\Big)^2\Big(\frac{1}{N+2}-\frac{1}{N-k}\Big)\\
&+\Big(S_2(N)-S_2(k)\Big)\Big(\frac{1}{3}\frac{1}{N-k}-\frac{13}{3}\frac{1}{N+1}+\frac{2}{(N+1)^2}+\frac{4}{N+2}\\
&-\frac{11}{3}\frac{1}{(N+2)^2}+\frac{1}{(N+2)^3}\Big)+\frac{2}{3}\Big(S_3(N)-S_3(k)\Big)\Big(\frac{5}{3}\frac{1}{N-k}+\frac{2}{N+1}\\
&-\frac{11}{3}\frac{1}{N+2}+\frac{1}{(N+2)^2}\Big)+\frac{1}{2}\Big(S_4(N)-S_4(k)\Big)\Big(\frac{1}{N+2}-\frac{1}{N-k}\Big)+\frac{2}{3}\frac{1}{N-k}\\
&-\frac{2}{3}\frac{1}{N+1}+\frac{2}{(N+1)^2}-\frac{26}{3}\frac{1}{(N+1)^3}+\frac{4}{(N+1)^4}-\frac{8}{3}\frac{1}{(N+2)^2}+\frac{8}{(N+2)^3}\\
&-\frac{22}{3}\frac{1}{(N+2)^4}+\frac{2}{(N+2)^5}\Bigg\}
\end{aligned}
\tag{5.58}
$$

and

$$
\hat{\gamma}^{\mathcal{D},(4)}_{N=5} = n_f^4 C_F \begin{pmatrix}
-\frac{562208549}{984150000} & \frac{8899139}{65610000} & \frac{1705289}{24603750} & \frac{2955389}{65610000} & \frac{15359729}{393660000}\\
0 & -\frac{990930013}{1968300000} & \frac{11153243}{82012500} & \frac{1831571}{27337500} & \frac{12500059}{246037500}\\
0 & 0 & -\frac{259993}{629856} & \frac{27955}{209952} & \frac{15439}{209952}\\
0 & 0 & 0 & -\frac{5504}{19683} & \frac{2752}{19683}\\
0 & 0 & 0 & 0 & 0
\end{pmatrix}. \tag{5.59}
$$

A suggestion for the prefactor of $[S_\alpha(N)-S_\alpha(k)]$ in the L-loop anomalous dimension is then[4]

$$
b_0\left(\frac{2}{3}\right)^{L+\alpha-4}\tilde{\gamma}^{(L-1)}_{N,k}\Bigg|_{[S_{\alpha-1}(N)-S_{\alpha-1}(k)]} \quad (\alpha\neq 0,1,L-1). \tag{5.60}
$$

$\tilde{\gamma}$ denotes that we only take into account the denominator structure and not the numerical prefactor multiplying it.

5.7 Anomalous dimensions beyond the leading-n_f limit

So far, we have focused our discussion on the anomalous dimensions in the leading-n_f limit. While this provides valuable checks of previous calculations, and extensions to higher orders in perturbation theory, the results in this limit are not phenomenologically useful, at least not by

[4] There is a typo in [132]. Eq.(4.41) there should be replaced by Eq.(5.60) here.

themselves. However, our method is in no way limited to this approximation, as we will now demonstrate. We present here two extensions. First, we present the two-loop mixing matrix in the leading-color limit. Second, we present some low-N results in full QCD up to order a_s^5.

5.7.1 Two-loop anomalous dimensions in the leading-color limit

The leading-color limit ($N_c \to \infty$), while more general than the leading-n_f one, is still somewhat simpler than the generic QCD case. The simplicity associated with the leading-n_f limit manifests itself in three ways: (1) only harmonic sums with positive indices appear, (2) because of the low maximum weight, the number of structures that could potentially contribute is reduced and (3) if we increase the order in a_s by one, the maximum weight is also increased by one. In the leading-color limit, point (1) remains true. However, now the structures will generically have weight $2L-1$ at L loops, and an increase in loop-order changes the maximum weight by more than one. Another difference comes from the details of the operator renormalization. In the leading-n_f limit, the $1/\varepsilon$-pole of the bare OMEs was simply determined by the operator anomalous dimensions. However, beyond this limit, the $1/\varepsilon$-pole can also get contributions from the finite (i.e. $O(\varepsilon^0)$) terms in the one-loop matrix elements. As we will see below, this has no significant consequences for our algorithm.

To illustrate this, we present here the two-loop mixing matrix in the leading-color approximation. The two-loop anomalous dimension can be decomposed as follows

$$\gamma_{N,k}^{\mathcal{D},(1)} = \gamma_{N,k}^{\mathcal{D},(1)}\Big|_{n_f} + \gamma_{N,k}^{\mathcal{D},(1)}\Big|_{\mathrm{LC}} + \gamma_{N,k}^{\mathcal{D},(1)}\Big|_{\mathrm{SLC}}. \tag{5.61}$$

The first term represents the leading-n_f piece discussed in the previous sections. The leading color term, represented by $\gamma_{N,k}^{\mathcal{D},(1)}\Big|_{\mathrm{LC}}$, is proportional to $C_F N_c/2$ while the subleading one, $\gamma_{N,k}^{\mathcal{D},(1)}\Big|_{\mathrm{SLC}}$ is proportional to $C_F/(2N_c)$. Hence in the limit $N_c \to \infty$, the latter can be neglected. The leading-color limit provides a good approximation to the full two-loop anomalous dimension. This is illustrated in Fig.5.1, which compares the full two-loop forward anomalous dimension to the leading-color limit in x-space. Hence, it is expected that also the leading-color mixing matrix provides a good approximation to the full matrix, making it a useful limit to consider for phenomenological studies. As already mentioned above, the $1/\varepsilon$-pole of the two-loop matrix elements gets contributions from the finite $O(\varepsilon^0)$ terms at one-loop. Collecting this in the quantity $\mathcal{F}(N)$ we find

$$\mathcal{F}(N) = C_F\left(\frac{4}{(N+1)^2} + \frac{2S_1(N)}{N+1} - S_1(N)^2 - 3S_2(N) - \frac{6}{N+1} + 4\right). \tag{5.62}$$

For completeness, we give here the pole-structure of the two-loop matrix elements in full QCD. There are three distinct contributions: those proportional to $C_F n_f$, to C_F^2 and $C_F C_A$. The first simply corresponds to the leading-n_f quantity discussed above. The other two are new and we have

$$\frac{1}{2}\left(\sum_{i=0}^{N}\gamma_{N,i}^{\mathcal{D},(1)} + \gamma_2^{(1)}\Big|_{C_F^2}\right) + \sum_{i=0}^{N}\left(\gamma_{N,i}^{\mathcal{D},(0)} + \delta_{N,i}\gamma_2^{(0)}\right)\mathcal{F}(i+1) \tag{5.63}$$

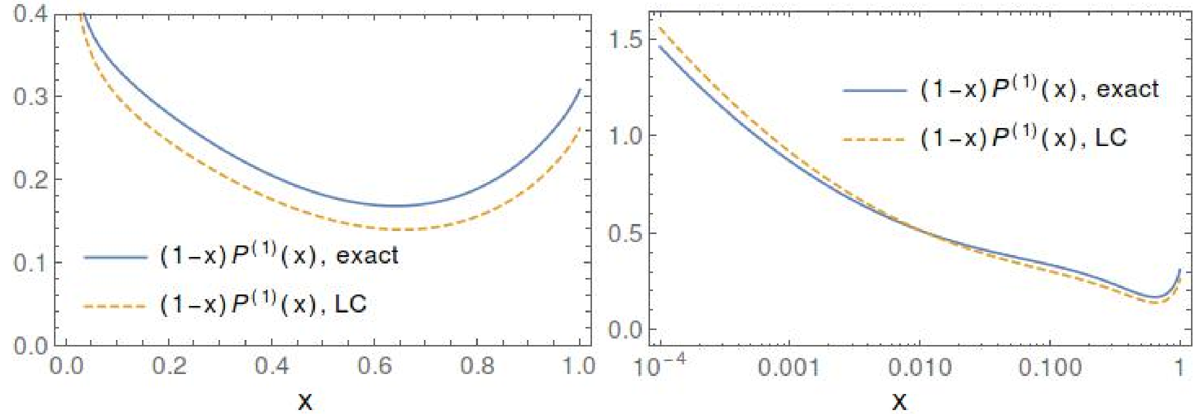

Figure 5.1: x-space comparison between the full two-loop forward anomalous dimension and the leading-color limit. We have employed the three-flavor scheme and included a normalization factor of $\frac{1}{16\pi^2}$.

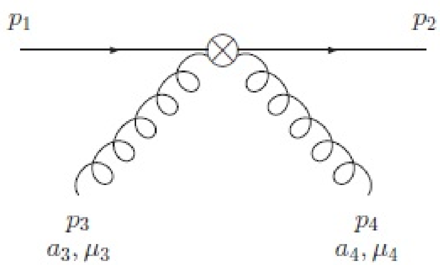

$$g^2 \not{\Delta}\Delta^{\mu_3}\Delta^{\mu_4} \sum_{j_1=0}^{N-3}\sum_{j_2=0}^{j_1} (p_2\cdot\Delta)^{N-3-j_1}(q\cdot\Delta - p_1\cdot\Delta)^{j_2}$$
$$\Big(t^{a_3}t^{a_4}(q\cdot\Delta - p_1\cdot\Delta - p_3\cdot\Delta)^{j_1-j_2}$$
$$+t^{a_4}t^{a_3}(q\cdot\Delta - p_1\cdot\Delta - p_4\cdot\Delta)^{j_1-j_2}\Big)$$

Figure 5.2: Feynman rule for the quark operator with two additional gluons, cf. [106]. The momenta are taken to be incoming and $q = \sum_i p_i$.

for the $1/\varepsilon$-pole proportional to C_F^2 and

$$\frac{1}{2}\left(\sum_{i=0}^{N}\gamma_{N,i}^{\mathcal{D},(1)} + \gamma_2^{(1)}\Big|_{C_F C_A}\right) \tag{5.64}$$

for the pole proportional to $C_F C_A$. They are related to the (sub)leading color pieces by

$$\gamma_{N,k}^{\mathcal{D},(1)}\Big|_{\mathrm{LC}} \sim C_F^2 \tag{5.65}$$

and

$$\gamma_{N,k}^{\mathcal{D},(1)}\Big|_{\mathrm{SLC}} \sim C_F\left(C_F - \frac{C_A}{2}\right). \tag{5.66}$$

We also have a new operator vertex to take into account, namely the one with two gluons attached to it, cf. Fig.5.2.

We now concentrate on the leading-color limit. The forward anomalous dimension is

$$
\begin{aligned}
\gamma^{(1)}_{N,N}\Big|_{\mathrm{LC}} = \frac{C_F N_c}{2}\Bigg[& -\frac{43}{6} - \frac{4}{(N+1)^3} + \frac{1}{(N+1)^2}\Big[-\frac{44}{3} - 8S_1(N)\Big] \\
& + \frac{1}{N+1}\Big[-\frac{32}{9} - 8S_2(N)\Big] - \frac{4}{(N+2)^3} \\
& + \frac{1}{(N+2)^2}\Big[-\frac{20}{3} - 8S_1(N)\Big] + \frac{1}{N+2}\Big[\frac{568}{9} - 8S_2(N)\Big] \\
& + \frac{536}{9}S_1(N) - 16S_{1,2}(N) - \frac{52}{3}S_2(N) - 16S_{2,1}(N) \\
& + 16S_3(N)\Bigg]
\end{aligned}
\tag{5.67}
$$

such that, using Eq.(4.66),

$$
\begin{aligned}
\gamma^{\mathcal{D},(1)}_{N,N-1}\Big|_{\mathrm{LC}} = & \frac{C_F N_c}{2}\Bigg[S_1(N)\Big(\frac{4}{N+2} - \frac{8}{(N+2)^2} + \frac{4}{N}\Big) + S_2(N)\Big(8 - \frac{8}{N+2}\Big) \\
& - \frac{268}{9} - \frac{100}{3}\frac{1}{N+1} + \frac{598}{9}\frac{1}{N+2} - \frac{14}{3}\frac{1}{(N+2)^2} - \frac{4}{(N+2)^3} \\
& + \frac{16}{3}\frac{1}{N} - \frac{2}{N^2}\Bigg].
\end{aligned}
\tag{5.68}
$$

Application of our algorithm then leads to

$$
\begin{aligned}
\gamma^{\mathcal{D},(1)}_{N,k}\Big|_{\mathrm{LC}} \;=\;& 4\frac{C_F N_c}{2}\Bigg\{\frac{\Big(S_1(N) - S_1(k)\Big)^2}{N-k} \\
& + \Big(S_1(N) - S_1(k)\Big)\Big(S_1(N-k) - S_1(k)\Big)\Big(\frac{1}{N+2} - \frac{2}{N-k}\Big) \\
& + \frac{1}{2}\Big(S_1(N) - S_1(k)\Big)\Big(\frac{13}{3}\frac{1}{N-k} + \frac{4}{(N-k)^2} - \frac{2}{N+1}\frac{1}{k+1} + \frac{2}{k+1}\frac{1}{N-k} \\
& - \frac{13}{3}\frac{1}{N+2} - \frac{2}{(N+2)^2}\Big) + \Big(S_1(N-k) - S_1(k)\Big)\Big(\frac{1}{N+1} + \frac{1}{N+1}\frac{1}{k+1} \\
& - \frac{1}{k+1}\frac{1}{N+2} - \frac{1}{N+2} + \frac{1}{(N+2)^2}\Big) - \Big(S_2(N) - S_2(k)\Big)\Big(\frac{1}{N+2} - \frac{1}{N-k}\Big) \\
& - 2S_2(k)\Big(\frac{1}{N+2} - \frac{1}{N-k}\Big) - \frac{67}{9}\frac{1}{N-k} - \frac{53}{6}\frac{1}{N+1} - \frac{1}{(N+1)^2} \\
& - \frac{1}{(N+1)^2}\frac{1}{k+1} - \frac{1}{2}\frac{1}{N+1}\frac{1}{k+1} + \frac{1}{2}\frac{1}{k+1}\frac{1}{N+2} + \frac{293}{18}\frac{1}{N+2} - \frac{5}{3}\frac{1}{(N+2)^2} \\
& - \frac{1}{(N+2)^3} - \frac{S_1(k)}{(N+2)^2}\Bigg\}.
\end{aligned}
\tag{5.69}
$$

For illustration, we quote the corresponding mixing matrix for spin-five operators

$$\hat{\gamma}^{\mathcal{D},(1)}_{N=5}\bigg|_{\mathrm{LC}} = \frac{C_F N_c}{2}\begin{pmatrix} \frac{654173}{13500} & -\frac{2551}{216} & -\frac{7999}{1800} & -\frac{1439}{600} & -\frac{511}{300} \\ 0 & \frac{255313}{6000} & -\frac{12881}{1125} & -\frac{39133}{9000} & -\frac{2936}{1125} \\ 0 & 0 & \frac{15085}{432} & -\frac{1615}{144} & -\frac{673}{144} \\ 0 & 0 & 0 & \frac{640}{27} & -\frac{320}{27} \\ 0 & 0 & 0 & 0 & 0 \end{pmatrix}. \tag{5.70}$$

To mimic the discussion for the leading-n_f part, we have written the expression in Eq.(5.69) in terms of differences of harmonic sums. By comparing the expressions in both limits, we see two differences for the anomalous dimensions. First, there is the appearance of denominators in $k+1$ in the leading-color expression. Second, we now also have higher powers of denominators in $N-k$. A final useful property of the leading-color expression is that the coefficients of the highest-weight terms are simple integers. This can be helpful when trying to determine higher-order expressions.

The algorithm should also be applicable to the subleading-color part of the anomalous dimensions, which originates from non-planar Feynman diagrams. However, these non-planar diagrams can generate harmonic sums with negative indices. This complicates the evaluation of the necessary sums, and we leave this to future studies.

5.7.2 Spin-five ADM in full QCD

We now present the mixing matrix for spin-five operators,

$$\begin{pmatrix} \gamma_{4,4} & \gamma^{\mathcal{D}}_{4,3} & \gamma^{\mathcal{D}}_{4,2} & \gamma^{\mathcal{D}}_{4,1} & \gamma^{\mathcal{D}}_{4,0} \\ 0 & \gamma_{3,3} & \gamma^{\mathcal{D}}_{3,2} & \gamma^{\mathcal{D}}_{3,1} & \gamma^{\mathcal{D}}_{3,0} \\ 0 & 0 & \gamma_{2,2} & \gamma^{\mathcal{D}}_{2,1} & \gamma^{\mathcal{D}}_{2,0} \\ 0 & 0 & 0 & \gamma_{1,1} & \gamma^{\mathcal{D}}_{1,0} \\ 0 & 0 & 0 & 0 & 0 \end{pmatrix}, \tag{5.71}$$

in full QCD. This means that we identify $C_A = 3$ and $C_F = 4/3$. The expressions for a general gauge group SU(N_c) can be found in Appendix B. Before presenting the results, we review the relevant identities used in their derivation.

Relevant identities

When the forward anomalous dimensions are known, the elements in the NTD can be directly calculated from them, cf. Eq.(4.66). Furthermore, if the anomalous dimensions are known in the Gegenbauer basis, we can use Eq.(4.82) to determine the elements of the last column in the total derivative basis. For the discussion at hand, we need $\gamma^{\mathcal{D}}_{2,0}, \gamma^{\mathcal{D}}_{3,0}$ and $\gamma^{\mathcal{D}}_{4,0}$, which can be calculated as

$$\gamma^{\mathcal{D}}_{2,0} = \frac{1}{30}\Big(\gamma^{\mathcal{G}}_{2,0} + 6\gamma_{2,2} + 30\gamma^{\mathcal{D}}_{1,0}\Big)$$
$$\gamma^{\mathcal{D}}_{3,0} = \frac{1}{140}\Big(-3\gamma^{\mathcal{G}}_{3,1} - 10\gamma_{3,3} - 90\gamma^{\mathcal{D}}_{1,0} + 210\gamma^{\mathcal{D}}_{2,0}\Big)$$

$$\gamma^{\mathcal{D}}_{4,0} = \frac{1}{630}\Big(\gamma^{\mathcal{G}}_{4,0} + 6\gamma^{\mathcal{G}}_{4,2} + 15\gamma_{4,4} + 210\gamma^{\mathcal{D}}_{1,0} - 840\gamma^{\mathcal{D}}_{2,0} + 1260\gamma^{\mathcal{D}}_{3,0}\Big). \tag{5.72}$$

Moreover we can use Eq.(4.71) to express $\gamma^{\mathcal{D}}_{3,1}$ in terms of known quantities

$$\gamma^{\mathcal{D}}_{3,1} = 3\gamma^{\mathcal{D}}_{2,0} - 3\gamma^{\mathcal{D}}_{1,0} - 2\gamma^{\mathcal{D}}_{3,0} - \gamma^{\mathcal{D}}_{3,2} - \gamma_{3,3}. \tag{5.73}$$

Unfortunately, at $N = 5$ not enough information is available to fix the full mixing matrix. In particular, there is no way to disentangle $\gamma^{\mathcal{D}}_{4,1}$ from $\gamma^{\mathcal{D}}_{4,2}$. Nevertheless, we can again use Eq.(4.71) to derive a relation between the two

$$\gamma^{\mathcal{D}}_{4,1} + \gamma^{\mathcal{D}}_{4,2} = -4\gamma^{\mathcal{D}}_{1,0} + 6\gamma^{\mathcal{D}}_{2,0} - 4\gamma^{\mathcal{D}}_{3,0} - \gamma^{\mathcal{D}}_{4,3} - \gamma_{4,4}. \tag{5.74}$$

With this information available, we can calculate the complete spin-two mixing matrix to five-loop order. The entry $\gamma^{\mathcal{D}}_{2,1}$ in the spin-three matrix can also be determined to the same order. When using the available three-loop anomalous dimensions in the Gegenbauer basis, cf. [16], the total derivative mixing matrix for spin-four operators can be calculated to order a_s^3. The relevant expressions for the fixed-N forward anomalous dimensions can be found in [106, 124–126] (four loops) and [127] (five loops). At order a_s^3, we only have access to the leading-n_f term of $\gamma^{\mathcal{D}}_{4,2}$. The remaining terms will be collected in $\tilde{\gamma}^{\mathcal{D}}_{4,2}$.

Results

$$\begin{aligned}
\gamma_{4,4} &= 8.08889\, a_s + (98.1994 - 7.68691\, n_f)\, a_s^2 \\
&\quad + (1720.94 - 279.180\, n_f - 2.36621\, n_f^2)\, a_s^3 \\
&\quad + (31273.3 - 7626.41\, n_f + 277.106\, n_f^2 + 4.53473\, n_f^3)\, a_s^4 + O(a_s^5) &(5.75)\\
\gamma^{\mathcal{D}}_{4,3} &= -2.22222\, a_s + (-23.8255 + 2.26667\, n_f)\, a_s^2 \\
&\quad + (-410.760 + 68.9025\, n_f + 0.515391\, n_f^2)\, a_s^3 \\
&\quad + (-6915.76 + 1844.48\, n_f - 76.8389\, n_f^2 - 1.30057\, n_f^3)\, a_s^4 + O(a_s^5) &(5.76)\\
\gamma^{\mathcal{D}}_{4,2} &= -0.888889\, a_s + \left(-8.88778 + \gamma^{\mathcal{D},(1)}_{4,2}\Big|_{\mathrm{SLC}} + 0.809877\, n_f \right) a_s^2 \\
&\quad + \left(\tilde{\gamma}^{\mathcal{D},(2)}_{4,2} + 0.287956\, n_f^2 \right) a_s^3 + O(a_s^4) &(5.77)\\
\gamma^{\mathcal{D}}_{4,1} &= -0.444444\, a_s + \left(-4.46178 - \gamma^{\mathcal{D},(1)}_{4,2}\Big|_{\mathrm{SLC}} + 0.340741\, n_f \right) a_s^2 \\
&\quad + \left(-234.566 + 40.5252\, n_f + 0.194403\, n_f^2 - \tilde{\gamma}^{\mathcal{D},(2)}_{4,2} \right) a_s^3 + O(a_s^4) &(5.78)\\
\gamma^{\mathcal{D}}_{4,0} &= -0.222222\, a_s + (-3.41128 + 0.106173\, n_f)\, a_s^2 \\
&\quad + (-61.8523 + 7.90849\, n_f + 0.132812\, n_f^2)\, a_s^3 + O(a_s^4) &(5.79)\\
\gamma_{3,3} &= 6.97778\, a_s + (86.2867 - 6.55358\, n_f)\, a_s^2
\end{aligned}$$

$$
\begin{aligned}
& +(1515.56-244.729\,n_f-2.10852\,n_f^2)\,a_s^3 \\
& +(27815.4-6704.17\,n_f+238.687\,n_f^2+3.88444\,n_f^3)\,a_s^4+O(a_s^5) \qquad (5.80)\\
\gamma^{\mathcal{D}}_{3,2} &= -2.13333\,a_s+(-23.1028+2.14519\,n_f)\,a_s^2 \\
& +(-405.973+67.6368\,n_f+0.51977\,n_f^2)\,a_s^3 \\
& +(-7071.4+1807.36\,n_f-74.6209\,n_f^2-1.23872\,n_f^3)\,a_s^4+O(a_s^5) \qquad (5.81)\\
\gamma^{\mathcal{D}}_{3,1} &= -0.8\,a_s+(-8.66775+0.693333\,n_f)\,a_s^2 \\
& +(-142.057+25.4966\,n_f+0.289975\,n_f^2)\,a_s^3+O(a_s^4) \qquad (5.82)\\
\gamma^{\mathcal{D}}_{3,0} &= -0.355556\,a_s+(-5.27039+0.209383\,n_f)\,a_s^2 \\
& +(-95.1612+12.9537\,n_f+0.193624\,n_f^2)\,a_s^3+O(a_s^4) \qquad (5.83)\\
\gamma_{2,2} &= 5.55556\,a_s+(70.8848-5.12346\,n_f)\,a_s^2 \\
& +(1244.91-199.637\,n_f-1.762\,n_f^2)\,a_s^3 \\
& +(23101.2-5499.27\,n_f+188.94\,n_f^2+3.05863\,n_f^3)\,a_s^4 \\
& +(547791-147144\,n_f+11176.3\,n_f^2+77.4206\,n_f^3-0.636764\,n_f^4)\,a_s^5 \\
& +O(a_s^6) \qquad (5.84)\\
\gamma^{\mathcal{D}}_{2,1} &= -2\,a_s+(-22.5556+1.96296\,n_f)\,a_s^2 \\
& +(-385.466+66.1992\,n_f+0.532922\,n_f^2)\,a_s^3 \\
& +(-6437.94+1751.72\,n_f-71.158\,n_f^2-1.1502\,n_f^3)\,a_s^4 \\
& +(-147044+43307.7\,n_f-3728.02\,n_f^2-15.8471\,n_f^3+0.293057\,n_f^4)\,a_s^5 \\
& +O(a_s^6) \qquad (5.85)\\
\gamma^{\mathcal{D}}_{2,0} &= -0.666667\,a_s+(-9.50617+0.481481\,n_f)\,a_s^2 \\
& +(-170.654+24.8232\,n_f+0.3107\,n_f^2)\,a_s^3+O(a_s^4) \qquad (5.86)\\
\gamma_{1,1} &= 3.55556\,a_s+(48.3292-3.16049\,n_f)\,a_s^2 \\
& +(859.448-133.438\,n_f-1.22908\,n_f^2)\,a_s^3 \\
& +(16663.2-3747.55\,n_f+117.781\,n_f^2+1.90843\,n_f^3)\,a_s^4 \\
& +(400747-103837\,n_f+7448.29\,n_f^2+61.5735\,n_f^3-0.343707\,n_f^4)\,a_s^5 \\
& +O(a_s^6) \qquad (5.87)\\
\gamma^{\mathcal{D}}_{1,0} &= -1.77778\,a_s+(-24.1646+1.58025\,n_f)\,a_s^2 \\
& +(-429.724+66.7191\,n_f+0.61454\,n_f^2)\,a_s^3 \\
& +(-8331.61+1873.78\,n_f-58.8907\,n_f^2-0.954217\,n_f^3)\,a_s^4 \\
& +(-200373+51918.3\,n_f-3724.15\,n_f^2-30.7867\,n_f^3+0.171853\,n_f^4)\,a_s^5 \\
& +O(a_s^6) \qquad (5.88)
\end{aligned}
$$

The values for $\gamma^{\mathcal{D},(2)}_{2,1}$ and $\gamma^{\mathcal{D},(2)}_{2,0}$ at order a_s^3 can be compared with those presented in [26], where the authors used numerical methods for their determination. We find agreement with their values of $\gamma_{2,1}^{\mathcal{D},(2)}$ and $\gamma_{2,0}^{\mathcal{D},(2)}$, in the latter case within the uncertainties of their numerical result[5]

$$\gamma_{2,0}^{\mathcal{D},(2)}\Big|_{\text{ref. [26]}} = -170.641(12) + 24.822(2)\,n_f + 0.3107(1)\,n_f^2\,. \tag{5.89}$$

We remind the reader that the results presented here are written in the $\overline{\text{MS}}$-scheme. When transformed to the RI-scheme, they will be useful for hadronic structure studies in the framework of lattice QCD.

[5]The numerical errors in the parentheses in Eq. (5.89) have been provided by the authors of [26] in private communication.

Chapter 6

Anomalous dimensions of transversity operators[1]

Introduction

Wilson operators, which we have discussed in previous chapters, are important in the study of the longitudinal structure of hadrons. However, there is also the transverse hadron structure to consider. This is less well-studied, both theoretically and phenomenologically. The transverse hadronic structure can be analyzed by considering hadronic matrix elements of so-called transversity operators, which are just the Wilson operators with the Dirac matrix replaced by a commutator of two Dirac matrices. The matrix elements of these operators are again to be calculated non-perturbatively, see e.g. [135–137] for recent progress in lattice QCD. They are related to the TDF of partons inside hadrons. Assuming we have a transversely polarized hadron, the TDF represents a measure of the difference in probabilities of finding a parton polarized parallel to the nucleon spin and an oppositely polarized one. Such distributions are relevant for processes like polarized Drell-Yan [9–13] and semi-inclusive deep-inelastic scattering [10, 138]. As was the case for PDFs, the scale-dependence of the TDF is related to the anomalous dimensions of the corresponding operators, which can be calculated in perturbation theory. The forward anomalous dimensions are known to third order in the strong coupling [10, 121, 139–148]. A related non-forward distribution is the so-called transverse distribution amplitude, which is related to vacuum-to-hadron transitions. Contrary to PDFs and GPDs, such distribution amplitudes are obtained by sandwiching the transversity operator between a hadronic state and the vacuum state. They are accessible in vector-meson production processes and can be studied e.g. by analyzing data collected at BELLE II [149]. As was the case for GPDs, their scale-dependence is determined by the ERBL equation, cf. Eq.(2.34). The corresponding off-forward anomalous dimension matrices are known to first order in the strong coupling [10, 139–141]. In momentum space, the evolution kernels were calculated to two-loop order in [150, 151].

As mentioned in Chapter 4, the consistency relation between the anomalous dimensions in the total derivative basis, cf. Eq.(4.87), does not depend on the Dirac structure of the corresponding quark operators. As such, we can use the methods of Chapter 4 to determine the anomalous dimen-

[1]The results of this chapter were originally presented in [134].

sions of the transversity operator, including mixing with total derivative operators. For simplicity, we focus our attention on the leading-n_f approximation, which implies that we can follow the discussion presented in Section 5.6. The resulting anomalous dimensions will be presented to order a_s^4. However, as the leading-n_f term of the forward transversity anomalous dimension is known to all orders, cf. [145], it would be easy to push the calculation of the mixing matrix to higher orders as well. We will also present the mixing matrices in the Gegenbauer basis. Fixed moments can be calculated using Eq.(5.12). In turn, these fixed moments can be used to check our results in the total derivative basis, cf. Eq.(4.82). If this consistency relation holds, it can subsequently be used to derive the full (N,k)-dependence of the Gegenbauer ADMs. These results will also be presented to fourth order in the strong coupling.

6.1 Transversity operators

The transversity operators are defined as

$$O^T_{\mu\nu_1\ldots\nu_N} = \mathcal{S}\overline{\psi}\lambda^\alpha\sigma_{\mu\nu_1}D_{\nu_2}\ldots D_{\nu_N}\psi \tag{6.1}$$

with

$$\sigma_{\mu\nu} = \frac{1}{2}[\gamma_\mu,\gamma_\nu]. \tag{6.2}$$

As in previous chapters, we consider only leading-twist flavor non-singlet operators. When calculating the partonic matrix elements of these operators, we again contract with a tensor composed of lightlike vectors, $\Delta^{\nu_1}\ldots\Delta^{\nu_N}$ and $\Delta^2 = 0$. Contrary to the Wilson OMEs, there will be one uncontracted Lorentz index left in the transversity matrix elements. This means that the analysis of these objects becomes more complicated. However, as we only consider the leading-n_f limit in this chapter, we only need to calculate the one-loop OMEs to extract the corresponding anomalous dimensions. The higher-order anomalous dimensions are then determined by implementing the discussion of Section 5.6.

In off-forward kinematics, the operators in Eq.(6.1) mix with total-derivative ones. In the total derivative basis, we write these additional operators generically as

$$O^{\mathcal{D},T}_{p,q,r} = S\partial^{\mu_1}\ldots\partial^{\mu_p}(D^{\nu_1}\ldots D^{\nu_q}\overline{\psi})\lambda^\alpha\sigma^{\mu\nu}(D^{\lambda_1}\ldots D^{\lambda_r}\psi) \tag{6.3}$$

such that

$$O^{\mathcal{D},T}_{k,0,N} = \sum_{j=0}^{N} Z^{\mathcal{D},T}_{N,N-j}[O^{\mathcal{D},T}_{k+j,0,N-j}]. \tag{6.4}$$

The corresponding anomalous dimensions are

$$\gamma^{\mathcal{D},T}_{N,k} = -(Z^{\mathcal{D},T}_{N,j})^{-1}\frac{\mathrm{d}\,Z^{\mathcal{D},T}_{j,k}}{\mathrm{d}\ln\mu^2}. \tag{6.5}$$

In the Gegenbauer basis, the transversity operators are written as

$$O^{\mathcal{G},T}_{N,k} = (\Delta\cdot\partial)^k\overline{\psi}(x)\frac{1}{2}[\gamma^\mu,\not{\Delta}]C_N^{3/2}\left(\frac{\overleftarrow{D}\cdot\Delta-\Delta\cdot\overrightarrow{D}}{\overleftarrow{\partial}\cdot\Delta+\Delta\cdot\overrightarrow{\partial}}\right)\psi(x) \tag{6.6}$$

and the corresponding off-diagonal entries of the mixing matrix can be calculated using Eq.(5.12).

6.2 One-loop anomalous dimensions

At this order, we need to perform the calculation of the matrix elements of the operators in Eq.(6.1) explicitly. The Feynman diagrams are exactly those that appear in the one-loop calculation of the Wilson OMEs, cf. Fig.4.3. Likewise, the Feynman rules of the transversity operators correspond to those of the Wilson operators with the replacement

$$\not{\Delta} \to \frac{1}{2}[\gamma_\mu, \not{\Delta}]. \tag{6.7}$$

Using *PACKAGE-X* in *MATHEMATICA* [152] we find

$$\mathcal{B}^{T,(0)}(N+1) = C_F\left(\frac{2}{N+1} + 2S_1(N) - 1\right) \tag{6.8}$$

such that, applying Eq.(4.74),

$$\gamma^{\mathcal{D},T,(0)}_{N,0} = C_F\left(\frac{2}{N+1} - \frac{2}{N}\right). \tag{6.9}$$

The value of $\gamma^{\mathcal{D},T,(0)}_{1,0}$ agrees with a previous calculation in [25]. The one-loop forward anomalous dimension was calculated in [10, 139–141] and reads

$$\gamma^{T,(0)}_{N,N} = C_F\left(\frac{4}{N+1} + 4S_1(N) - 3\right). \tag{6.10}$$

Note that, contrary to the Wilson operators, the $N = 1$ transversity operator does not correspond to a conserved current, such that $\gamma^{T}_{0,0} \neq 0$. The all-k expression can then be determined using the conjugation relation in Eq.(4.87). The result is

$$\gamma^{\mathcal{D},T,(0)}_{N,k} = C_F\left(\frac{2}{N+1} - \frac{2}{N-k}\right). \tag{6.11}$$

For $N = 5$ this implies that

$$\hat{\gamma}^{\mathcal{D},T,(0)}_{N=5} = C_F\begin{pmatrix} \frac{92}{15} & -\frac{8}{5} & -\frac{3}{5} & -\frac{4}{15} & -\frac{1}{10} \\ 0 & \frac{16}{3} & -\frac{3}{2} & -\frac{1}{2} & -\frac{1}{6} \\ 0 & 0 & \frac{13}{3} & -\frac{4}{3} & -\frac{1}{3} \\ 0 & 0 & 0 & 3 & -1 \\ 0 & 0 & 0 & 0 & 1 \end{pmatrix}. \tag{6.12}$$

The complete one-loop mixing matrix was also calculated in [10, 139–141] using different methods, and we find full agreement with these results. As mentioned in Chapter 5, the one-loop mixing matrix in the Gegenbauer basis is diagonal, such that

$$\hat{\gamma}^{\mathcal{G},T,(0)}_{N=5} = C_F \begin{pmatrix} \frac{92}{15} & 0 & 0 & 0 & 0 \\ 0 & \frac{16}{3} & 0 & 0 & 0 \\ 0 & 0 & \frac{13}{3} & 0 & 0 \\ 0 & 0 & 0 & 3 & 0 \\ 0 & 0 & 0 & 0 & 1 \end{pmatrix}. \tag{6.13}$$

We have checked that Eq.(4.82) is obeyed.

6.3 Two-loop anomalous dimensions

At two-loop order, the leading-n_f term of the forward anomalous dimension reads [142–144]

$$\gamma^{T,(1)}_{N,N} = \frac{8}{9} n_f C_F \left(3S_2(N+1) - 5S_1(N+1) + \frac{3}{8} \right). \tag{6.14}$$

We now follow the discussion of Section 5.6. The only difference with the Wilson anomalous dimensions there is that now the maximal shift in the forward anomalous dimension is $N+1$ instead of $N+2$. This leads to

$$\begin{aligned} \gamma^{\mathcal{D},T,(1)}_{N,k} =& \frac{4}{3} n_f C_F \left\{ \frac{1}{(N+1)^2} + [S_1(N) - S_1(k)] \left(\frac{1}{N+1} - \frac{1}{N-k} \right) \right\} \\ &+ n_f C_F \left(\frac{a_1}{N+1} + \frac{a_2}{N-k} \right) \end{aligned} \tag{6.15}$$

where $a_1, a_2 \in \mathbb{Q}$ are a priori unknown. They can be fixed however by using the consistency relation in Eq.(4.87), and we find

$$\begin{aligned} \gamma^{\mathcal{D},T,(1)}_{N,k} =& \frac{4}{3} n_f C_F \left\{ \frac{1}{(N+1)^2} + [S_1(N) - S_1(k)] \left(\frac{1}{N+1} - \frac{1}{N-k} \right) \right. \\ & \left. - \frac{5}{3} \left(\frac{1}{N+1} - \frac{1}{N-k} \right) \right\}. \end{aligned} \tag{6.16}$$

The corresponding value for $\gamma^{\mathcal{D},T,(1)}_{1,0}$ agrees with the one in [25]. The $N=5$ mixing matrix is then

$$\hat{\gamma}^{\mathcal{D},T,(1)}_{N=5} = n_f C_F \begin{pmatrix} -\frac{7981}{1350} & \frac{352}{225} & \frac{73}{150} & \frac{106}{675} & \frac{23}{900} \\ 0 & -\frac{277}{54} & \frac{17}{12} & \frac{13}{36} & \frac{7}{108} \\ 0 & 0 & -\frac{113}{27} & \frac{32}{27} & \frac{5}{27} \\ 0 & 0 & 0 & -3 & \frac{7}{9} \\ 0 & 0 & 0 & 0 & -\frac{13}{9}. \end{pmatrix}. \tag{6.17}$$

Fixed moments of the Gegenbauer mixing matrix can be computed using Eq.(5.12), and to two-loop accuracy we find for $N = 5$

$$\hat{\gamma}^{\mathcal{G},T,(1)}_{N=5} = n_f C_F \begin{pmatrix} -\frac{7981}{1350} & 0 & -\frac{14}{15} & 0 & -\frac{11}{15} \\ 0 & -\frac{277}{54} & 0 & -\frac{10}{9} & 0 \\ 0 & 0 & -\frac{113}{27} & 0 & -\frac{4}{3} \\ 0 & 0 & 0 & -3 & 0 \\ 0 & 0 & 0 & 0 & -\frac{13}{9} \end{pmatrix}. \tag{6.18}$$

We checked that the two-loop result in the total derivative basis and the Gegenbauer moments are consistent with one another[2]. As such, the relation in Eq.(4.82) can now be used to reconstruct the full (N,k)-dependence of the Gegenbauer mixing matrix. We find

$$\gamma^{\mathcal{G},T,(1)}_{N,k} = -\frac{16}{3}\frac{n_f C_F}{a(N,k)}\vartheta_{N,k}\left\{(3+2k)\left(S_1(N) - S_1(k) + \frac{1}{N+1}\right) - \frac{1}{k+1} - 2\right\}. \tag{6.19}$$

6.4 Three-loop anomalous dimensions

The forward anomalous dimension at three-loop order was calculated in [145–147]. Its leading-n_f term is

$$\begin{aligned} \gamma^{T,(2)}_{N,N} = 16 n_f^2 C_F \Bigg(&\frac{17}{144} - \frac{1}{27}S_1(N+1) - \frac{5}{27}S_2(N+1) \\ &+ \frac{1}{9}S_3(N+1) - \frac{1}{18}\frac{1}{(N+1)(N+2)}\Bigg). \end{aligned} \tag{6.20}$$

Of note is the appearance of a new structure, namely a weight-one denominator in $N+2$. This has to be accounted for when applying the method. We find

$$\begin{aligned} \gamma^{\mathcal{D},T,(2)}_{N,k} = \frac{4}{9} n_f^2 C_F \Bigg\{ &\frac{2}{(N+1)^3} + [S_2(N) - S_2(k)]\left(\frac{1}{N+1} - \frac{1}{N-k}\right) \\ &+ [S_1(N) - S_1(k)]^2\left(\frac{1}{N+1} - \frac{1}{N-k}\right) + \frac{2[S_1(N) - S_1(k)]}{(N+1)^2} \\ &- \frac{10}{3}[S_1(N) - S_1(k)]\left(\frac{1}{N+1} - \frac{1}{N-k}\right) - \frac{10}{3}\frac{1}{(N+1)^2} \\ &- \frac{8}{3}\frac{1}{N+1} + \frac{2}{N+2} + \frac{2}{3}\frac{1}{N-k}\Bigg\} \end{aligned} \tag{6.21}$$

[2]While only presenting the $N = 5$ Gegenbauer moments here, the consistency check was performed up to $N = 50$.

and for $N=5$

$$\hat{\gamma}_{N=5}^{\mathcal{D},T,(2)} = n_f^2 C_F \begin{pmatrix} -\frac{209297}{121500} & \frac{52}{125} & \frac{2951}{13500} & \frac{3511}{30375} & \frac{2701}{81000} \\ 0 & -\frac{7361}{4860} & \frac{149}{360} & \frac{611}{3240} & \frac{533}{9720} \\ 0 & 0 & -\frac{301}{243} & \frac{94}{243} & \frac{25}{243} \\ 0 & 0 & 0 & -\frac{23}{27} & \frac{7}{27} \\ 0 & 0 & 0 & 0 & -\frac{1}{3} \end{pmatrix}. \tag{6.22}$$

We agree with [25] for the value of $\gamma_{1,0}^{\mathcal{D},T,(2)}$. The Gegenbauer ADM can again be calculated using Eq.(5.12), and for $N=5$ we find

$$\hat{\gamma}_{N=5}^{\mathcal{G},T,(2)} = n_f^2 C_F \begin{pmatrix} -\frac{209297}{121500} & 0 & \frac{511}{675} & 0 & \frac{253}{1350} \\ 0 & -\frac{7361}{4860} & 0 & \frac{65}{81} & 0 \\ 0 & 0 & -\frac{301}{243} & 0 & \frac{20}{27} \\ 0 & 0 & 0 & -\frac{23}{27} & 0 \\ 0 & 0 & 0 & 0 & -\frac{1}{3} \end{pmatrix}. \tag{6.23}$$

Consistency between the Gegenbauer moments and the result in the total derivative basis was explicitly checked. As before, we can then use Eq.(4.82) to derive the full (N,k)-dependence of the off-diagonal elements of the Gegenbauer mixing matrix. The result is

$$\begin{aligned} \gamma_{N,k}^{\mathcal{G},T,(2)} = \frac{32}{9}\frac{n_f^2 C_F}{a(N,k)}\vartheta_{N,k}\Bigg\{ &(3+2k)\Big(2S_1(N)S_1(k) - 2[S_{1,1}(N)+S_{1,1}(k)] + [S_2(N) \\ &+ S_2(k)]\Big) - (3+2k)\left(2\frac{S_1(N)-S_1(k)}{N+1} + \frac{1}{(N+1)^2}\right) + \Bigg(S_1(N) - S_1(k) \\ &+ \frac{1}{N+1}\Bigg)\left(\frac{2}{k+1} + 9 + \frac{10k}{3}\right) - \frac{1}{(k+1)^2} - \frac{11}{3}\frac{1}{k+1} - \frac{10}{3}\Bigg\}. \end{aligned} \tag{6.24}$$

6.5 Four-loop anomalous dimensions

Finally, we consider the mixing matrix to fourth order in the strong coupling. The corresponding leading-n_f forward anomalous dimension was calculated in [145]

$$\begin{aligned} \gamma_{N,N}^{T,(3)} = \frac{32}{27}n_f^3 C_F \Bigg(&S_4(N+1) - \frac{5}{3}S_3(N+1) - \frac{1}{3}S_2(N+1) - \frac{1}{3}S_1(N+1) \\ &+ \frac{1}{2}\frac{1}{(N+2)^2} - \frac{1}{2}\frac{1}{(N+1)^2} - \frac{5}{6}\frac{1}{N+2} + \frac{5}{6}\frac{1}{N+1} + \frac{131}{96} \\ &+ \zeta_3\left[2(N+1) - \frac{3}{2}\right]\Bigg). \end{aligned} \tag{6.25}$$

Application of our method then yields

$$
\begin{aligned}
\gamma_{N,k}^{\mathcal{D},T,(3)} = \frac{16}{27} n_f^3 C_F \Bigg\{ & \frac{1}{(N+1)^4} - \frac{5}{3}\frac{1}{(N+1)^3} + [S_1(N) - S_1(k)] \Bigg(\frac{1}{(N+1)^3} \\
& - \frac{5}{3}\frac{1}{(N+1)^2} - \frac{4}{3}\frac{1}{N+1} + \frac{1}{N+2} + \frac{1}{3}\frac{1}{N-k} \Bigg) + \Bigg([S_1(N) - S_1(k)]^2 + S_2(N) \\
& - S_2(k) \Bigg) \Bigg(\frac{1}{2}\frac{1}{(N+1)^2} - \frac{5}{6}\frac{1}{N+1} + \frac{5}{6}\frac{1}{N-k} \Bigg) + \Bigg(\frac{1}{N+1} - \frac{1}{N-k} \Bigg) \Bigg(\frac{1}{6}[S_1(N) \\
& - S_1(k)]^3 + \frac{1}{2}[S_2(N) - S_2(k)][S_1(N) - S_1(k)] + \frac{1}{3}[S_3(N) - S_3(k)] \Bigg) \\
& - \frac{4}{3}\frac{1}{(N+1)^2} + \frac{4}{3}\frac{1}{N+1} + \frac{1}{(N+2)^2} - \frac{5}{3}\frac{1}{N+2} + \frac{1}{3}\frac{1}{N-k} \Bigg\}
\end{aligned} \tag{6.26}
$$

and

$$
\hat{\gamma}_{N=5}^{\mathcal{D},T,(3)} = n_f^3 C_F \begin{pmatrix} -\frac{9829939}{10935000} & \frac{12058}{50625} & \frac{166537}{1215000} & \frac{249257}{2733750} & \frac{277787}{7290000} \\ 0 & -\frac{341107}{437400} & \frac{8123}{32400} & \frac{40237}{291600} & \frac{49891}{874800} \\ 0 & 0 & -\frac{1340}{2187} & \frac{575}{2187} & \frac{212}{2187} \\ 0 & 0 & 0 & -\frac{85}{243} & \frac{53}{243} \\ 0 & 0 & 0 & 0 & \frac{7}{81} \end{pmatrix} \tag{6.27}
$$

for the ζ_3-independent terms. The structure multiplying ζ_3 in Eq.(6.25) has a maximum weight of one. Hence using our algorithm, the determination of the ζ_3-terms in the off-forward anomalous dimensions is no more complex than a one-loop calculation. We find

$$
\gamma_{N,k}^{\mathcal{D},T,(3)} \Big|_{\zeta_3} = \frac{32}{27} \zeta_3 n_f^3 C_F \left(\frac{1}{N+1} - \frac{1}{N-k} \right) \tag{6.28}
$$

and, for the spin-five mixing matrix,

$$
\hat{\gamma}_{N=5}^{\mathcal{D},T,(3)} \Big|_{\zeta_3} = \zeta_3 n_f^3 C_F \begin{pmatrix} \frac{1472}{405} & -\frac{128}{135} & -\frac{16}{45} & -\frac{64}{405} & -\frac{8}{135} \\ 0 & \frac{256}{81} & -\frac{8}{9} & -\frac{8}{27} & -\frac{8}{81} \\ 0 & 0 & \frac{208}{81} & -\frac{64}{81} & -\frac{16}{81} \\ 0 & 0 & 0 & \frac{16}{9} & -\frac{16}{27} \\ 0 & 0 & 0 & 0 & \frac{16}{27} \end{pmatrix}. \tag{6.29}
$$

The corresponding mixing matrices in the Gegenbauer basis are

$$\hat{\gamma}_{N=5}^{\mathcal{G},T,(3)} = n_f^3 C_F \begin{pmatrix} -\frac{9829939}{10935000} & 0 & \frac{22057}{60750} & 0 & \frac{45311}{121500} \\ 0 & -\frac{341107}{437400} & 0 & \frac{683}{1458} & 0 \\ 0 & 0 & -\frac{1340}{2187} & 0 & \frac{136}{243} \\ 0 & 0 & 0 & -\frac{85}{243} & 0 \\ 0 & 0 & 0 & 0 & \frac{7}{81} \end{pmatrix} \tag{6.30}$$

and

$$\hat{\gamma}_{N=5}^{\mathcal{G},T,(3)}\Big|_{\zeta_3} = \zeta_3 n_f^3 C_F \begin{pmatrix} \frac{1472}{405} & 0 & 0 & 0 & 0 \\ 0 & \frac{256}{81} & 0 & 0 & 0 \\ 0 & 0 & \frac{208}{81} & 0 & 0 \\ 0 & 0 & 0 & \frac{16}{9} & 0 \\ 0 & 0 & 0 & 0 & \frac{16}{27} \end{pmatrix}. \tag{6.31}$$

The consistency check, Eq.(4.82), was again explicitly checked to hold. In turn this implies that

$$\begin{aligned} \gamma_{N,k}^{\mathcal{G},T,(3)} = & \frac{64}{27}\frac{n_f^3 C_F}{a(N,k)}\vartheta_{N,k}\Bigg\{-\frac{3+2k}{3}\Big(S_3(N)-S_3(k)+2[S_1(N)-S_1(k)]^3\Big) \\ & +[S_1(N)-S_1(k)]^2\left(9+\frac{10}{3}k+\frac{2}{k+1}-\frac{2(3+2k)}{N+1}\right)+[S_1(N)-S_1(k)]\Bigg(-\frac{17}{3} \\ & +\frac{2}{3}k-\frac{22}{3}\frac{1}{k+1}-\frac{2}{(k+1)^2}+\frac{2}{3}\frac{27+10k}{N+1}+\frac{4}{(N+1)(k+1)}-\frac{2(3+2k)}{(N+1)^2}\Bigg) \\ & +\frac{1}{(k+1)^3}-\frac{2}{(N+1)(k+1)}\left(\frac{11}{3}+\frac{1}{k+1}-\frac{1}{N+1}\right)-\frac{3+2k}{(N+1)^3}+\frac{11}{3}\frac{1}{(k+1)^2} \\ & +\frac{1}{3}\frac{27+10k}{(N+1)^2}+\frac{5}{2}\frac{1}{k+1}-\frac{5}{6}\frac{5-2k}{N+1}-\frac{1}{2}\frac{1}{k+2}-\frac{1}{2}\frac{3+2k}{N+2}-\frac{2}{3}\Bigg\}. \end{aligned} \tag{6.32}$$

To conclude, we reiterate that the method used in this chapter can be easily applied to derive the higher-order leading-n_f anomalous dimensions as well. However, going beyond the leading-n_f limit is more complicated. In the total derivative basis, this involves calculating the higher-order matrix elements of the transversity operator in off-forward kinematics. In the Gegenbauer basis, one would need to calculate the transversity conformal anomaly at two-loop order and beyond (the one-loop transversity conformal anomaly corresponds to the one-loop Wilson one, cf. [19]). These points are left for future studies.

Chapter 7

Ongoing research

In this final chapter, we collect some recent research results, which are as-of-yet unpublished. In the first section, we derive another consistency relation for the off-forward anomalous dimensions. Contrary to before, this relation does not originate from physical considerations, but instead from mathematical ones. The next section introduces a relation between the off-forward anomalous dimensions for the gluon operator, which is valid to one-loop order. In the final section we consider the renormalization of polarized flavor non-singlet quark operators in the leading-n_f limit.

7.1 A mathematics based relation for the anomalous dimensions

Consider some sequence $\{a_k\}$ with associated sum

$$A_N \equiv \sum_{k=0}^{N} a_k. \tag{7.1}$$

Then, according to Eq.(14) of [153], the following identity holds

$$\sum_{k=0}^{N} (-1)^k \binom{N+1}{k} A_k = (-1)^N \binom{N+s-1}{N} A_N + \sum_{k=0}^{N-1} (-1)^{k+1} \binom{N+s-1}{k} a_{k+1} \tag{7.2}$$

with $s \in \mathbb{C} \setminus \mathbb{Z}^-$. We have introduced a shift in indices compared to [153] to start the summations at zero. We can now apply Eq.(7.2) to the elements of the ADM. Identifying as usual

$$\sum_{j=0}^{N} \gamma_{N,j} \equiv \mathcal{B}(N+1) \tag{7.3}$$

we have

$$\sum_{k=0}^{N} (-1)^k \binom{N+s}{k} \sum_{j=0}^{k} \gamma_{N,j} - (-1)^N \binom{N+s-1}{N} \mathcal{B}(N+1) = \sum_{j=0}^{N} (-1)^j \binom{N+s-1}{j-1} \gamma_{N,j}. \tag{7.4}$$

Assuming $\mathcal{B}(N+1)$ and $\gamma_{N,N}$ to be known, we split off these quantities, leading to

$$(-1)^N \binom{N+s-1}{N-1}\Big(\mathcal{B}(N+1)-\gamma_{N,N}\Big) = \sum_{j=0}^{N-1}(-1)^j\left[\binom{N+s-1}{j-1}\gamma_{N,j} - \binom{N+s}{j}\sum_{i=0}^{j}\gamma_{N,i}\right]. \tag{7.5}$$

The right-hand side of this identity depends only on the off-diagonal part of the ADM. With an Ansatz, this then gives a system of equations different from the one we get from using the consistency relation in Eq.(4.87). Furthermore, as the systems of equations for different s-values are equivalent, we can stick to a particular value. The simplest case is $s=0$ which gives

$$(-1)^N\Big(\mathcal{B}(N+1)-\gamma_{N,N}\Big) = \sum_{j=0}^{N-1}(-1)^j\left[\binom{N-1}{j-1}\gamma_{N,j} - \binom{N}{j}\sum_{i=0}^{j}\gamma_{N,i}\right]. \tag{7.6}$$

As a check, we consider the one-loop Wilson quantities in the total derivative basis. With

$$\mathcal{B}^{(0)}(N+1) = C_F\left(2S_1(N+1) - \frac{2}{N+2} - 1\right) \tag{7.7}$$

and

$$\gamma^{(0)}_{N,N} = C_F\left(4S_1(N) + \frac{2}{N+2} + \frac{2}{N+1} - 3\right) \tag{7.8}$$

the left-hand side of Eq.(7.6) becomes

$$2(-1)^N C_F\left(1 - S_1(N) - \frac{2}{N+2}\right). \tag{7.9}$$

The off-diagonal terms of the one-loop ADM are given by

$$\gamma^{\mathcal{D},(0)}_{N,k} = 2C_F\left(\frac{1}{N+2} - \frac{1}{N-k}\right). \tag{7.10}$$

Evaluating the corresponding sums on the right-hand side of Eq.(7.6) then exactly reproduces Eq.(7.9). The relation was also explicitly checked to hold for the two-loop leading-color anomalous dimensions, cf. Eq.(5.69).

7.2 A one-loop relation for gluon operators

We consider matrix elements of the spin-N twist-two gluon operator

$$O^{\mathrm{G}}_{\mu_1\ldots\mu_N} \equiv \mathcal{S} F_{\nu\mu_1} D_{\mu_2}\ldots D_{\mu_{N-1}} F_{\mu_N}{}^{\nu}. \tag{7.11}$$

These operators will be contracted with a tensor of light-like Δ, which we denote as

$$\Delta^{\mu_1}\ldots\Delta^{\mu_N} F_{\nu\mu_1} D_{\mu_2}\ldots D_{\mu_{N-1}} F_{\mu_N}{}^{\nu} \to F\underbrace{D\ldots D}_{N-1}F \tag{7.12}$$

for notational simplicity. Under renormalization, this operator mixes with the quark flavor singlet operator of the same dimension, cf. Eq.(1.114). Moreover, in the case of off-forward kinematics, there is also mixing with total derivative operators. Throughout this section, we work exclusively in the total derivative basis. To avoid cluttering the notation too much, we omit the superscript $\mathcal{D}$ on the anomalous dimensions. For explicitness, we consider the insertion of the gluon operator into a quark two-point function. In this case, the odd-N matrix elements vanish in the forward limit. This is because odd-N gluon operators can be written as a linear combination of total derivative operators. For example, for the simple case of $N = 3$ we just have

$$FDF = \partial F^2 - (DF)F \tag{7.13}$$

and hence

$$2FDF = \partial F^2. \tag{7.14}$$

Note that this would work for any spin-N operator of the type

$$(\text{field })D\ldots D(\text{ field}). \tag{7.15}$$

The matrix elements of even-spin gluon operators are non-trivial and require an explicit calculation. Throughout this section, all such calculations are performed using *PACKAGE-X*. With no contributions of self-energy corrections at one-loop order, the $1/\varepsilon$-pole of the bare OME corresponds to the anomalous dimension in the forward limit. This gives

$$\gamma_{N,N}^{(0),\mathrm{gq}} = 2C_F\left(-\frac{1}{N+2}+\frac{2}{N+1}-\frac{2}{N}\right) \tag{7.16}$$

for odd N, as expected. The $1/\varepsilon$-pole in the off-forward limit is

$$\mathcal{B}(N) = C_F\left(\frac{2}{N+1}-\frac{2}{N}-\frac{1}{N-1}\right) \tag{7.17}$$

which should correspond to the sum of anomalous dimensions, with the argument appropriately shifted

$$\mathcal{B}(N+1) = \sum_{i=0}^{N}\gamma_{N,i}. \tag{7.18}$$

For $N = 2$ this gives

$$\gamma_{1,0}^{(0),\mathrm{gq}} = \frac{4}{3}C_F. \tag{7.19}$$

This is exactly what we would have expected from the relations in the non-singlet sector. However, rather than assuming that these would generalize to gluon operators in the singlet sector, we follow a different strategy. Eq.(7.14), as a relation at the operator level, is always valid. When considering forward kinematics, it leads to the conclusion that the matrix elements of odd-N operators vanish. In off-forward kinematics, it implies that for $N = 3$ we only have to take into account one of the gluon operators, as the other one is not independent. For arbitrary odd N-values, it means that we have $(N-2)$ independent gluon operators. Inserting the gluon operator in a quark two-point function, we then have $(N-2)$ gluon operators mixing into N quark operators. For example, for $N=3$ we can replace the matrix equation

$$\begin{pmatrix} FDF \\ \partial F^2 \end{pmatrix} = \begin{pmatrix} Z_{22}^{\mathrm{gq}} & Z_{21}^{\mathrm{gq}} & Z_{20}^{\mathrm{gq}} \\ 0 & Z_{11}^{\mathrm{gq}} & Z_{10}^{\mathrm{gq}} \end{pmatrix} \begin{pmatrix} [\overline{\psi}\gamma D^2\psi] \\ [\partial\overline{\psi}\gamma D\psi] \\ [\partial^2\overline{\psi}\gamma\psi] \end{pmatrix} \tag{7.20}$$

by one of the two rows only. Eq.(7.14) holds for bare gluon operators. Introducing the renormalization then leads to a relation between the anomalous dimensions

$$\gamma_{2,1}^{(0),\mathrm{g}} = \frac{\gamma_{1,1}^{(0),\mathrm{g}} + \gamma_{1,0}^{(0),\mathrm{g}}}{2} - \gamma_{2,2}^{(0),\mathrm{g}} - \gamma_{2,0}^{(0),\mathrm{g}}. \tag{7.21}$$

This relation only holds at one-loop order, where we can simply put all renormalized operators equal to one[1]. As it is independent of the external legs of the matrix element, we do not specify them. An interesting feature of Eq.(7.21) is that it *does not hold in the non-singlet sector*. This implies that we cannot simply take the relations between the anomalous dimensions in the non-singlet sector and apply them to those of the gluon operators. Nevertheless, also the gluon anomalous dimensions are not all independent. Generalizing Eq.(7.14) to arbitrary N we have

$$2FD^NF - \partial\sum_{i=0}^{N-1}(-1)^i(D^{N-1-i}F)(D^iF) = 0 \quad (N \text{ odd}). \tag{7.22}$$

For our purposes, it is more convenient to have operators with covariant derivatives only acting on one field strength. It is straightforward to make this transformation, and we find

$$2FD^NF - \partial FD^{N-1}F - \sum_{i=1}^{N-1}(-1)^i\binom{N-1}{i-1}\partial^{N-i}FD^iF = 0 \quad (N \text{ odd}). \tag{7.23}$$

This relation holds for bare operators. The corresponding one between the renormalized operators gives a relation between the anomalous dimensions. Again we assume to work at one-loop order, such that we can put $[O] \equiv 1$. We then find

$$2\sum_{i=0}^{N+1}\gamma_{N+1,i}^{(0),\mathrm{g}} - \sum_{i=0}^{N}\gamma_{N,i}^{(0),\mathrm{g}} - \sum_{i=1}^{N-1}(-1)^i\binom{N-1}{i-1}\sum_{j=0}^{i+1}\gamma_{i+1,j}^{(0),\mathrm{g}} = 0 \quad (N \text{ odd}). \tag{7.24}$$

Note that, while the last relation only holds for odd N-values, it does mix odd and even moments. Our result Eq.(7.17) obeys this condition.

7.2.1 Extension to even-N operators

Let us now see whether we find a similar condition between the anomalous dimensions when starting from even-spin operators. A similar calculation as above shows that the following operator identity holds

$$\sum_{i=0}^{N-1}(-1)^i\binom{N}{i}\partial^{N-i}FD^iF = 0 \quad (N \text{ even}). \tag{7.25}$$

[1] At higher orders, the finite pieces of the renormalized operators will give additional non-trivial contributions.

This in turn leads to a relation between the anomalous dimensions

$$\sum_{i=0}^{N-1}(-1)^i\binom{N}{i}\sum_{j=0}^{i+1}\gamma_{i+1,j}^{(0),g}=0 \;\; (N \text{ even}). \tag{7.26}$$

Our diagram result, Eq.(7.17), obeys this relation. Unfortunately, this does not actually seem to contain new information about the anomalous dimensions. With the identification of Eq.(7.18) this is equivalent to

$$\mathcal{C}\mathcal{B}(N+2)=(-1)^N\mathcal{B}(N+2) \;\; (N \text{ even}) \tag{7.27}$$

with

$$\mathcal{C}f(N)\equiv\sum_{i=0}^{N}(-1)^i\binom{N}{i}f(i). \tag{7.28}$$

Recall that for the non-singlet quark operators, the transform of $\mathcal{B}$ was related to the last column,

$$\mathcal{C}\mathcal{B}(N+1)=\gamma_{N,0} \;\; (\text{non-singlet case}). \tag{7.29}$$

We could then define an adapted transformation $\tilde{\mathcal{C}}$

$$\tilde{\mathcal{C}}f(N)\equiv\sum_{i=0}^{N}(-1)^{N-i}\binom{N}{i}f(i), \tag{7.30}$$

such that $\mathcal{B}$ is invariant when N is even

$$\tilde{\mathcal{C}}\mathcal{B}(N+2)=\mathcal{B}(N+2). \tag{7.31}$$

From our discussion in Chapter 3, we see that this corresponds to the inverse binomial transform, cf. Eq.(3.24).

7.3 Renormalization of polarized non-singlet operators

7.3.1 Introduction

We consider the renormalization of polarized flavor non-singlet quark operators in the leading-n_f limit, including mixing with total derivative operators. The operators of interest are defined as

$$O^A_{\mu_1\ldots\mu_N}=\mathcal{S}\overline{\psi}\lambda^\alpha\gamma_{\mu_1}\gamma_5 D_{\mu_2}\ldots D_{\mu_N}\psi. \tag{7.32}$$

In forward kinematics, the corresponding anomalous dimensions determine the scale-dependence of the polarized PDFs through the DGLAP equation, cf. Eq.(2.23). These distributions can be studied by analyzing data from longitudinally polarized DIS experiments [154], collected e.g. by the HERMES and COMPASS collaborations. See e.g. [155] and references therein. For the case of off-forward kinematics, the corresponding mixing matrices characterize, through the ERBL equation introduced in Eq.(2.34), the scale-dependence of polarized GPDs [14] and polarized distribution amplitudes. An example of the latter is associated to the $\gamma\gamma^*\to\pi^0$ transition [156–159], which has been studied e.g. by analyzing data from the CLEO II detector [160]. These distributions form important ingredients to gain insight into the proton spin puzzle.

Let us briefly summarize the current knowledge about the polarized non-singlet anomalous dimensions. The forward anomalous dimensions are known to three-loop order [82, 161–167, 121] in full QCD and to all orders in the leading-n_f limit [168, 169]. For off-forward kinematics, the Gegenbauer evolution kernel was determined to three-loop order in [170]. Finally, the one-loop anomalous dimensions were also calculated in the Geyer basis [23].

As is well known, care has to be taken when dealing with γ_5 in the framework of dimensional regularization. The reason is that its standard definition involves the anti-symmetric tensor $\varepsilon_{\mu\nu\rho\sigma}$, which is a fundamentally four-dimensional object, i.e. it does not have a well-defined continuation to $D = 4 - 2\varepsilon$ dimensions. A plethora of possible γ_5 prescriptions has been developed over time, see e.g. [171–176]. We employ here the so-called Larin scheme [176], in which one defines γ_5 as

$$\gamma_5 = \frac{i}{4!}\varepsilon_{\mu\nu\rho\sigma}\gamma^\mu\gamma^\nu\gamma^\rho\gamma^\sigma. \tag{7.33}$$

When dealing with massless quarks, this is equivalent to the 't Hooft-Veltman scheme [171]. Within this scheme we have

$$\gamma_\mu\gamma_5 = \frac{i}{6}\varepsilon_{\mu\nu\rho\sigma}\gamma^\nu\gamma^\rho\gamma^\sigma \tag{7.34}$$

which means that the polarized operators can be written as

$$\mathcal{O}_N^A = \frac{i}{6}\overline{\psi}\Delta^{\mu_1}\varepsilon_{\mu_1\nu\rho\sigma}\overline{\psi}\gamma^\nu\gamma^\rho\gamma^\sigma(\Delta\cdot D)^{N-1}\psi. \tag{7.35}$$

As before, we have selected the leading-twist contributions by contracting with $\Delta^{\mu_1}\ldots\Delta^{\mu_N}$ for $\Delta^2 = 0$.

An important consequence of the definition Eq.(7.33) is that γ_5 no longer anti-commutes with D-dimensional Dirac matrices. This leads to a violation of the Ward identities. In particular, while the non-singlet current $\mathcal{O}_1^A$ is conserved, its Z-factor in the $\overline{\text{MS}}$-scheme is no longer equal to one. Instead, some non-zero anomalous dimension is generated. The way to fix this is by introducing an additional *finite* renormalization factor Z_5. The renormalization of the polarized current then follows

$$J \equiv \mathcal{O}_1^A = Z_5 Z_{0,0}^A[J]. \tag{7.36}$$

The scale-dependence of the current is determined by its anomalous dimension

$$\frac{\mathrm{d}}{\mathrm{d}\ln\mu^2}[J] = \gamma_J[J] \tag{7.37}$$

which in turn is determined from the renormalization factor as

$$\gamma_J = -Z_J^{-1}\frac{\mathrm{d}Z_J}{\mathrm{d}\ln\mu^2}. \tag{7.38}$$

The renormalization group equation for Eq.(7.36) is then

$$0 = \mu^2\frac{\mathrm{d}}{\mathrm{d}\mu^2}(Z_5 Z_{0,0}^A) + \gamma_J. \tag{7.39}$$

We can rewrite this as

$$0=\beta(a_s)\frac{\partial Z_5}{\partial a_s}-Z_5\gamma^A_{0,0}+\gamma_J \tag{7.40}$$

with

$$\gamma^A_{0,0}=-(Z^A_{0,0})^{-1}\frac{\mathrm{d}Z^A_{0,0}}{\mathrm{d}\ln\mu^2}. \tag{7.41}$$

Note the difference in interpretation of the RG-parameters in Eq.(7.40). The anomalous dimension γ_J determines the scale-dependence of the polarized current. As this is a conserved quantity, we set $\gamma_J\equiv 0$ to all orders in a_s. The anomalous dimension $\gamma^A_{0,0}$ is extracted from the renormalization of the matrix elements of J and is non-zero starting from order a_s^2. This is caused by the violation of the anti-commutativity of γ_5 with the D-dimensional Dirac matrices. Using the perturbative expansions

$$Z_5=1+z_5^{(0)}a_s+z_5^{(1)}a_s^2+z_5^{(2)}a_s^3+\ldots \tag{7.42}$$

and

$$\gamma^A_{0,0}=\gamma^{A,(0)}_{0,0}a_s+\gamma^{A,(1)}_{0,0}a_s^2+\gamma^{A,(2)}_{0,0}a_s^3+\ldots, \tag{7.43}$$

we can determine the finite renormalization factor Z_5 order per order from Eq.(7.40). Because the first term in Eq.(7.40) is multiplied by the beta-function, whose perturbative expansion starts at order a_s^2, we need to know the anomalous dimension $\gamma^A_{0,0}$ to order $(L+1)$ to obtain Z_5 to L-loop order. For example, at leading order, the equation to solve is

$$a_s^2\left(\frac{\beta_0 z_5^{(0)}}{1+a_s z_5^{(0)}}+\gamma^{A,(1)}_{0,0}\right)=0 \tag{7.44}$$

which leads to

$$z_5^{(0)}=-4C_F. \tag{7.45}$$

Here we used that [177]

$$\gamma^{A,(1)}_{0,0}=\frac{44}{3}C_FC_A-\frac{8}{3}n_fC_F. \tag{7.46}$$

The finite renormalization factor Z_5 is currently known to three-loop order [166].

7.3.2 One-loop anomalous dimensions

At the one-loop level, the operator matrix elements are easily calculated using e.g. *PACKAGE-X* in *MATHEMATICA*. The Feynman rules are the same as those of the unpolarized non-singlet operators, cf. [106], with the replacement

$$\not{\Delta}\to\frac{i}{6}\Delta^\mu\varepsilon_{\mu\nu\rho\sigma}\gamma^\nu\gamma^\rho\gamma^\sigma. \tag{7.47}$$

Both in forward and off-forward kinematics, we then find that the anomalous dimensions correspond to those of the unpolarized operators, i.e.

$$\gamma^{A,(0)}_{N,N}=C_F\left(4S_1(N)+\frac{2}{N+2}+\frac{2}{N+1}-3\right) \tag{7.48}$$

and

$$\gamma_{N,k}^{\mathcal{D},A,(0)} = C_F \left(\frac{2}{N+2} - \frac{2}{N-k} \right). \tag{7.49}$$

Note that this implies that $\gamma_{0,0}^{A,(0)} = 0$, as it should be.

In the following, we once again focus the leading-n_f limit in the total derivative basis. For the calculation of the off-forward anomalous dimensions, we can then follow the same strategy as we did in the determination of the transversity anomalous dimensions.

7.3.3 Higher-order anomalous dimensions

The leading-n_f part of the two-loop forward anomalous dimensions is [163–165]

$$\begin{aligned}\gamma_{N,N}^{A,(1)} = \frac{4}{3} n_f C_F \Bigg[& \frac{1}{4} + \frac{11}{3}\Big(\frac{1}{N+1}\Big) - \Big(\frac{1}{N+1}\Big)^2 - \frac{11}{3}\Big(\frac{1}{N+2}\Big) \\ & + \Big(\frac{1}{N+2}\Big)^2 - \frac{10}{3} S_1(N+1) + 2S_2(N+1) \Bigg].\end{aligned}$$

Note that this is exactly the same expression as for the unpolarized operators, cf. Eq.(5.20). Hence also the off-diagonal part of the mixing matrix is the same as for the Wilson operators, i.e.

$$\begin{aligned}\gamma_{N,k}^{\mathcal{D},A,(1)} = \frac{4}{3} n_f C_F \Bigg\{ & \Big(S_1(N) - S_1(k)\Big)\Big(\frac{1}{N+2} - \frac{1}{N-k}\Big) + \frac{5}{3}\frac{1}{N-k} + \frac{2}{N+1} - \frac{11}{3}\frac{1}{N+2} \\ & + \frac{1}{(N+2)^2} \Bigg\}.\end{aligned} \tag{7.50}$$

Also at higher orders in α_s, the leading-n_f terms of the forward polarized and unpolarized anomalous dimensions coincide. As such, the off-forward mixing matrices in this limit are identical. This implies that Eqs.(5.37), (5.39), (5.41) and (5.58) are valid for the three- to five-loop unpolarized and polarized ADMs.

Chapter 8

Conclusions and outlook

In this thesis, we considered the renormalization of non-singlet quark operators appearing in exclusive hard scattering processes, allowing for mixing with total derivative operators. For a consistent study of such mixing, a basis has to be chosen for the additional derivative operators. We have discussed three options, which appeared in separate branches of the literature. The first one was based on an expansion in terms of Gegenbauer polynomials, while the others were based on counting derivatives. It was shown that, using appropriate transformations, the anomalous dimensions in distinct bases can be related to one another. This connects previously unrelated branches of the literature, and provides non-trivial cross-checks of the respective calculations. In the Gegenbauer basis, this lead to an independent check of the three-loop evolution kernel of the Wilsonian non-singlet quark operators. In the Geyer basis, it provides a check of the one-loop anomalous dimensions of the same operators. The expressions in terms of harmonic sums in the Gegenbauer and total derivative bases presented in this thesis are new.

Moreover, by performing a detailed analysis of the renormalization structure of the operators in the chiral limit, we have derived consistency relations between the off-forward anomalous dimensions in the total derivative basis. This allowed us to derive, in the leading-n_f limit, the Wilson mixing matrices up to the five-loop level and the transversity matrices to four loops. Furthermore, we have presented the mixing matrices for low-spin Wilson operators in full QCD. All these results are presented in the $\overline{\text{MS}}$-scheme. When transformed to the regularization-invariant scheme, they will also be useful for the study of hadronic structure on the lattice.

The main algorithm presented in this thesis, i.e. the combination of consistency relations with explicit Feynman diagram calculations, is nicely suited for automation using computer algebra programs. Examples given in the text are the computation of Feynman graphs using *FORCER* in *FORM* or *PACKAGE-X* in *MATHEMATICA* and symbolic summation using SIGMA .

As the consistency relation for the anomalous dimensions derived in this work is a direct consequence of the renormalization structure of the operators, it should be straightforward to generalize to other types of operators. A particularly interesting application of this type would be the determination of the mixing matrices for the flavor singlet operators in QCD. Besides the mixing with total derivatives operators in off-forward kinematics, one would also have to take into account here the mixing between same-dimension quark and gluon operators. Furthermore, there would also be contributions from equation of motion and non-gauge invariant operators. The long-term goal of this would be to extend the calculation to the polarized singlet sector, where one also has to take into account that (a) the spin-one current is anomalous and (b) an additional finite renormalization factor has to be introduced because of the properties of the Dirac matrix γ_5. These aspects are left for future studies.

Acknowledgments

This thesis could not have been written without the help and support of a large group of people. First of all, the author would like to thank his supervisor, S. Moch, for the guidance, useful discussions and everlasting patience when asked a seemingly endless stream of questions. Next, I would also like to express my gratitude to J. Gracey, for taking time out of his busy schedule to have some interesting discussions on the difficulties of operator renormalization, and for carefully going through drafts of publications and sharing some useful comments to improve them. Finally I want to thank A. Manashov for the discussions (often accompanied by coffee and chocolate) and comments on papers.

Next, I want to thank M. Diehl, A. Geiser, B. Kniehl and R. Santra for agreeing to be part of the PhD committee.

Staying sane as a PhD student in theoretical physics is not easy, which is why I now want to thank some people who made some valiant efforts in this regards. First, there is of course my primordial office buddy, V. Magerya, whom I want to thank for nice discussions, exciting movie nights, changing the fundamental quantum structure of my carpet and empirically showing that I am, in fact, red-green color blind. Next, I also want to thank B. Chargeishvili for the deep philosophical discussions, excursions to perfectly normal locations to spend a Saturday afternoon and for introducing me to the greatest movie of all time. Finally, I want to thank my colleagues at the Second Institute S. Alekhin, V. Chestnov, E. Duarte, M.V. Garzelli, C. Harder, L. Kemmler, V. Lingadahally, T. Mäkelä, O. Veretin and K. Voβ for all the help, nice discussions and making the office feel like a second home.

En dan nu in het Vlaams! Eerst en vooral wil ik uiteraard mijn ouders, broer en grootouders bedanken voor de continue steun, die zich nu reeds uitstekt over meerdere decennia. Natuurlijk mogen Bram, Jeroen en Robin ook zeker niet ontbreken in dit bedankje, dus bij deze: merci voor de jarenlange vriendschap en steun (in dit Duitse avontuur en daarbuiten)!

Appendix A

Conventions

In this appendix, we briefly summarize some of the conventions used in this thesis.

- Throughout this work we use natural units, i.e. $\hbar = c = 1$.
- For the Minkowski spacetime metric, we use the mostly-minus convention

$$g_{\mu\nu} = g^{\mu\nu} = \begin{pmatrix} 1 & 0 & 0 & 0 \\ 0 & -1 & 0 & 0 \\ 0 & 0 & -1 & 0 \\ 0 & 0 & 0 & -1 \end{pmatrix}. \tag{A.1}$$

- The totally anti-symmetric tensor is defined as

$$\varepsilon^{\mu\nu\rho\sigma} = \begin{cases} 0 & \text{(if two indices are equal)} \\ 1 & (\text{if } \mu\nu\rho\sigma = 0123) \\ -1 & (\text{if } \mu\nu\rho\sigma = 1023). \end{cases} \tag{A.2}$$

- Certain calculations are most conveniently done using lightcone coordinates. For some four-vector $v \equiv (v^0, v^1, v^2, v^3)$ these are defined as

$$v^{\pm} = \frac{1}{\sqrt{2}}(v^0 \pm v^3) \tag{A.3}$$

$$\vec{v} = (v^1, v^2). \tag{A.4}$$

  Four-dimensional integration measures in turn are rewritten as

$$\mathrm{d}^4 z = \mathrm{d}z^+ \mathrm{d}z^- \mathrm{d}^2\vec{z}. \tag{A.5}$$

Appendix B

$SU(N_c)$ Wilson anomalous dimensions

Here we present the off-diagonal elements of the spin-five Wilson mixing matrix for a general gauge group $SU(N_c)$. Starting from the four-loop level, the following color factors contribute

$$\frac{d_F^{abcd}d_A^{abcd}}{N_F} = \frac{(N_c^2+6)(N_c^2-1)}{48}, \tag{B.1}$$

$$\frac{d_F^{abcd}d_F^{abcd}}{N_F} = \frac{(N_c^4-6N_c^2+18)(N_c^2-1)}{96N_c^3}, \tag{B.2}$$

$$\frac{d_A^{abcd}d_A^{abcd}}{N_A} = \frac{N_c^2(N_c^2+36)}{24}. \tag{B.3}$$

The subscripts F and A denote the fundamental and adjoint representation, and $N_F = N_c$ and $N_A = N_c^2 - 1$ represent their dimensions. Hence in QCD $d_F^{abcd}d_A^{abcd}/N_F = 5/2$, $d_F^{abcd}d_F^{abcd}/N_F = 5/36$ and $d_A^{abcd}d_A^{abcd}/N_A = 135/8$.

B.1 Two-loop anomalous dimensions

$$\gamma_{4,3}^{\mathcal{D},(1)} = -\frac{191}{30}C_FC_A + \frac{997}{1080}C_F^2 + \frac{17}{10}n_fC_F, \tag{B.4}$$

$$\gamma_{4,2}^{\mathcal{D},(1)} = -\frac{7999}{1800}C_F^2 + \gamma_{4,2}^{\mathcal{D},(1)}\Big|_{\text{SLC}} + \frac{82}{135}n_fC_F, \tag{B.5}$$

$$\gamma_{4,1}^{\mathcal{D},(1)} = \frac{5339}{225}C_FC_A - \frac{37769}{27000}C_F^2 + \frac{23}{90}n_fC_F - \gamma_{4,2}^{\mathcal{D},(1)}\Big|_{\text{SLC}}, \tag{B.6}$$

$$\gamma_{4,0}^{\mathcal{D},(1)} = -\frac{931}{1080}C_FC_A + \frac{14}{675}C_F^2 + \frac{43}{540}n_fC_F, \tag{B.7}$$

$$\gamma_{3,2}^{\mathcal{D},(1)} = -\frac{1391}{225}C_FC_A + \frac{343}{375}C_F^2 + \frac{362}{225}n_fC_F, \tag{B.8}$$

$$\gamma_{3,1}^{\mathcal{D},(1)} = -\frac{211}{100}C_FC_A - \frac{1153}{9000}C_F^2 + \frac{13}{25}n_fC_F, \tag{B.9}$$

$$\gamma_{3,0}^{\mathcal{D},(1)} = -\frac{958}{675}C_F C_A + \frac{772}{3375}C_F^2 + \frac{106}{675}n_f C_F\,, \tag{B.10}$$

$$\gamma_{2,1}^{\mathcal{D},(1)} = -\frac{53}{9}C_F C_A + \frac{9}{16}C_F^2 + \frac{53}{36}n_f C_F\,, \tag{B.11}$$

$$\gamma_{2,0}^{\mathcal{D},(1)} = -\frac{97}{36}C_F C_A + \frac{103}{144}C_F^2 + \frac{13}{36}n_f C_F\,, \tag{B.12}$$

$$\gamma_{1,0}^{\mathcal{D},(1)} = -\frac{188}{27}C_F C_A + \frac{56}{27}C_F^2 + \frac{32}{27}n_f C_F\,. \tag{B.13}$$

B.2 Three-loop anomalous dimensions

$$\begin{aligned}\gamma_{4,3}^{\mathcal{D},(2)} = {} & C_F C_A^2\Big(-\frac{6642011}{194400} + \frac{2}{3}\zeta_3\Big) + C_F^2 C_A\Big(-\frac{2291861}{972000} - 2\zeta_3\Big) \\ & + C_F^3\Big(\frac{4602059}{972000} + \frac{4}{3}\zeta_3\Big) + n_f C_F C_A\Big(\frac{28703}{12150} + \frac{40}{3}\zeta_3\Big) \\ & + n_f C_F^2\Big(\frac{6516293}{486000} - \frac{40}{3}\zeta_3\Big) + n_f^2 C_F\Big(\frac{3131}{8100}\Big)\,,\end{aligned} \tag{B.14}$$

$$\gamma_{4,2}^{\mathcal{D},(2)} = \frac{1312}{6075}n_f^2 C_F + \tilde{\gamma}_{4,2}^{\mathcal{D},(2)}\,, \tag{B.15}$$

$$\begin{aligned}\gamma_{4,1}^{\mathcal{D},(2)} = {} & C_F C_A^2\Big(-\frac{2331353}{129600} + \frac{6}{5}\zeta_3\Big) + C_F^2 C_A\Big(-\frac{1620737}{243000} - \frac{18}{5}\zeta_3\Big) \\ & + C_F^3\Big(\frac{3600253}{540000} + \frac{12}{5}\zeta_3\Big) + n_f C_F C_A\Big(\frac{124163}{97200} + 8\zeta_3\Big) \\ & + n_f C_F^2\Big(\frac{3839747}{486000} - 8\zeta_3\Big) + n_f^2 C_F\Big(\frac{1181}{8100}\Big) - \tilde{\gamma}_{4,2}^{\mathcal{D},(2)}\,,\end{aligned} \tag{B.16}$$

$$\begin{aligned}\gamma_{4,0}^{\mathcal{D},(2)} = {} & C_F C_A^2\Big(-\frac{5439839}{777600} - \frac{19}{5}\zeta_3\Big) + C_F^2 C_A\Big(\frac{11200081}{1944000} + \frac{57}{5}\zeta_3\Big) \\ & + C_F^3\Big(-\frac{14346169}{6480000} - \frac{38}{5}\zeta_3\Big) + n_f C_F C_A\Big(\frac{155383}{194400} + \frac{4}{3}\zeta_3\Big) \\ & + n_f C_F^2\Big(\frac{34921}{54000} - \frac{4}{3}\zeta_3\Big) + n_f^2 C_F\Big(\frac{4841}{48600}\Big)\,,\end{aligned} \tag{B.17}$$

$$\begin{aligned}\gamma_{3,2}^{\mathcal{D},(2)} = {} & C_F C_A^2\Big(-\frac{1555453}{40500} - \frac{32}{25}\zeta_3\Big) + C_F^2 C_A\Big(\frac{755417}{67500} + \frac{96}{25}\zeta_3\Big) \\ & + C_F^3\Big(-\frac{3114527}{2025000} - \frac{64}{25}\zeta_3\Big) + n_f C_F C_A\Big(\frac{63841}{20250} + \frac{64}{5}\zeta_3\Big) \\ & + n_f C_F^2\Big(\frac{197764}{16875} - \frac{64}{5}\zeta_3\Big) + n_f^2 C_F\Big(\frac{3947}{10125}\Big)\,,\end{aligned} \tag{B.18}$$

$$\begin{aligned}\gamma_{3,1}^{\mathcal{D},(2)} = {} & C_F C_A^2\Big(-\frac{328189}{54000} + \frac{78}{25}\zeta_3\Big) + C_F^2 C_A\Big(-\frac{30661727}{1620000} - \frac{234}{25}\zeta_3\Big) \\ & + C_F^3\Big(\frac{22052171}{1800000} + \frac{156}{25}\zeta_3\Big) + n_f C_F C_A\Big(\frac{2351}{3375} + \frac{24}{5}\zeta_3\Big)\end{aligned}$$

$$+n_f C_F^2\Big(\frac{9010739}{1620000}-\frac{24}{5}\zeta_3\Big)+n_f^2 C_F\Big(\frac{734}{3375}\Big)\,, \tag{B.19}$$

$$\begin{aligned}\gamma_{3,0}^{\mathcal{D},(2)} &= C_F C_A^2\Big(-\frac{319316}{30375}-\frac{376}{75}\zeta_3\Big)+C_F^2 C_A\Big(\frac{18468637}{2430000}+\frac{376}{25}\zeta_3\Big)\\ &\quad +C_F^3\Big(-\frac{52103569}{24300000}-\frac{752}{75}\zeta_3\Big)+n_f C_F C_A\Big(\frac{81233}{60750}+\frac{32}{15}\zeta_3\Big)\\ &\quad +n_f C_F^2\Big(\frac{1302883}{1215000}-\frac{32}{15}\zeta_3\Big)+n_f^2 C_F\Big(\frac{4411}{30375}\Big)\,,\end{aligned} \tag{B.20}$$

$$\begin{aligned}\gamma_{2,1}^{\mathcal{D},(2)} &= C_F C_A^2\Big(-\frac{73331}{2592}+3\zeta_3\Big)+C_F^2 C_A\Big(-\frac{78193}{5184}-9\zeta_3\Big)\\ &\quad +C_F^3\Big(\frac{23185}{1728}+6\zeta_3\Big)+n_f C_F C_A\Big(\frac{4067}{1296}+12\zeta_3\Big)+n_f C_F^2\Big(\frac{31481}{2592}-12\zeta_3\Big)\\ &\quad +n_f^2 C_F\Big(\frac{259}{648}\Big)\,,\end{aligned} \tag{B.21}$$

$$\begin{aligned}\gamma_{2,0}^{\mathcal{D},(2)} &= C_F C_A^2\Big(-\frac{47225}{2592}-7\zeta_3\Big)+C_F^2 C_A\Big(\frac{56393}{5184}+21\zeta_3\Big)\\ &\quad +C_F^3\Big(-\frac{130}{81}-14\zeta_3\Big)+n_f C_F C_A\Big(\frac{3335}{1296}+4\zeta_3\Big)+n_f C_F^2\Big(\frac{2803}{1296}-4\zeta_3\Big)\\ &\quad +n_f^2 C_F\Big(\frac{151}{648}\Big)\,,\end{aligned} \tag{B.22}$$

$$\begin{aligned}\gamma_{1,0}^{\mathcal{D},(2)} &= C_F C_A^2\Big(-\frac{10460}{243}-\frac{32}{3}\zeta_3\Big)+C_F^2 C_A\Big(\frac{4264}{243}+32\zeta_3\Big)+C_F^3\Big(\frac{280}{243}-\frac{64}{3}\zeta_3\Big)\\ &\quad +n_f C_F C_A\Big(\frac{1564}{243}+\frac{32}{3}\zeta_3\Big)+n_f C_F^2\Big(\frac{1706}{243}-\frac{32}{3}\zeta_3\Big)+n_f^2 C_F\Big(\frac{112}{243}\Big)\,.\end{aligned} \tag{B.23}$$

B.3 Four-loop anomalous dimensions

$$\begin{aligned}\gamma_{1,0}^{\mathcal{D},(3)} &= \frac{d_F^{abcd}d_A^{abcd}}{N_F}\Big(\frac{368}{9}-\frac{2560}{9}\zeta_5-\frac{992}{9}\zeta_3\Big)\\ &\quad +C_F C_A^3\Big(-\frac{867065}{2187}+\frac{6080}{27}\zeta_5+\frac{176}{3}\zeta_4-\frac{17468}{81}\zeta_3\Big)\\ &\quad +C_F^2 C_A^2\Big(\frac{813032}{2187}-\frac{2240}{9}\zeta_5-176\zeta_4+\frac{12872}{27}\zeta_3\Big)\\ &\quad +C_F^3 C_A\Big(-\frac{119338}{2187}-\frac{640}{3}\zeta_5+\frac{352}{3}\zeta_4-\frac{15520}{81}\zeta_3\Big)\\ &\quad +C_F^4\Big(-\frac{97196}{2187}+\frac{640}{3}\zeta_5-\frac{5440}{81}\zeta_3\Big)\\ &\quad +n_f\frac{d_F^{abcd}d_F^{abcd}}{N_F}\Big(-\frac{416}{9}+\frac{1280}{9}\zeta_5-\frac{512}{9}\zeta_3\Big)\\ &\quad +n_f C_F C_A^2\Big(\frac{26509}{243}-\frac{2240}{27}\zeta_5-\frac{208}{3}\zeta_4+\frac{2020}{9}\zeta_3\Big)\\ &\quad +n_f C_F^2 C_A\Big(\frac{88874}{2187}-\frac{160}{9}\zeta_5+\frac{272}{3}\zeta_4-\frac{6464}{27}\zeta_3\Big)\end{aligned}$$

$$
\begin{aligned}
&+n_f C_F^3\Big(-\frac{95456}{2187}+\frac{320}{3}\zeta_5-\frac{64}{3}\zeta_4+\frac{1264}{81}\zeta_3\Big)\\
&+n_f^2 C_F C_A\Big(-\frac{3175}{729}+\frac{32}{3}\zeta_4-\frac{64}{3}\zeta_3\Big)\\
&+n_f^2 C_F^2\Big(-\frac{12472}{2187}-\frac{32}{3}\zeta_4+\frac{64}{3}\zeta_3\Big)+n_f^3 C_F\Big(\frac{512}{2187}-\frac{64}{81}\zeta_3\Big)\,, \qquad \text{(B.24)}
\end{aligned}
$$

$$
\begin{aligned}
\gamma_{2,1}^{\mathcal{D},(3)} \;=\;& \frac{d_F^{abcd}d_A^{abcd}}{N_F}\Big(-\frac{481}{9}+1380\zeta_5-624\zeta_3\Big)+C_F C_A^3\Big(-\frac{5725127}{23328}-230\zeta_5\\
&-\frac{33}{2}\zeta_4+\frac{17141}{72}\zeta_3\Big)+C_F^2 C_A^2\Big(\frac{29201815}{186624}+645\zeta_5+\frac{99}{2}\zeta_4-\frac{6967}{9}\zeta_3\Big)\\
&+C_F^3 C_A\Big(-\frac{1128755}{31104}-540\zeta_5-33\zeta_4+\frac{43153}{72}\zeta_3\Big)\\
&+C_F^4\Big(-\frac{15839393}{248832}+240\zeta_5-\frac{500}{3}\zeta_3\Big)+n_f\frac{d_F^{abcd}d_F^{abcd}}{N_F}\Big(\frac{7}{9}+160\zeta_5-104\zeta_3\Big)\\
&+n_f C_F C_A^2\Big(\frac{223465}{2592}-\frac{280}{3}\zeta_5-63\zeta_4+\frac{3403}{18}\zeta_3\Big)+n_f C_F^2 C_A\Big(\frac{3855247}{46656}-20\zeta_5\\
&+57\zeta_4-\frac{1897}{18}\zeta_3\Big)+n_f C_F^3\Big(-\frac{1549993}{31104}+120\zeta_5+6\zeta_4-\frac{223}{3}\zeta_3\Big)\\
&+n_f^2 C_F C_A\Big(-\frac{9649}{1944}+12\zeta_4-\frac{226}{9}\zeta_3\Big)+n_f^2 C_F^2\Big(-\frac{171745}{23328}-12\zeta_4+\frac{226}{9}\zeta_3\Big)\\
&+n_f^3 C_F\Big(\frac{2401}{11664}-\frac{8}{9}\zeta_3\Big)\,, \qquad \text{(B.25)}
\end{aligned}
$$

$$
\begin{aligned}
\gamma_{3,2}^{\mathcal{D},(3)} \;=\;& \frac{d_F^{abcd}d_A^{abcd}}{N_F}\Big(-\frac{292963}{900}+\frac{21184}{15}\zeta_5-\frac{12784}{15}\zeta_3\Big)\\
&+C_F C_A^3\Big(-\frac{1009689359}{7290000}-\frac{5552}{45}\zeta_5+\frac{176}{25}\zeta_4+\frac{136949}{3375}\zeta_3\Big)\\
&+C_F^2 C_A^2\Big(-\frac{359381531}{24300000}+\frac{160}{3}\zeta_5-\frac{528}{25}\zeta_4-\frac{88256}{1875}\zeta_3\Big)\\
&+C_F^3 C_A\Big(-\frac{522421339}{7290000}+\frac{5248}{15}\zeta_5+\frac{352}{25}\zeta_4-\frac{151912}{1125}\zeta_3\Big)\\
&+C_F^4\Big(\frac{9662914729}{121500000}-\frac{2432}{15}\zeta_5+\frac{366368}{16875}\zeta_3\Big)\\
&+n_f\frac{d_F^{abcd}d_F^{abcd}}{N_F}\Big(-\frac{4193}{90}+\frac{1152}{5}\zeta_5-\frac{9328}{75}\zeta_3\Big)\\
&+n_f C_F C_A^2\Big(\frac{19831099}{202500}-\frac{1456}{15}\zeta_5-\frac{1792}{25}\zeta_4+\frac{235459}{1125}\zeta_3\Big)\\
&+n_f C_F^2 C_A\Big(\frac{367343971}{6075000}-\frac{64}{3}\zeta_5+\frac{1856}{25}\zeta_4-\frac{17924}{125}\zeta_3\Big)\\
&+n_f C_F^3\Big(-\frac{87346403}{1822500}+128\zeta_5-\frac{64}{25}\zeta_4-\frac{21352}{375}\zeta_3\Big)\\
&+n_f^2 C_F C_A\Big(-\frac{2581429}{607500}+\frac{64}{5}\zeta_4-\frac{2032}{75}\zeta_3\Big)\\
&+n_f^2 C_F^2\Big(-\frac{6850267}{759375}-\frac{64}{5}\zeta_4+\frac{2032}{75}\zeta_3\Big)+n_f^3 C_F\Big(\frac{191989}{911250}-\frac{128}{135}\zeta_3\Big)\,, \qquad \text{(B.26)}
\end{aligned}
$$

$$
\begin{aligned}
\gamma_{4,3}^{\mathcal{D},(3)} &= \frac{d_F^{abcd}d_A^{abcd}}{N_F}\Big(-\frac{3138061}{5400}+\frac{22840}{9}\zeta_5-\frac{315746}{225}\zeta_3\Big) \\
&+C_FC_A^3\Big(-\frac{339793967}{34992000}-\frac{12896}{27}\zeta_5-\frac{11}{3}\zeta_4+\frac{451817}{2025}\zeta_3\Big) \\
&+C_F^2C_A^2\Big(-\frac{69304250621}{174960000}+\frac{9506}{9}\zeta_5+11\zeta_4-\frac{348659}{675}\zeta_3\Big) \\
&+C_F^3C_A\Big(\frac{170996951743}{437400000}-\frac{6488}{9}\zeta_5-\frac{22}{3}\zeta_4+\frac{62749}{300}\zeta_3\Big) \\
&+C_F^4\Big(-\frac{652403846867}{3499200000}+\frac{3184}{9}\zeta_5-\frac{194876}{2025}\zeta_3\Big) \\
&+n_f\frac{d_F^{abcd}d_F^{abcd}}{N_F}\Big(-\frac{57823}{675}+\frac{832}{3}\zeta_5-\frac{29552}{225}\zeta_3\Big) \\
&+n_fC_FC_A^2\Big(\frac{170258047}{1749600}-\frac{896}{9}\zeta_5-\frac{218}{3}\zeta_4+\frac{9409}{45}\zeta_3\Big) \\
&+n_fC_F^2C_A\Big(\frac{2705226287}{43740000}-\frac{200}{9}\zeta_5+\frac{214}{3}\zeta_4-\frac{85819}{675}\zeta_3\Big) \\
&+n_fC_F^3\Big(-\frac{17459684723}{437400000}+\frac{400}{3}\zeta_5+\frac{4}{3}\zeta_4-\frac{48094}{675}\zeta_3\Big) \\
&+n_f^2C_FC_A\Big(-\frac{580649}{145800}+\frac{40}{3}\zeta_4-\frac{3836}{135}\zeta_3\Big) \\
&+n_f^2C_F^2\Big(-\frac{210054821}{21870000}-\frac{40}{3}\zeta_4+\frac{3836}{135}\zeta_3\Big)+n_f^3C_F\Big(\frac{154397}{729000}-\frac{80}{81}\zeta_3\Big). \qquad \text{(B.27)}
\end{aligned}
$$

B.4 Five-loop anomalous dimensions

$$
\begin{aligned}
\gamma_{1,0}^{\mathcal{D},(4)} &= C_A\frac{d_F^{abcd}d_A^{abcd}}{N_F}\Big(\frac{41384}{81}+6384\zeta_7+\frac{70400}{27}\zeta_6-\frac{646480}{81}\zeta_5+\frac{5456}{9}\zeta_4 \\
&-\frac{277760}{81}\zeta_3+\frac{42176}{27}\zeta_3^2\Big)+C_F\frac{d_A^{abcd}d_A^{abcd}}{N_A}\Big(\frac{7672}{81}-\frac{9520}{9}\zeta_7+\frac{29200}{27}\zeta_5 \\
&-\frac{352}{3}\zeta_4-\frac{6032}{27}\zeta_3-\frac{3008}{3}\zeta_3^2\Big)+C_F\frac{d_F^{abcd}d_A^{abcd}}{N_F}\Big(-\frac{11984}{81}-\frac{38528}{9}\zeta_7 \\
&-\frac{88160}{81}\zeta_5+\frac{366752}{81}\zeta_3-\frac{3200}{3}\zeta_3^2\Big)+C_FC_A^4\Big(-\frac{266532611}{78732}-\frac{89488}{27}\zeta_7 \\
&-\frac{167200}{81}\zeta_6+\frac{1551104}{243}\zeta_5+\frac{110960}{81}\zeta_4-\frac{1294072}{729}\zeta_3-\frac{37456}{81}\zeta_3^2\Big) \\
&+C_F^2C_A^3\Big(\frac{110112362}{19683}+\frac{165928}{27}\zeta_7+\frac{61600}{27}\zeta_6-\frac{1820312}{243}\zeta_5-\frac{85484}{27}\zeta_4 \\
&+\frac{2057768}{729}\zeta_3+\frac{35200}{27}\zeta_3^2\Big)+C_F^3C_A^2\Big(-\frac{31670203}{6561}-7840\zeta_7+\frac{17600}{9}\zeta_6 \\
&-\frac{30848}{27}\zeta_5+\frac{114736}{81}\zeta_4+\frac{501596}{243}\zeta_3-\frac{15488}{9}\zeta_3^2\Big) \\
&+C_F^4C_A\Big(\frac{40931372}{19683}+9968\zeta_7-\frac{17600}{9}\zeta_6-\frac{71120}{27}\zeta_5+\frac{29920}{81}\zeta_4
\end{aligned}
$$

$$
\begin{aligned}
& -\frac{800296}{243}\zeta_3+1536\zeta_3^2\Big)+C_F^5\Big(-\frac{4653188}{19683}-4256\zeta_7+\frac{278720}{81}\zeta_5 \\
& +\frac{401392}{729}\zeta_3-\frac{6272}{9}\zeta_3^2\Big)+n_f\frac{d_F^{abcd}d_A^{abcd}}{N_F}\Big(-\frac{11048}{27}+1232\zeta_7-\frac{12800}{27}\zeta_6 \\
& +\frac{108640}{81}\zeta_5+\frac{256}{9}\zeta_4-\frac{21856}{81}\zeta_3+\frac{12544}{27}\zeta_3^2\Big) \\
& +n_fC_A\frac{d_F^{abcd}d_F^{abcd}}{N_F}\Big(-\frac{103912}{81}+\frac{14560}{9}\zeta_7-\frac{35200}{27}\zeta_6+\frac{261440}{81}\zeta_5 \\
& +\frac{2816}{9}\zeta_4-\frac{125696}{81}\zeta_3-\frac{7936}{27}\zeta_3^2\Big)+n_fC_F\frac{d_F^{abcd}d_F^{abcd}}{N_F}\Big(\frac{85376}{81}-\frac{17920}{9}\zeta_7 \\
& +\frac{325120}{81}\zeta_5-\frac{164416}{81}\zeta_3-\frac{4096}{9}\zeta_3^2\Big)+n_fC_FC_A^3\Big(\frac{24423290}{19683}+\frac{19544}{27}\zeta_7 \\
& +\frac{92000}{81}\zeta_6-\frac{694540}{243}\zeta_5-\frac{137384}{81}\zeta_4+\frac{2157154}{729}\zeta_3+\frac{13904}{81}\zeta_3^2\Big) \\
& +n_fC_F^2C_A^2\Big(-\frac{15291499}{26244}-\frac{5600}{27}\zeta_7-\frac{6800}{27}\zeta_6+\frac{126272}{243}\zeta_5+\frac{57268}{27}\zeta_4 \\
& -\frac{780800}{243}\zeta_3-\frac{12448}{27}\zeta_3^2\Big)+n_fC_F^3C_A\Big(\frac{1687541}{6561}+\frac{2240}{3}\zeta_7-\frac{4000}{3}\zeta_6 \\
& +\frac{229016}{81}\zeta_5-\frac{24128}{81}\zeta_4-\frac{210034}{243}\zeta_3+\frac{1984}{3}\zeta_3^2\Big) \\
& +n_fC_F^4\Big(-\frac{912482}{19683}-\frac{4480}{3}\zeta_7+\frac{3200}{9}\zeta_6+\frac{8240}{81}\zeta_5-\frac{10624}{81}\zeta_4 \\
& +\frac{231760}{243}\zeta_3-\frac{3328}{9}\zeta_3^2\Big)+n_f^2\frac{d_F^{abcd}d_F^{abcd}}{N_F}\Big(\frac{21872}{81}+\frac{6400}{27}\zeta_6-\frac{26240}{81}\zeta_5 \\
& -\frac{896}{9}\zeta_4-\frac{17824}{81}\zeta_3+\frac{1024}{27}\zeta_3^2\Big)+n_f^2C_FC_A^2\Big(-\frac{315700}{6561}-\frac{11200}{81}\zeta_6 \\
& +\frac{26672}{243}\zeta_5+392\zeta_4-\frac{107134}{243}\zeta_3-\frac{12736}{81}\zeta_3^2\Big) \\
& +n_f^2C_F^2C_A\Big(-\frac{166127}{2187}-\frac{800}{27}\zeta_6+\frac{14272}{81}\zeta_5-\frac{10376}{27}\zeta_4+\frac{42508}{243}\zeta_3 \\
& +\frac{6976}{27}\zeta_3^2\Big)+n_f^2C_F^3\Big(-\frac{1082297}{13122}+\frac{1600}{9}\zeta_6-\frac{27776}{81}\zeta_5-\frac{536}{81}\zeta_4 \\
& +\frac{72896}{243}\zeta_3-\frac{896}{9}\zeta_3^2\Big)+n_f^3C_FC_A\Big(-\frac{168677}{39366}+\frac{2048}{81}\zeta_5-\frac{1376}{81}\zeta_4 \\
& -\frac{5936}{729}\zeta_3\Big)+n_f^3C_F^2\Big(-\frac{132755}{19683}-\frac{256}{27}\zeta_5+\frac{64}{3}\zeta_4-\frac{5936}{729}\zeta_3\Big) \\
& +n_f^4C_F\Big(\frac{2752}{19683}-\frac{64}{81}\zeta_4+\frac{512}{729}\zeta_3\Big), \qquad \text{(B.28)}
\end{aligned}
$$

$$
\begin{aligned}
\gamma_{2,1}^{\mathcal{D},(4)} = {} & C_A\frac{d_F^{abcd}d_A^{abcd}}{N_F}\Big(-\frac{663149}{162}-\frac{43547}{4}\zeta_7-12650\zeta_6+\frac{2347355}{54}\zeta_5 \\
& +3432\zeta_4-\frac{235195}{54}\zeta_3-10416\zeta_3^2\Big) \\
& +C_F\frac{d_A^{abcd}d_A^{abcd}}{N_A}\Big(\frac{51037}{162}+\frac{3115}{4}\zeta_7+\frac{39275}{54}\zeta_5-132\zeta_4
\end{aligned}
$$

$$
\begin{aligned}
&-\frac{76387}{54}\zeta_3-328\zeta_3^2\Big)+C_F\frac{d_F^{abcd}d_A^{abcd}}{N_F}\Big(\frac{2180047}{324}-13706\zeta_7\\
&-\frac{31785}{2}\zeta_5+\frac{1139143}{108}\zeta_3+9870\zeta_3^2\Big)\\
&+C_FC_A^4\Big(-\frac{2566577183}{3359232}-\frac{2296}{3}\zeta_7+\frac{6325}{3}\zeta_6-\frac{5133413}{648}\zeta_5\\
&-\frac{195499}{144}\zeta_4+\frac{36838057}{7776}\zeta_3+\frac{6356}{3}\zeta_3^2\Big)\\
&+C_F^2C_A^3\Big(-\frac{19615708519}{6718464}+\frac{88879}{12}\zeta_7-\frac{11825}{2}\zeta_6+\frac{9916061}{432}\zeta_5\\
&+\frac{79391}{18}\zeta_4-\frac{5873293}{324}\zeta_3-7570\zeta_3^2\Big)\\
&+C_F^3C_A^2\Big(\frac{1361909845}{373248}-\frac{77175}{4}\zeta_7+4950\zeta_6-\frac{1478507}{216}\zeta_5\\
&-\frac{489371}{144}\zeta_4+\frac{106509385}{7776}\zeta_3+10534\zeta_3^2\Big)\\
&+C_F^4C_A\Big(-\frac{16427221735}{26873856}+\frac{75411}{4}\zeta_7-2200\zeta_6-\frac{1899115}{108}\zeta_5\\
&+\frac{2750}{3}\zeta_4+\frac{9100805}{2592}\zeta_3-7562\zeta_3^2\Big)\\
&+C_F^5\Big(-\frac{178411603}{331776}-\frac{17661}{2}\zeta_7+\frac{84485}{6}\zeta_5-\frac{4632269}{864}\zeta_3+2466\zeta_3^2\Big)\\
&+n_f\frac{d_F^{abcd}d_A^{abcd}}{N_F}\Big(-\frac{165313}{162}-1554\zeta_7+2300\zeta_6-\frac{3500}{3}\zeta_5\\
&-468\zeta_4-\frac{12362}{9}\zeta_3+\frac{4168}{3}\zeta_3^2\Big)\\
&+n_fC_A\frac{d_F^{abcd}d_F^{abcd}}{N_F}\Big(\frac{173813}{162}+4760\zeta_7-\frac{4400}{3}\zeta_6-\frac{68660}{27}\zeta_5\\
&+572\zeta_4-\frac{27365}{27}\zeta_3-544\zeta_3^2\Big)\\
&+n_fC_F\frac{d_F^{abcd}d_F^{abcd}}{N_F}\Big(-\frac{97597}{81}-11060\zeta_7+\frac{108040}{9}\zeta_5-\frac{1726}{27}\zeta_3-32\zeta_3^2\Big)\\
&+n_fC_FC_A^3\Big(\frac{837883325}{839808}+\frac{10507}{12}\zeta_7+\frac{4250}{9}\zeta_6-\frac{139930}{81}\zeta_5\\
&-\frac{72251}{72}\zeta_4+\frac{3727589}{1944}\zeta_3-\frac{2957}{9}\zeta_3^2\Big)\\
&+n_fC_F^2C_A^2\Big(-\frac{191432243}{373248}-\frac{595}{12}\zeta_7+\frac{3775}{3}\zeta_6-\frac{84596}{27}\zeta_5\\
&-\frac{215}{36}\zeta_4+\frac{15259}{18}\zeta_3+1108\zeta_3^2\Big)\\
&+n_fC_F^3C_A\Big(\frac{669771445}{1119744}+840\zeta_7-2000\zeta_6+\frac{259217}{54}\zeta_5\\
&+\frac{72013}{72}\zeta_4-\frac{14222911}{3888}\zeta_3-896\zeta_3^2\Big)
\end{aligned}
$$

$$
\begin{aligned}
&+n_f C_F^4\Big(\frac{653668241}{13436928}-1680\zeta_7+400\zeta_6+\frac{4615}{27}\zeta_5-\frac{446}{3}\zeta_4\\
&+\frac{135293}{162}\zeta_3+184\zeta_3^2\Big)+n_f^2\frac{d_F^{abcd}d_F^{abcd}}{N_F}\Big(\frac{14561}{81}+\frac{800}{3}\zeta_6-\frac{5840}{27}\zeta_5\\
&-152\zeta_4-\frac{5906}{27}\zeta_3+\frac{128}{3}\zeta_3^2\Big)\\
&+n_f^2 C_F C_A^2\Big(-\frac{7112759}{139968}-\frac{1400}{9}\zeta_6+\frac{11882}{81}\zeta_5+\frac{1151}{3}\zeta_4\\
&-\frac{86963}{216}\zeta_3-\frac{1592}{9}\zeta_3^2\Big)+n_f^2 C_F^2 C_A\Big(-\frac{582217}{17496}-\frac{100}{3}\zeta_6+\frac{4772}{27}\zeta_5\\
&-\frac{549}{2}\zeta_4-\frac{535}{12}\zeta_3+\frac{872}{3}\zeta_3^2\Big)+n_f^2 C_F^3\Big(-\frac{78593429}{559872}+200\zeta_6\\
&-\frac{1144}{3}\zeta_5-\frac{298}{3}\zeta_4+\frac{222397}{486}\zeta_3-112\zeta_3^2\Big)\\
&+n_f^3 C_F C_A\Big(-\frac{977951}{419904}+\frac{256}{9}\zeta_5-\frac{182}{9}\zeta_4-\frac{1025}{243}\zeta_3\Big)\\
&+n_f^3 C_F^2\Big(-\frac{3921833}{419904}-\frac{32}{3}\zeta_5+\frac{226}{9}\zeta_4-\frac{121}{9}\zeta_3\Big)\\
&+n_f^4 C_F\Big(\frac{27955}{209952}-\frac{8}{9}\zeta_4+\frac{212}{243}\zeta_3\Big)\,. \qquad \text{(B.29)}
\end{aligned}
$$

Bibliography

[1] C.A. Aidala, S.D. Bass, D. Hasch and G.K. Mallot, *The Spin Structure of the Nucleon*, *Rev. Mod. Phys.* **85** (2013) 655 [arXiv:1209.2803].

[2] E. Leader and C. Lorcé, *The angular momentum controversy: What's it all about and does it matter?*, *Phys. Rept.* **541** (2014) 163 [arXiv:1309.4235].

[3] A. Deur, S.J. Brodsky and G.F. De Téramond, *The Spin Structure of the Nucleon*, arXiv:1807.05250.

[4] X. Ji, F. Yuan and Y. Zhao, *What we know and what we don't know about the proton spin after 30 years*, *Nature Rev. Phys.* **3** (2021) 27 [arXiv:2009.01291].

[5] H1, ZEUS collaboration, H. Abramowicz et al., *Combination of measurements of inclusive deep inelastic $e^{\pm}p$ scattering cross sections and QCD analysis of HERA data*, *Eur. Phys. J. C* **75** (2015) 580 [arXiv:1506.06042].

[6] A. Accardi et al., *A Critical Appraisal and Evaluation of Modern PDFs*, *Eur. Phys. J. C* **76** (2016) 471 [arXiv:1603.08906].

[7] D. Boer et al., *Gluons and the quark sea at high energies: Distributions, polarization, tomography*, arXiv:1108.1713.

[8] R. Abdul Khalek et al., *Science Requirements and Detector Concepts for the Electron-Ion Collider: EIC Yellow Report*, arXiv:2103.05419.

[9] J.P. Ralston and D.E. Soper, *Production of Dimuons from High-Energy Polarized Proton Proton Collisions*, *Nucl. Phys. B* **152** (1979) 109.

[10] X. Artru and M. Mekhfi, *Transversely Polarized Parton Densities, their Evolution and their Measurement*, *Z. Phys. C* **45** (1990) 669.

[11] R.L. Jaffe and X.D. Ji, *Chiral odd parton distributions and polarized Drell-Yan*, *Phys. Rev. Lett.* **67** (1991) 552.

[12] R.L. Jaffe and X.D. Ji, *Chiral odd parton distributions and Drell-Yan processes*, *Nucl. Phys. B* **375** (1992) 527.

[13] J.L. Cortes, B. Pire and J.P. Ralston, *Measuring the transverse polarization of quarks in the proton*, *Z. Phys. C* **55** (1992) 409.

[14] M. Diehl, *Generalized parton distributions*, *Phys. Rept.* **388** (2003) 41 [hep-ph/0307382].

[15] A.V. Belitsky and A.V. Radyushkin, *Unraveling hadron structure with generalized parton distributions*, *Phys. Rept.* **418** (2005) 1 [hep-ph/0504030].

[16] V.M. Braun, A.N. Manashov, S. Moch and M. Strohmaier, *Three-loop evolution equation for flavor-nonsinglet operators in off-forward kinematics*, *JHEP* **06** (2017) 037 [arXiv:1703.09532].

[17] V.M. Braun, G.P. Korchemsky and D. Müller, *The Uses of conformal symmetry in QCD*, *Prog. Part. Nucl. Phys.* **51** (2003) 311 [hep-ph/0306057].

[18] D. Müller, *Conformal constraints and the evolution of the nonsinglet meson distribution amplitude*, *Phys. Rev. D* **49** (1994) 2525.

[19] A.V. Belitsky and D. Müller, *Broken conformal invariance and spectrum of anomalous dimensions in QCD*, *Nucl. Phys. B* **537** (1999) 397 [hep-ph/9804379].

[20] V.M. Braun and A.N. Manashov, *Evolution equations beyond one loop from conformal symmetry*, *Eur. Phys. J. C* **73** (2013) 2544 [arXiv:1306.5644].

[21] D. Müller, *Constraints for anomalous dimensions of local light cone operators in ϕ^3 in six-dimensions theory*, *Z. Phys. C* **49** (1991) 293.

[22] V.M. Braun, A.N. Manashov, S. Moch and M. Strohmaier, *Two-loop conformal generators for leading-twist operators in QCD*, *JHEP* **03** (2016) 142 [arXiv:1601.05937].

[23] J. Blümlein, B. Geyer and D. Robaschik, *The Virtual Compton amplitude in the generalized Bjorken region: twist-2 contributions*, *Nucl. Phys. B* **560** (1999) 283 [hep-ph/9903520].

[24] B. Geyer, *Anomalous dimensions in local and non-local light cone expansion. (Talk)*, *Czech. J. Phys. B* **32** (1982) 645.

[25] J.A. Gracey, *Three loop anti-MS operator correlation functions for deep inelastic scattering in the chiral limit*, *JHEP* **04** (2009) 127 [arXiv:0903.4623].

[26] B.A. Kniehl and O.L. Veretin, *Moments $n = 2$ and $n = 3$ of the Wilson twist-two operators at three loops in the RI′/SMOM scheme*, *Nucl. Phys. B* **961** (2020) 115229 [arXiv:2009.11325].

[27] R.P. Feynman, *Very high-energy collisions of hadrons*, *Phys. Rev. Lett.* **23** (1969) 1415.

[28] D.J. Gross and F. Wilczek, *Ultraviolet Behavior of Nonabelian Gauge Theories*, *Phys. Rev. Lett.* **30** (1973) 1343.

[29] H.D. Politzer, *Reliable Perturbative Results for Strong Interactions?*, *Phys. Rev. Lett.* **30** (1973) 1346.

[30] C. Gignoux, B. Silvestre-Brac and J.M. Richard, *Possibility of Stable Multi - Quark Baryons*, *Phys. Lett. B* **193** (1987) 323.

[31] *LHCb experiment discovers a new pentaquark, https://home.cern/news/news/physics/lhcb-experiment-discovers-new-pentaquark*, 2019.

[32] J. Ellis, *TikZ-Feynman: Feynman diagrams with TikZ*, *Comput. Phys. Commun.* **210** (2017) 103 [arXiv:1601.05437].

[33] F.J. Yndurain, *The Theory of Quark and Gluon Interactions*, Springer (1983).

[34] L. Faddeev and V. Popov, *Feynman diagrams for the yang-mills field*, *Physics Letters B* **25** (1967) 29.

[35] T. Chupp, P. Fierlinger, M. Ramsey-Musolf and J. Singh, *Electric dipole moments of atoms, molecules, nuclei, and particles*, *Rev. Mod. Phys.* **91** (2019) 015001 [`arXiv:1710.02504`].

[36] M.D. Schwarz, *Quantum field theory and the standard model*, Cambridge Univ. Press (2014).

[37] R.D. Peccei and H.R. Quinn, *CP Conservation in the Presence of Instantons*, *Phys. Rev. Lett.* **38** (1977) 1440.

[38] MADMAX WORKING GROUP collaboration, B. Majorovits and J. Redondo, *MADMAX: A new Dark Matter Axion Search using a Dielectric Haloscope*, in *12th Patras Workshop on Axions, WIMPs and WISPs*, p. 94, 2017. `arXiv:1611.04549`. DOI.

[39] S. Beurthey et al., *MADMAX Status Report*, `arXiv:2003.10894`.

[40] R. Bähre et al., *Any light particle search II —Technical Design Report*, *JINST* **8** (2013) T09001 [`arXiv:1302.5647`].

[41] ALPS collaboration, K.S. Isleif, *The Any Light Particle Search experiment at DESY*, `arXiv:2202.07306`.

[42] J. Goldstone, *Field Theories with Superconductor Solutions*, *Nuovo Cim.* **19** (1961) 154.

[43] J. Goldstone, A. Salam and S. Weinberg, *Broken Symmetries*, *Phys. Rev.* **127** (1962) 965.

[44] S.L. Adler and W.A. Bardeen, *Absence of higher order corrections in the anomalous axial vector divergence equation*, *Phys. Rev.* **182** (1969) 1517.

[45] J.C. Collins, D.E. Soper and G.F. Sterman, *Factorization of Hard Processes in QCD*, *Adv. Ser. Direct. High Energy Phys.* **5** (1989) 1 [`hep-ph/0409313`].

[46] T. Ohl, *Drawing Feynman diagrams with Latex and Metafont*, *Comput. Phys. Commun.* **90** (1995) 340 [`hep-ph/9505351`].

[47] G. 't Hooft, *Renormalization of Massless Yang-Mills Fields*, *Nucl. Phys. B* **33** (1971) 173.

[48] C.G. Bollini and J.J. Giambiagi, *Dimensional Renormalization: The Number of Dimensions as a Regularizing Parameter*, *Nuovo Cim. B* **12** (1972) 20.

[49] G.M. Cicuta and E. Montaldi, *Analytic renormalization via continuous space dimension*, *Lett. Nuovo Cim.* **4** (1972) 329.

[50] J.F. Ashmore, *A Method of Gauge Invariant Regularization*, *Lett. Nuovo Cim.* **4** (1972) 289.

[51] J.C. Collins, *Renormalization: An Introduction to Renormalization, The Renormalization Group, and the Operator Product Expansion*, vol. 26 of *Cambridge Monographs on Mathematical Physics*, Cambridge University Press, Cambridge (1986), 10.1017/CBO9780511622656.

[52] C.G. Callan, Jr., *Broken scale invariance in scalar field theory*, *Phys. Rev. D* **2** (1970) 1541.

[53] K. Symanzik, *Small distance behavior in field theory and power counting*, *Commun. Math. Phys.* **18** (1970) 227.

[54] W.E. Caswell, *Asymptotic Behavior of Nonabelian Gauge Theories to Two Loop Order*, *Phys. Rev. Lett.* **33** (1974) 244.

[55] D.R.T. Jones, *Asymptotic Behavior of Supersymmetric Yang-Mills Theories in the Two Loop Approximation*, *Nucl. Phys. B* **87** (1975) 127.

[56] O.V. Tarasov, A.A. Vladimirov and A.Y. Zharkov, *The Gell-Mann-Low Function of QCD in the Three Loop Approximation*, *Phys. Lett. B* **93** (1980) 429.

[57] S.A. Larin and J.A.M. Vermaseren, *The Three loop QCD Beta function and anomalous dimensions*, *Phys. Lett. B* **303** (1993) 334 [hep-ph/9302208].

[58] T. van Ritbergen, J.A.M. Vermaseren and S.A. Larin, *The Four loop beta function in quantum chromodynamics*, *Phys. Lett. B* **400** (1997) 379 [hep-ph/9701390].

[59] M. Czakon, *The Four-loop QCD beta-function and anomalous dimensions*, *Nucl. Phys. B* **710** (2005) 485 [hep-ph/0411261].

[60] P.A. Baikov, K.G. Chetyrkin and J.H. Kühn, *Five-loop running of the QCD coupling constant*, *Phys. Rev. Lett.* **118** (2017) 082002 [arXiv:1606.08659].

[61] K.G. Wilson, *Nonlagrangian models of current algebra*, *Phys. Rev.* **179** (1969) 1499.

[62] W. Zimmermann, *Normal products and the short distance expansion in the perturbation theory of renormalizable interactions*, *Annals Phys.* **77** (1973) 570.

[63] M.E. Peskin and D.V. Schroeder, *An Introduction to quantum field theory*, Addison-Wesley, Reading, USA (1995).

[64] D.J. Gross and S.B. Treiman, *Light cone structure of current commutators in the gluon quark model*, *Phys. Rev. D* **4** (1971) 1059.

[65] S.D. Bass, *The Spin Structure of the Proton*, World Scientific (2008).

[66] X.D. Ji, *Deeply virtual Compton scattering*, *Phys. Rev. D* **55** (1997) 7114 [hep-ph/9609381].

[67] C.G. Callan, Jr. and D.J. Gross, *High-energy electroproduction and the constitution of the electric current*, *Phys. Rev. Lett.* **22** (1969) 156.

[68] A. Bodek et al., *Experimental Studies of the Neutron and Proton Electromagnetic Structure Functions*, *Phys. Rev. D* **20** (1979) 1471.

[69] D.J. Griffiths, *Introducion to Elementary Particles*, Wiley (1987).

[70] J.D. Bjorken, *Asymptotic Sum Rules at Infinite Momentum*, *Phys. Rev.* **179** (1969) 1547.

[71] PARTICLE DATA GROUP collaboration, J. Beringer et al., *Review of Particle Physics (RPP)*, *Phys. Rev. D* **86** (2012) 010001.

[72] QCDSF collaboration, M. Göckeler, R. Horsley, D. Pleiter, P.E.L. Rakow and G. Schierholz, *A Lattice determination of moments of unpolarised nucleon structure functions using improved Wilson fermions*, *Phys. Rev. D* **71** (2005) 114511 [hep-ph/0410187].

[73] M. Göckeler et al., *Perturbative and Nonperturbative Renormalization in Lattice QCD*, *Phys. Rev. D* **82** (2010) 114511 [arXiv:1003.5756].

[74] V.M. Braun, S. Collins, M. Göckeler, P. Pérez-Rubio, A. Schäfer, R.W. Schiel et al., *Second Moment of the Pion Light-cone Distribution Amplitude from Lattice QCD*, *Phys. Rev. D* **92** (2015) 014504 [arXiv:1503.03656].

[75] V.M. Braun et al., *The* ρ*-meson light-cone distribution amplitudes from lattice QCD*, *JHEP* **04** (2017) 082 [arXiv:1612.02955].

[76] G.S. Bali, S. Collins, M. Göckeler, R. Rödl, A. Schäfer and A. Sternbeck, *Nucleon generalized form factors from two-flavor lattice QCD*, *Phys. Rev. D* **100** (2019) 014507 [arXiv:1812.08256].

[77] RQCD collaboration, G.S. Bali, V.M. Braun, S. Bürger, M. Göckeler, M. Gruber, F. Hutzler et al., *Light-cone distribution amplitudes of pseudoscalar mesons from lattice QCD*, *JHEP* **08** (2019) 065 [arXiv:1903.08038].

[78] T. Harris, G. von Hippel, P. Junnarkar, H.B. Meyer, K. Ottnad, J. Wilhelm et al., *Nucleon isovector charges and twist-2 matrix elements with* $N_f = 2+1$ *dynamical Wilson quarks*, *Phys. Rev. D* **100** (2019) 034513 [arXiv:1905.01291].

[79] C. Alexandrou, S. Bacchio, M. Constantinou, J. Finkenrath, K. Hadjiyiannakou, K. Jansen et al., *Complete flavor decomposition of the spin and momentum fraction of the proton using lattice QCD simulations at physical pion mass*, *Phys. Rev. D* **101** (2020) 094513 [arXiv:2003.08486].

[80] CTEQ collaboration, R. Brock et al., *Handbook of perturbative QCD: Version 1.0*, *Rev. Mod. Phys.* **67** (1995) 157.

[81] V.N. Gribov and L.N. Lipatov, *Deep inelastic e p scattering in perturbation theory*, *Sov. J. Nucl. Phys.* **15** (1972) 438.

[82] G. Altarelli and G. Parisi, *Asymptotic Freedom in Parton Language*, *Nucl. Phys. B* **126** (1977) 298.

[83] Y.L. Dokshitzer, *Calculation of the Structure Functions for Deep Inelastic Scattering and* e^+e^- *Annihilation by Perturbation Theory in Quantum Chromodynamics.*, *Sov. Phys. JETP* **46** (1977) 641.

[84] B. Pasquini and S. Boffi, *The Structure of the nucleon from generalized parton distributions*, *PoS* **LC2008** (2008) 014 [arXiv:0810.3835].

[85] R. Kaiser, *The 3D structure of the proton*, *J. Phys. Conf. Ser.* **381** (2012) 012018.

[86] A. Bacchetta, *Where do we stand with a 3-D picture of the proton?*, *Eur. Phys. J. A* **52** (2016) 163 [arXiv:2107.06772].

[87] A.V. Efremov and A.V. Radyushkin, *Asymptotical Behavior of Pion Electromagnetic Form-Factor in QCD*, *Theor. Math. Phys.* **42** (1980) 97.

[88] A.V. Efremov and A.V. Radyushkin, *Factorization and Asymptotical Behavior of Pion Form-Factor in QCD*, *Phys. Lett. B* **94** (1980) 245.

[89] G.P. Lepage and S.J. Brodsky, *Exclusive Processes in Quantum Chromodynamics: Evolution Equations for Hadronic Wave Functions and the Form-Factors of Mesons*, *Phys. Lett. B* **87** (1979) 359.

[90] G.P. Lepage and S.J. Brodsky, *Exclusive Processes in Perturbative Quantum Chromodynamics*, *Phys. Rev. D* **22** (1980) 2157.

[91] F.M. Dittes, D. Müller, D. Robaschik, B. Geyer and J. Hořejši, *The Altarelli-Parisi Kernel as Asymptotic Limit of an Extended Brodsky-Lepage Kernel*, *Phys. Lett. B* **209** (1988) 325.

[92] J.A.M. Vermaseren, *Harmonic sums, Mellin transforms and integrals*, *Int. J. Mod. Phys. A* **14** (1999) 2037 [hep-ph/9806280].

[93] J. Blümlein and S. Kurth, *Harmonic sums and Mellin transforms up to two loop order*, *Phys. Rev. D* **60** (1999) 014018 [hep-ph/9810241].

[94] F.W.J. Olver, D.W. Lozier, R.F. Boisvert and C.W. Clark, *The NIST Handbook of Mathematical Functions*, Cambridge Univ. Press (2010).

[95] K. Boyadzhiev, *Notes on the Binomial Transform*, World Scientific (2018).

[96] N. Nielsen, *Traité élémentaire des nombres de Bernoulli*, *Gauthier-Villars* (1923).

[97] Z.A. Melzak, V.D. Gokhale and W.V. Parker, *Advanced problems and solutions: 4458*, *The American Mathematical Monthly* **60** (1953) 53.

[98] C. Schneider, *Symbolic summation assists combinatorics*, *Seminaire Lotharingien de Combinatoire* **56** (01, 2007) 1.

[99] C. Schneider, *Simplifying Multiple Sums in Difference Fields*, in *LHCPhenoNet School: Integration, Summation and Special Functions in Quantum Field Theory*, p. 325, 2013. DOI.

[100] R.W. Gosper, *Decision procedure for indefinite hypergeometric summation*, *Proceedings of the National Academy of Sciences* **75** (1978) 40.

[101] M. Kauers and P. Paule, *The Concrete Tetrahedron: Symbolic Sums, Recurrence Equations, Generating Functions, Asymptotic Estimates*, Springer Publishing Company, Incorporated (2011).

[102] D. Zeilberger, *The method of creative telescoping*, *Journal of Symbolic Computation* **11** (1991) 195.

[103] R.L. Graham, D.E. Knuth and O. Patashnik, *Concrete mathematics - a foundation for computer science.*, Addison-Wesley (1989).

[104] M. Petkovŝek, H.S. Wilf and D. Zeilberger, *A=B*, A K Peters (1996).

[105] P. Nogueira, *Automatic Feynman graph generation*, *J. Comput. Phys.* **105** (1993) 279.

[106] S. Moch, B. Ruijl, T. Ueda, J.A.M. Vermaseren and A. Vogt, *Four-Loop Non-Singlet Splitting Functions in the Planar Limit and Beyond*, *JHEP* **10** (2017) 041 [`arXiv:1707.08315`].

[107] J.A.M. Vermaseren, *New features of FORM*, `math-ph/0010025`.

[108] J. Kuipers, T. Ueda, J.A.M. Vermaseren and J. Vollinga, *FORM version 4.0*, *Comput. Phys. Commun.* **184** (2013) 1453 [`arXiv:1203.6543`].

[109] B. Ruijl, T. Ueda and J.A.M. Vermaseren, *Forcer, a FORM program for the parametric reduction of four-loop massless propagator diagrams*, *Comput. Phys. Commun.* **253** (2020) 107198 [`arXiv:1704.06650`].

[110] S.G. Gorishnii, S.A. Larin, L.R. Surguladze and F.V. Tkachov, *Mincer: Program for Multiloop Calculations in Quantum Field Theory for the Schoonschip System*, *Comput. Phys. Commun.* **55** (1989) 381.

[111] S.A. Larin, F.V. Tkachov and J.A.M. Vermaseren, *The FORM version of MINCER*, preprint `NIKHEF-H-91-18`, 1991.

[112] K.G. Chetyrkin, A.L. Kataev and F.V. Tkachov, *New Approach to Evaluation of Multiloop Feynman Integrals: The Gegenbauer Polynomial x Space Technique*, *Nucl. Phys. B* **174** (1980) 345.

[113] F.V. Tkachov, *A Theorem on Analytical Calculability of Four Loop Renormalization Group Functions*, *Phys. Lett. B* **100** (1981) 65.

[114] S.A. Larin, P. Nogueira, T. van Ritbergen and J.A.M. Vermaseren, *The Three loop QCD calculation of the moments of deep inelastic structure functions*, *Nucl. Phys. B* **492** (1997) 338 [`hep-ph/9605317`].

[115] F. Herzog, B. Ruijl, T. Ueda, J.A.M. Vermaseren and A. Vogt, *FORM, Diagrams and Topologies*, *PoS* **LL2016** (2016) 073 [`arXiv:1608.01834`].

[116] T. van Ritbergen, A.N. Schellekens and J.A.M. Vermaseren, *Group theory factors for Feynman diagrams*, *Int. J. Mod. Phys. A* **14** (1999) 41 [`hep-ph/9802376`].

[117] J. Vermaseren, *Automatization of the computation of structure function moments at the three loop level*, *Nucl. Instrum. Meth. A* **389** (1997) 350.

[118] D.J. Gross and F. Wilczek, *Asymptotically Free Gauge Theories - I*, *Phys. Rev. D* **8** (1973) 3633.

[119] E.G. Floratos, D.A. Ross and C.T. Sachrajda, *Higher Order Effects in Asymptotically Free Gauge Theories: The Anomalous Dimensions of Wilson Operators*, *Nucl. Phys. B* **129** (1977) 66.

[120] S. Moch, J.A.M. Vermaseren and A. Vogt, *The Three loop splitting functions in QCD: The Nonsinglet case*, *Nucl. Phys. B* **688** (2004) 101 [hep-ph/0403192].

[121] J. Blümlein, P. Marquard, C. Schneider and K. Schönwald, *The three-loop unpolarized and polarized non-singlet anomalous dimensions from off shell operator matrix elements*, *Nucl. Phys. B* **971** (2021) 115542 [arXiv:2107.06267].

[122] J.A. Gracey, *Anomalous dimension of nonsinglet Wilson operators at $O(1/n_f)$ in deep inelastic scattering*, *Phys. Lett. B* **322** (1994) 141 [hep-ph/9401214].

[123] J. Davies, A. Vogt, B. Ruijl, T. Ueda and J.A.M. Vermaseren, *Large-n_f contributions to the four-loop splitting functions in QCD*, *Nucl. Phys. B* **915** (2017) 335 [arXiv:1610.07477].

[124] V.N. Velizhanin, *Four loop anomalous dimension of the second moment of the non-singlet twist-2 operator in QCD*, *Nucl. Phys. B* **860** (2012) 288 [arXiv:1112.3954].

[125] V.N. Velizhanin, *Four-loop anomalous dimension of the third and fourth moments of the nonsinglet twist-2 operator in QCD*, *Int. J. Mod. Phys. A* **35** (2020) 2050199 [arXiv:1411.1331].

[126] B. Ruijl, T. Ueda, J.A.M. Vermaseren, J. Davies and A. Vogt, *First Forcer results on deep-inelastic scattering and related quantities*, *PoS* **LL2016** (2016) 071 [arXiv:1605.08408].

[127] F. Herzog, S. Moch, B. Ruijl, T. Ueda, J.A.M. Vermaseren and A. Vogt, *Five-loop contributions to low-N non-singlet anomalous dimensions in QCD*, *Phys. Lett. B* **790** (2019) 436 [arXiv:1812.11818].

[128] E. Remiddi and J.A.M. Vermaseren, *Harmonic polylogarithms*, *Int. J. Mod. Phys. A* **15** (2000) 725 [hep-ph/9905237].

[129] I.I. Balitsky and V.M. Braun, *Evolution Equations for QCD String Operators*, *Nucl. Phys. B* **311** (1989) 541.

[130] J.A. Gracey, *Two loop renormalization of the n = 2 Wilson operator in the RI'/SMOM scheme*, *JHEP* **03** (2011) 109 [arXiv:1103.2055].

[131] J.A. Gracey, *Amplitudes for the n = 3 moment of the Wilson operator at two loops in the RI'/SMOM scheme*, *Phys. Rev. D* **84** (2011) 016002 [arXiv:1105.2138].

[132] S. Moch and S. Van Thurenhout, *Renormalization of non-singlet quark operator matrix elements for off-forward hard scattering*, *Nucl. Phys. B* **971** (2021) 115536 [arXiv:2107.02470].

[133] Y.M. Makeenko, *Conformal Operators in Quantum Chromodynamics*, *Sov. J. Nucl. Phys.* **33** (1981) 440.

[134] S. Van Thurenhout, *Off-forward anomalous dimensions of non-singlet transversity operators*, arXiv:2204.02140.

[135] C. Alexandrou, K. Cichy, M. Constantinou, K. Hadjiyiannakou, K. Jansen, A. Scapellato et al., *Transversity GPDs of the proton from lattice QCD*, *Phys. Rev. D* **105** (2022) 034501 [arXiv:2108.10789].

[136] A. Scapellato, C. Alexandrou, K. Cichy, M. Constantinou, K. Hadjiyiannakou, K. Jansen et al., *Proton generalized parton distributions from lattice QCD*, in *19th International Conference on Hadron Spectroscopy and Structure*, 1, 2022. arXiv:2201.06519.

[137] C. Alexandrou et al., *First moments of the nucleon transverse quark spin densities using lattice QCD*, arXiv:2202.09871.

[138] X. Artru and M. Mekhfi, *What can we learn from unpolarized and polarized electroproduction of fast baryons?*, *Nucl. Phys. A* **532** (1991) 351.

[139] M.A. Shifman and M.I. Vysotsky, *Form-Factors of Heavy Mesons in QCD*, *Nucl. Phys. B* **186** (1981) 475.

[140] F. Baldracchini, N.S. Craigie, V. Roberto and M. Socolovsky, *A Survey of Polarization Asymmetries Predicted by QCD*, *Fortschritte der Physik* **29** (1981) 505.

[141] J. Blümlein, *On the anomalous dimension of the transversity distribution $h_1(x,Q^2)$*, *Eur. Phys. J. C* **20** (2001) 683 [hep-ph/0104099].

[142] A. Hayashigaki, Y. Kanazawa and Y. Koike, *Next-to-leading order q^2 evolution of the transversity distribution $h_1(x,q^2)$*, *Phys. Rev. D* **56** (1997) 7350 [hep-ph/9707208].

[143] S. Kumano and M. Miyama, *Two loop anomalous dimensions for the structure function h1*, *Phys. Rev. D* **56** (1997) R2504 [hep-ph/9706420].

[144] W. Vogelsang, *Next-to-leading order evolution of transversity distributions and Soffer's inequality*, *Phys. Rev. D* **57** (1998) 1886 [hep-ph/9706511].

[145] J.A. Gracey, *Three loop anomalous dimension of the second moment of the transversity operator in the MS-bar and RI-prime schemes*, *Nucl. Phys. B* **667** (2003) 242 [hep-ph/0306163].

[146] J. Ablinger, J. Blümlein, S. Klein, C. Schneider and F. Wissbrock, *The $O(\alpha_s^3)$ Massive Operator Matrix Elements of $O(n_f)$ for the Structure Function $F_2(x,Q^2)$ and Transversity*, *Nucl. Phys. B* **844** (2011) 26 [arXiv:1008.3347].

[147] V.N. Velizhanin, *Three loop anomalous dimension of the non-singlet transversity operator in QCD*, *Nucl. Phys. B* **864** (2012) 113 [arXiv:1203.1022].

[148] J. Ablinger, A. Behring, J. Blümlein, A. De Freitas, A. Hasselhuhn, A. von Manteuffel et al., *The 3-Loop Non-Singlet Heavy Flavor Contributions and Anomalous Dimensions for the Structure Function $F_2(x,Q^2)$ and Transversity*, *Nucl. Phys. B* **886** (2014) 733 [arXiv:1406.4654].

[149] BELLE-II collaboration, W. Altmannshofer et al., *The Belle II Physics Book*, *PTEP* **2019** (2019) 123C01 [arXiv:1808.10567].

[150] A.V. Belitsky, A. Freund and D. Mueller, *NLO evolution kernels for skewed transversity distributions*, *Phys. Lett. B* **493** (2000) 341 [hep-ph/0008005].

[151] S. Mikhailov and A. Vladimirov, *Erbl and dglap kernels for transversity distributions. two-loop calculations in covariant gauge*, *Physics Letters B* **671** (2009) 111 [hep-ph/0810.1647].

[152] H.H. Patel, *Package-X: A Mathematica package for the analytic calculation of one-loop integrals*, *Comput. Phys. Commun.* **197** (2015) 276 [arXiv:1503.01469].

[153] N. Batir, *Finite binomial sum identities with harmonic numbers*, *Journal of Integer Sequences* **24** (2021).

[154] ASYMMETRY ANALYSIS collaboration, Y. Goto et al., *Polarized parton distribution functions in the nucleon*, *Phys. Rev. D* **62** (2000) 034017 [hep-ph/0001046].

[155] H. Nematollahi, P. Abolhadi, S. Atashbar, A. Mirjalili and M.M. Yazdanpanah, *Polarized parton distribution functions: parametrization and transverse momentum dependence*, *Eur. Phys. J. C* **81** (2021) 18.

[156] R. Jakob, P. Kroll and M. Raulfs, *Meson - photon transition form-factors*, *J. Phys. G* **22** (1996) 45 [hep-ph/9410304].

[157] P. Kroll and M. Raulfs, *The $\pi\gamma$ transition form-factor and the pion wave function*, *Phys. Lett. B* **387** (1996) 848 [hep-ph/9605264].

[158] A.V. Radyushkin and R.T. Ruskov, *Transition form-factor $\gamma\gamma^* \to \pi^0$ and QCD sum rules*, *Nucl. Phys. B* **481** (1996) 625 [hep-ph/9603408].

[159] I.V. Musatov and A.V. Radyushkin, *Transverse momentum and Sudakov effects in exclusive QCD processes: $\gamma^*\gamma\pi^0$ form-factor*, *Phys. Rev. D* **56** (1997) 2713 [hep-ph/9702443].

[160] CLEO collaboration, J. Gronberg et al., *Measurements of the meson - photon transition form-factors of light pseudoscalar mesons at large momentum transfer*, *Phys. Rev. D* **57** (1998) 33 [hep-ex/9707031].

[161] K. Sasaki, *Polarized Electroproduction in Asymptotically Free Gauge Theories*, *Prog. Theor. Phys.* **54** (1975) 1816.

[162] M.A. Ahmed and G.G. Ross, *Polarized Lepton - Hadron Scattering in Asymptotically Free Gauge Theories*, *Nucl. Phys. B* **111** (1976) 441.

[163] R. Mertig and W.L. van Neerven, *The Calculation of the two loop spin splitting functions $P_{ij}^{(1)}(x)$*, *Z. Phys. C* **70** (1996) 637 [hep-ph/9506451].

[164] W. Vogelsang, *A Rederivation of the spin dependent next-to-leading order splitting functions*, *Phys. Rev. D* **54** (1996) 2023 [hep-ph/9512218].

[165] W. Vogelsang, *The Spin dependent two loop splitting functions*, *Nucl. Phys. B* **475** (1996) 47 [hep-ph/9603366].

[166] S. Moch, J.A.M. Vermaseren and A. Vogt, *The Three-Loop Splitting Functions in QCD: The Helicity-Dependent Case*, *Nucl. Phys. B* **889** (2014) 351 [arXiv:1409.5131].

[167] A. Behring, J. Blümlein, A. De Freitas, A. Goedicke, S. Klein, A. von Manteuffel et al., *The Polarized Three-Loop Anomalous Dimensions from On-Shell Massive Operator Matrix Elements*, *Nucl. Phys. B* **948** (2019) 114753 [arXiv:1908.03779].

[168] D.J. Broadhurst and A.L. Kataev, *Connections between deep inelastic and annihilation processes at next to next-to-leading order and beyond*, *Phys. Lett. B* **315** (1993) 179 [hep-ph/9308274].

[169] J.A. Gracey, *Anomalous dimensions of operators in polarized deep inelastic scattering at O(1/N(f))*, *Nucl. Phys. B* **480** (1996) 73 [hep-ph/9609301].

[170] V.M. Braun, A.N. Manashov, S. Moch and M. Strohmaier, *Three-loop off-forward evolution kernel for axial-vector operators in Larin's scheme*, *Phys. Rev. D* **103** (2021) 094018 [arXiv:2101.01471].

[171] G. 't Hooft and M.J.G. Veltman, *Regularization and Renormalization of Gauge Fields*, *Nucl. Phys. B* **44** (1972) 189.

[172] D.A. Akyeampong and R. Delbourgo, *Dimensional regularization, abnormal amplitudes and anomalies*, *Nuovo Cim. A* **17** (1973) 578.

[173] P. Breitenlohner and D. Maison, *Dimensional Renormalization and the Action Principle*, *Commun. Math. Phys.* **52** (1977) 11.

[174] M.S. Chanowitz, M. Furman and I. Hinchliffe, *The Axial Current in Dimensional Regularization*, *Nucl. Phys. B* **159** (1979) 225.

[175] W. Siegel, *Supersymmetric Dimensional Regularization via Dimensional Reduction*, *Phys. Lett. B* **84** (1979) 193.

[176] S.A. Larin, *The Renormalization of the axial anomaly in dimensional regularization*, *Phys. Lett. B* **303** (1993) 113 [hep-ph/9302240].

[177] S.A. Larin and J.A.M. Vermaseren, *The α_s^3 corrections to the Bjorken sum rule for polarized electroproduction and to the Gross-Llewellyn Smith sum rule*, *Phys. Lett. B* **259** (1991) 345.

Eidesstattliche Versicherung / Declaration on oath

Hiermit versichere ich an Eides statt, die vorliegende Dissertationsschrift selbst verfasst und keine anderen als die angegebenen Hilfsmittel und Quellen benutzt zu haben.

Hamburg, den 06.07.2022 Unterschrift